Spring 2016

Immobilization of cellulase for large scale reactors to reduce cellulosic ethanol cost

Dezhi Zhang

IMMOBILIZATION OF CELLULASE FOR LARGE SCALE REACTORS TO REDUCE CELLULOSIC ETHANOL COST

by

Dezhi Zhang, B.S., M.S.

A Dissertation Presented in Partial Fulfillment
of the Requirements of the Degree
Doctor of Philosophy

COLLEGE OF ENGINEERING AND SCIENCE
LOUISIANA TECH UNIVERSITY

May 2016

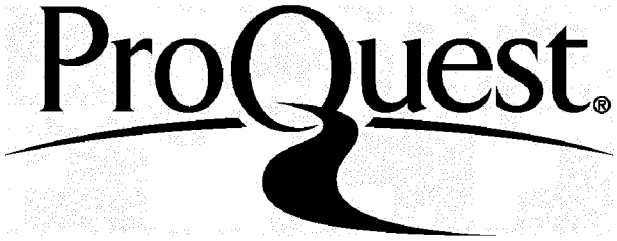

LOUISIANA TECH UNIVERSITY

THE GRADUATE SCHOOL

APRIL 8, 2016
Date

We hereby recommend that the dissertation prepared under our supervision by

Dezhi Zhang, B.S., M.S.

entitled **Immobilization of Cellulase for Large Scale Reactors to Reduce Cellulosic Ethanol Cost**

be accepted in partial fulfillment of the requirements for the Degree of

Doctor of Philosophy in Engineering

Supervisor of Dissertation Research

Head of Department
Engineering
Department

Recommendation concurred in:

Advisory Committee

Approved:

Director of Graduate Studies

Dean of the College

Approved:

Dean of the Graduate School

ABSTRACT

Cellulosic ethanol is an alternative renewable energy source. Cellulase used in the production of cellulosic ethanol is very expensive. The difficulty in separating cellulase from the cellulose solution after the hydrolysis process limits the reusability of the cellulase, which highly precludes the scales of this application because of the high cost of the enzyme. Immobilization of cellulase provides a promising approach to allow the enzyme to be recycled, thus reducing the production cost. This research focused on immobilizing cellulase for reuse to reduce the cellulosic ethanol cost.

Four immobilization techniques were explored for the immobilization of cellulase on four different immobilization carriers. The immobilized cellulases by Layer-by-Layer Nano-Assembly (LbL) and Ca^{2+}-$Al(OH)_x$ modification methods had high initial activities but low reusabilities. Enzyme desorption was observed during the hydrolysis of cellulose solutions by the immobilized cellulases for both LbL and Ca^{2+}-$Al(OH)_x$ modification methods. Efforts were focused on improving the reusability of the immobilized cellulase, yet rarely worked. For the immobilized cellulase by the combination of Ca^{2+}-$Al(OH)_x$ modification and LbL, the reusability of the immobilized cellulase was improved with the number of enzyme layers. Unfortunately, for the present moment, the initial activity decreased with the number of enzyme layers. Immobilization of cellulase on silica gel by 3-APTES and glutaraldehyde modification showed the highest reusability. No enzyme desorption was observed during the hydrolysis of cellulose solution. It indicated that the

cellulase molecules firmly covalent bound to the silica gel. The immobilized cellulase on silica gel by 3-APTES and glutaraldehyde modification had the highest activity per unit mass of immobilization carriers because of the porous structure of the silica gel.

Key Words: Cellulosic ethanol, Immobilization of cellulase, LbL, 3-APTES, Silica gel

APPROVAL FOR SCHOLARLY DISSEMINATION

The author grants to the Prescott Memorial Library of Louisiana Tech University the right to reproduce, by appropriate methods, upon request, any or all portions of this Dissertation. It is understood that "proper request" consists of the agreement, on the part of the requesting party, that said reproduction is for his personal use and that subsequent reproduction will not occur without written approval of the author of this Dissertation. Further, any portions of the Dissertation used in books, papers, and other works must be appropriately referenced to this Dissertation.

Finally, the author of this Dissertation reserves the right to publish freely, in the literature, at any time, any or all portions of this Dissertation.

Author Dezhi Zhang

Date 04/28/2016

TABLE OF CONTENTS

LIST OF TABLES

LIST OF FIGURES

ACKNOWLEDGMENTS

First and foremost, I would like to express my sincere gratitude to my advisor, Dr. James Palmer, for his suggestions and advice throughout the project. I would also like to thank my current committee members: Dr. Hisham Hegab, Dr. Yuri Lvov, Dr. Shengnian Wang, and Dr. Sven Eklund, along with my previous advisory committee member, Dr. L. Dale Snow, for their time and contributions to my research.

I cannot forget my fellow lab mates: Juan Lin, Qi Xing, Bam Aryal, Joe Nealy, and Bibek Uprety for their advice and assistance in the laboratory. Additionally, the IfM faculty and staff have always been there when I needed their assistance.

I would like to thank the Department of Energy for their support of this project (DE-EE0003120).

Finally, I would like to thank my parents, Mr. Xiuzhong Zhang and Mrs. Xiukun Li, as well as my wife, Mrs. Lei Yang, for their understanding, unyielding support and encouragement.

CHAPTER 1

INTRODUCTION

1.1 Motivation

The global demand of energy has enormously increased in recent years due to industrial development and population growth. The petroleum consumption had risen from 13,315 in 1,950 trillion Btu to 34,016 trillion Btu in 2012, in which the consumption for transportation sector had risen from 6,690 to 24,202 trillion Btu [1]. Also, massive fossil fuel consumption causes several environmental problems, such as pollution, global warming, and destruction of landscapes and habitats [2]. Because of these facts, the interest in developing a new, clean, and sustainable energy source has risen dramatically. Biofuel is an alternative renewable energy source which has several advantages including improvement of air quality, reduction of greenhouse gases, and preservation of the ecological environment [2]. Biofuel includes bioethanol, biodiesel, and biomethanol.

In 2013, bioethanol production in the USA was 25 million tonnes of oil equivalent, which was 88% of the total biofuel production in the USA [1]. In the past, bioethanol was produced mainly from starch in corn kernels in the USA and sugarcane in Brazil, which was known as the first-generation bioethanol [2]. However, its competition with the food industry limits its scales due to rapidly increasing population growth.

Therefore, the second-generation bioethanol produced from lignocellulosic biomass, such as cellulose, is one of the most promising biofuels [3].

In order to produce bioethanol, the lignocellulosic biomass are broken down into fermentable sugars (glucose) by hydrolysis. Although this process can be performed by either a chemical or an enzymatic process, the latter one is preferred because it is cleaner and the process can be controlled by adjusting the reaction conditions easily (such as pH and temperature) [4]. Currently, the degradation of cellulose materials to glucose uses free enzyme. The difficulty of the separation of the free enzyme from the solution after the hydrolysis process limits the reusability of the enzyme which highly precludes the scales of this application because of the high cost of the enzyme. Therefore, the interest in immobilizing enzyme is increasingly high. The immobilized enzyme can be reused several times, which would dramatically decrease the cost of bioethanol producing processes.

1.2 Objectives

The overall objectives of this research work are to explore and demonstrate one enzyme (cellulase) immobilization method for reuse to reduce bioethanol producing costs in commercial scale reactors.

Specifically:

(1) Explore enzyme immobilization methods. Layer-by-Layer Nano-Assembly (LbL) and self-assembly monolayer nanotechnology were studied. In order to find a suitable immobilization carrier, different materials were tested for immobilization of the enzyme.

(2) Adjust the immobilization steps to achieve the immobilization of the enzyme. Monitor and calculate the mass of the immobilized enzyme.

(3) Design and set up bioreactors for hydrolysis of different cellulose materials by free enzyme and immobilized enzyme onto different carriers. Different immobilization carriers require different bioreactors to perform hydrolysis of cellulose material.

(4) Test the activity of the free and immobilized enzyme in hydrolysis of cellulose materials. Optimize the immobilization and hydrolysis steps to achieve high specific activity of the immobilized enzyme by comparing it with the same amount of the free enzyme. Characterize material properties, such as pore size.

(5) Test hydrolysis performances of the immobilized enzyme under different conditions (temperature and pH)

(6) Demonstrate the reusability of the immobilized enzyme for multiple recycles. Further optimize the immobilization and hydrolysis steps to improve the reusability of the immobilized enzyme.

1.3 Background

Enzymes are macromolecules that act as biological catalysts. They can catalyze many different kinds of chemical reactions under very mild conditions. Enzymes have a high level of substrate specificity. It is rare for by-products to be formed from the enzyme catalyzed reactions. These advantages make them very interesting for industrial use. However, most enzymes are expensive, and it is difficult to separate them from the substrate/product solution after the catalystic reaction. Immobilization of enzymes allows enzymes to be recycled, thereby reducing the cost of the overall industrial process.

Chibata *et al.* reported the first industrial use of the immobilized enzymes in 1967, with the immobilization of *Aspergillus oryzae* aminoacylase [5].

Techniques for immobilization have developed rapidly in the past four decades [6]. There are two main immobilization techniques: physical adsorption and chemical binding [6]. Both of these main immobilization techniques have their own inherent advantages and disadvantages. The immobilization techniques will be discussed in Section 1.7 in detail. Besides application in the industrial processes, the immobilization techniques are fundamental with application in diagnostics, bioaffinity chromatography, and biosensors [7, 8]. Although the immobilization techniques have developed rapidly in the past decades, further development is still needed. Application in the current field and further extension of the use of the immobilized enzymes to other domains will require new methodologies and a better understanding of current techniques.

1.4 Cellulose

1.4.1 Crystalline Cellulose

Cellulose is one of the most abundant polysaccharide in nature. Its sources include agricultural and forestry residues (e.g. corn stover, sawdust, and mill wastes), portion of municipal solid waste (e.g. waste paper), and herbaceous and woody crops (e.g. switchgrass) [9]. The chemical structure of cellulose is a linear polymer of β-(1→4)-linked D-glucopyranose monomer units (also called D-glucose units). Although the chemical repeating unit is β-(1→4)-linker D-glucose, the structural repeat of cellulose is β-cellobiose because every glucose residue is rotated approximately 180° [10, 11]. **Figure 1-1** shows the structure of a single cellulose chain.

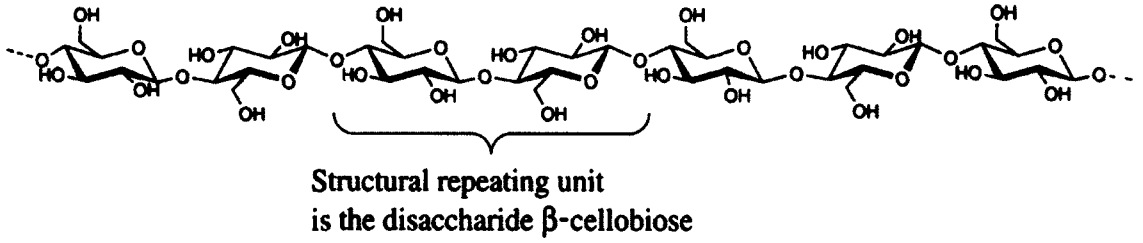

Figure 1-1: The structure of a single cellulose chain. While β-(1→4)-linker D-glucose is the chemical repeating unit, the structure repeat is cellobiose and each glucoside is orientated at 180° [10].

The single cellulose chains (also called glucose chains) are bound to each other by Van der Waals forces and hydrogen bonds to form crystalline structures in the cellulose. There are seven crystal structures for cellulose, including I_α, I_β, II, III_I, III_{II}, IV_I, and IV_{II} [12]. In nature, the most abundant crystal forms of cellulose are I_α and I_β. **Figure 1-2** shows the structure of crystalline cellulose (conformation I_α).

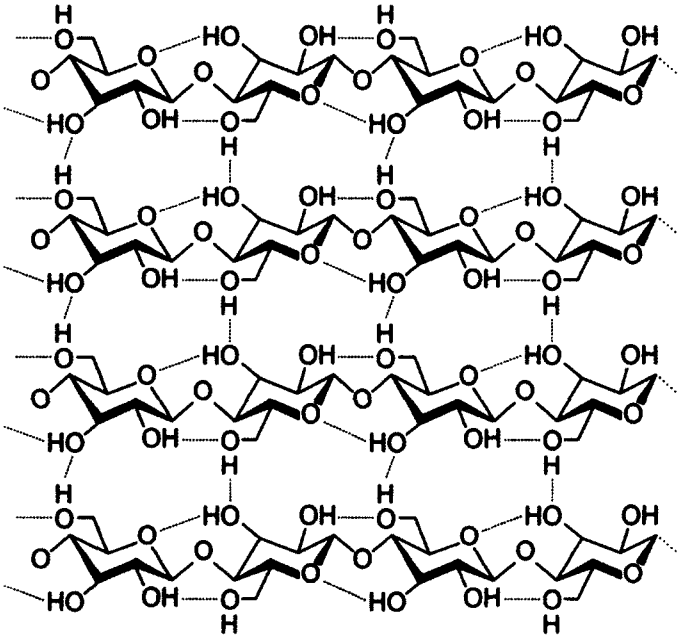

Figure 1-2: The structure of a crystalline cellulose (conformation I_α) [13].

1.4.2 Carboxymethyl Cellulose Sodium Salt

Carboxymethyl Cellulose (CMC) is a cellulose derivative which is soluble in water [14]. The hydroxyl groups of the glucopyranose monomer units in cellulose are substituted by carboxymethyl groups in CMC repeating units. **Figure 1-3** shows the structure of CMC sodium salt.

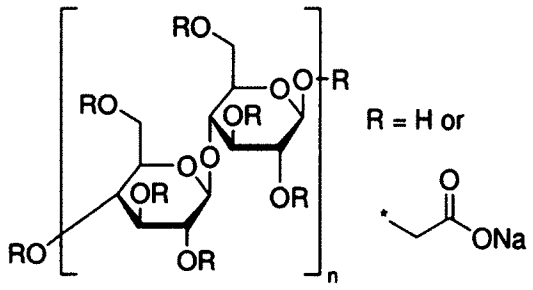

Figure 1-3: The structure of CMC Sodium Salt, in which R is H or CH_2CO_2Na [15].

1.5 Cellulase and Hydrolysis of Cellulose

Cellulases refer to a class of enzymes which can catalyze the hydrolysis of cellulose to glucose. In general, cellulases have been classified into three distinct classes based on their types of catalyzed reaction: cellobiohydrolases (CBH) which are also called exo-1,4-β-D-glucanases (EC 3.2.1.91), endo-1,4-β-D-glucanases (EG) (EC 3.2.1.4), and β-glucosidases (BG) (EC 3.2.1.21). Endoglucanases have an affinity to the interior of the cellulose chain, while exoglucanases have an affinity towards the cellulose chain's ends. β-glucosidases work with CBH and EG to hydrolyze the cleaved units into individual monosaccharides, i.e. glucose. However, these three classes of cellulase often have overlapping specificities [16].

Endo-glucanases are responsible for decreasing the degree of polymerization of the cellulose by randomly cutting the internal amorphous sites of the cellulose chain

(such as bent, flexible and hydrated disordered regions in the cellulose chain) to form oligosaccharides at different lengths [17]. The products can easily react with cellobiohydrolases in the later hydrolysis steps [18]. **Figure 1-4** shows the structure of endoglucanase from termite Nasutitermes takasagoensis [19]. **Figure 1-5** shows the computer animation of endoglucanase on the surface of the cellulose chain [Picture from National Renewable Energy Laboratories (NREL) and Pixel Kitchen].

Figure 1-4: The structure of endoglucanase from termite Nasutitermes takasagoensis [19].

Figure 1-5: Computer animation of endoglucanase on the surface of the cellulose chain [Picture from National Renewable Energy Laboratories (NREL) and Pixel Kitchen].

Exo-glucanases cut the ends of the cellulose chains to produce cellobiose [16, 20, 21]. A small amount of glucose and cellotriose are also procduced at the beginning of hydrolysis [22]. There are two exo-glucanases, CBH I and CBH II, which react with reducing and non-reducing ends of cellulose chain, respectively [17, 23, 24]. All exoglucanases (CBH I, CBH II) can react with microcrystalline cellulose [25]. **Figure 1-6** shows the three dimensional structure of cellobiohydrolase (CBH I) (Cel7A). **Figure 1-7** shows the computer animation of cellobiohydrolase on the cellulose surface [Picture from National Renewable Energy Laboratories (NREL) and Pixel Kitchen].

Figure 1-6: Structure of cellobiohydrolase CBH I (Cel7A) catalytic domain from T. reesei [26].

Figure 1-7: Computer animation of cellobiohydrolase on the cellulose surface [Picture from National Renewable Energy Laboratories (NREL) and Pixel Kitchen].

β-glucosidases react with cellobiose (the hydrolysis products of endo-glucanases and exo-glucanases catalyzed reactions) to produce glucose [27, 28]. The reaction is performed in the liquid phase. **Figure 1-8** shows the structure of β-glucosidase from fungus Trichoderma reesei (TrBgl2) [29].

Figure 1-8: The structure of β-glucosidase from fungus Trichoderma reesei (TrBgl2) [29].

1.6 Choice of Immobilization Carriers

Selection of immobilization carriers plays an important role in enzyme immobilization. Ideal support properties include chemical stability, physical strength, non-toxicity, biological compatibility, resistance to microbial attack, and cost-effectiveness [30-32]. According to the chemical composition, immobilization carriers can be classified as inorganic and organic carriers. The organic carriers can be subdivided into natural and synthetic materials [33].

Researchers have paid attention to cellulose and its derivatives, dextran, chitin, chitosan, and other natural organic carriers because of their wide range of sources, non-toxicity, biological compatibility, and easy modification. Chitosan is a typical natural

organic carrier, which can provide some advantages, such as inert, hydrophilic, biocompatible, and cost-effectiveness [34]. Chitosan and its amino acids condensation adducts were reported for the immobilization of cellulase [35]. The retained activities were found to be 63%-85% for chitosan and its adducts [35]. In addition, Rodolfo Darias and Reynaldo Villalonga reported covalent binding of cellulase with chitosan [36]. The specific activity was 39% of the native cellulase [36]. Also, the thermostability and pH stability were reported a significant increase for the cellulase-chitosan complex [36]. Carbon nanotubes have gained much attention for its efficient carrier properties, such as high mechanical strength, electrical, and thermal properties [37, 38]. The functionalized multiwall carbon nanotubes were used for the immobilization of cellulase [39]. The enzyme loading of the immobilized cellulase reached approximately 97% under the optimal conditions, and 52% retained activity was observed after the six cycles [39].

As important carriers, synthetic organic materials exhibit some advantages, such as good mechanical rigidity, easy modification, and large surface area. Therefore, they have been widely studied and applied for enzyme immobilization. Lei and Jiang synthesized the macroporous polyacrylamide (PAM) microspheres for the immobilization of pectinase [40]. The enzyme loading was reported up to be 296 mg of enzyme per gram of the supports [40]. Also, the thermal stability and storage stability was improved after immobilization [40]. Polystyrene (PST) microspheres were used as immobilization carriers by Li *et al.* to immobilize lipase, and they found that the pore size of the PST microspheres played a critical role in the properties (specific activity, thermal stability and storage stability) of the immobilized enzyme [41].

When it comes to the inorganic carriers, much attention has been paid to nano-particles, which can provide large surface areas. Immobilization carriers with large surface areas always provide great help in obtaining good immobilization efficiency. Recently, researchers have paid much attention to Fe_3O_4 magnetic nanoparticle for immobilization of cellulase, due to its easy separation from the hydrolysis solution when applying magnetic field [42-46]. Unfortunately, the preferred pH condition for the hydrolysis of cellulose is slightly acidic (pH 5) dissolving the Fe_3O_4 back to Fe^{2+} and Fe^{3+}. Also, the aggregation of Fe_3O_4 magnetic nanoparticle was commonly found in the research, which decreases the mass transfer rate in the solution [43, 46]. Many other inorganic carriers were used for the immobilization of cellulase, such as nano-silver and gold particle [47], silicate clay minerals [48], and modified activated carbon [49]. Silica gel has been widely used in the immobilization of enzymes [50-57]. Its advantages of low cost, chemical stability in acid environment, good dispersion in the solution and large surface area make it more favorable for the immobilization of cellulase.

The physical properties of the immobilization carriers (such as particle size, mechanical strength, density) are of critical importance for the performance of the immobilized enzyme. Density of the carriers determines the dispersion of the immobilized enzyme in the substrate's solution. For porous materials, the total surface area which significantly affects the loading of enzyme is determined by pore parameters and particle size. By contrast, for non-porous materials, there will be few mass diffusional limitations but low enzyme loading. **Table 1-1** shows the classification of immobilization carriers.

Table 1-1: Classification of immobilization carriers.

Classification of carriers	Name of carriers	Density
Natural organic	Chitosan	0.3-0.45 g/cm^3
	Cellulose	1.5 g/cm^3
	Carbon nanotube	1.3-1.4 g/cm^3
Synthetic organic	Polystyrene	1.05 g/cm^3
	Polyacrylamide	1.11 g/cm^3
Inorganic	Silica	2.2 g/cm^3 (amorphous)
	Silica gel	0.7 g/cm^3
	Glass	2.5 g/cm^3
	Iron oxides	5.24 g/cm^3

1.7 Immobilization Techniques

The immobilization methods and immobilized carriers are two important factors that significantly influence the properties of biocatalysts. The immobilization methods can be classified into physical adsorption and covalent binding [58].

1.7.1 Physical Adsorption

Physical adsorption is one of the earliest immobilization methods reported in the literature. It can be further categorized into adsorption (by electrical binding, hydrogen binding, and hydrophobic adsorption), and entrapment (inside polymer matrix) (**Figure 1-9**) [59]. It is still widely used due to its simple and economical process, and initial reported enzymatic activity [43]. Wenjuan Zhang *et al.* demonstrated that cellulase immobilized on modified Fe_3O_4 magnetic nanosphere by electrostatic binding can retain 87% native activity for the first use [43]. N.M. Mubarak *et al.* reported that the specific activity of the immobilized cellulase on functionalized multiwall carbon nanotubes by hydrogen binding was even higher than that of free cellulase [39].This high retention of immobilized cellulase is reportedly due to the weak interaction between carriers and

cellulase molecules, which minimize the change of conformational structure and the active center of cellulase molecules [59]. However, this weak interaction also causes enzyme desorption, and poor reusability of immobilized cellulase is a major disadvantage of physical adsorption [59].

Abhijeet Mishra *et al.* reported that, with 30 min incubation in CMC for each cycle, the immobilized cellulase on nano-silver and gold can be reused six times with 73-78% initial activity retained [47]. The retained activities of the immobilized cellulase on functionalized multiwall carbon nanotubes by N.M. Mubarak *et al.* were 52% for the 6^{th} recycle and 26% for the 8^{th} recycle [39]. The majority of the literature for physical absorption immobilization of enzymes do not report reusability [43, 48, 60-63].

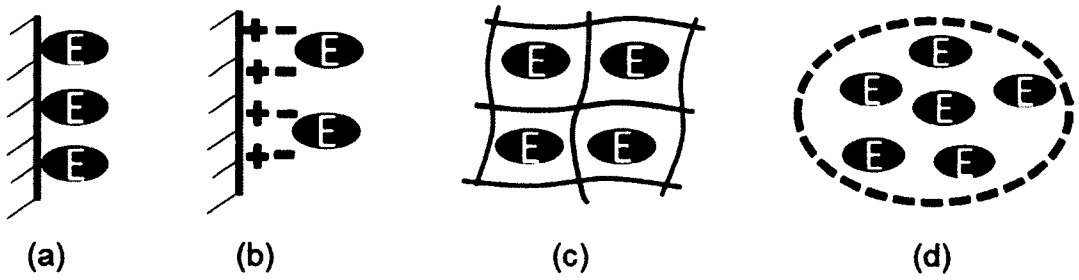

Figure 1-9: Physical binding. (a) Adsorption, (b) Electrical binding, (c) Entrapment, (d) Encapsulation.

1.7.2 Layer-by-Layer Nano-Assembly

Layer-by-Layer Nano-Assembly (LbL) is a very simple and effective way to form the multilayers. It uses electrostatic force as a driving force between layers. LbL was first reported by Iler in 1966 [64], and it was further studied by Decher and Lvov in the 1990s [65, 66]. The fundamental principle of LbL is that the surface charge is reversed by alternating adsorption of oppositely charged polyions. **Figure 1-10** shows the scheme of LbL processes.

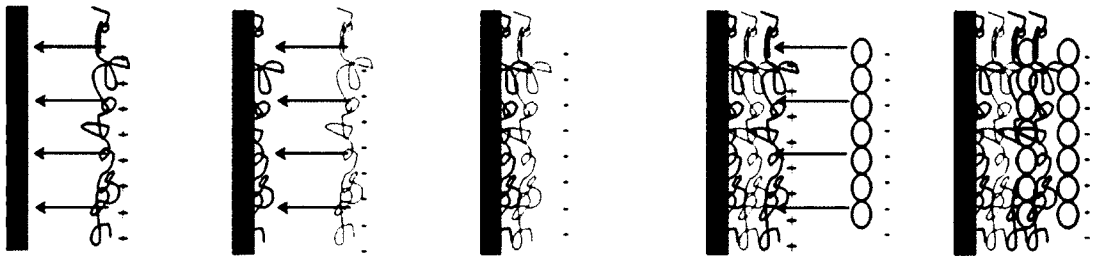

Figure 1-10: The scheme of LbL processes.

The multiple layers can be formed by sequential deposition of oppositely charged molecules. The film's thickness was linearly increased with the number of adsorbed layers, and the films were remarkably uniform [67]. This technique works not only with polyions but also with proteins [68], viruses [69], ceramics [70], and charged nanoparticles [71-77]. **Figure 1-11** illustrates the basic LbL operation procedure.

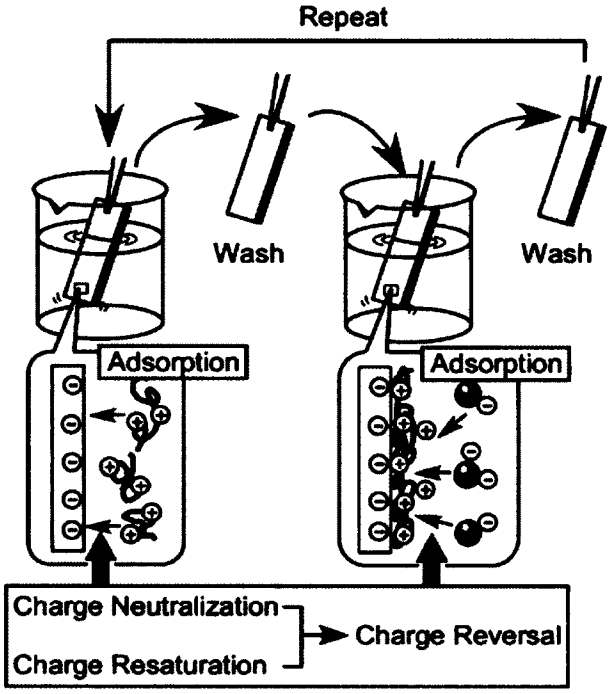

Figure 1-11: The basic operation procedure of LbL [78].

For a weakly charged carrier, the first polyion layer may not cover the whole surface, but forming an island-type pattern [79]. However, the islands will spread and cover the entire surface of the carrier in the following steps. It is the reason that non-linear film growth is often observed at the beginning of the LbL processes, which is followed by linear growth of multiple layers. Because of this phenomenon, three or four precursor layers are needed before coating the target molecules. The precursor layers provide a well-defined surface charged carrier [79].

Many kinds of charged molecules can be adsorbed by using LbL technique such as polyelectrolytes, nanoparticles and proteins (i.e. DNA, enzymes) [80-87]. **Figure 1-12** shows the structural formula of the predominately used polyelectrolytes.

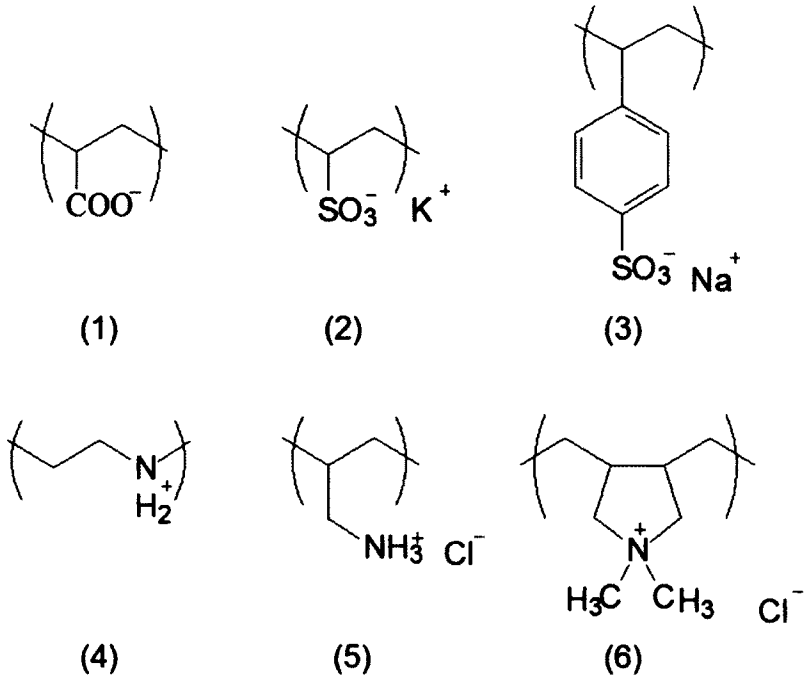

Figure 1-12: Polyion structural formula: (1) PAA, (2) PVS, (3) PSS, (4) PEI, (5) PAH, (6) PDDA.

Frequently used polyions are: 1) Polycations: poly(dimethyl diallyl ammonium chloride) (PDDA), poly(allylamine) (PAH), poly(ethylenimine) (PEI), polylysine, chitosan; 2) Polyanions: poly(styrene sulfonate) (PSS), poly(vinyl sulfate) (PVS), poly(acrylic acid) (PAA), dextran sulfate, and many proteins [79]. The isoelectric point is the pH at which the molecule carries no net electrical charge. The net charge of the molecule can be influenced by the surrounding environment and become positively or negatively charged due to the gain or loss of protons, respectively [79]. In order to make the polyions sufficiently charged, the pH of the polyion solution must be adjusted away from the isoelectric point. **Table 1-2** shows the isoelectric points of the polyions.

Table 1-2: Isoelectric point of some polyelectrolytes and proteins.

	Compound	Isoelectric Point
Polycation	PDDA	12
	PEI	11.5
	PAH	8.2
Polyanion	PAA	4.2
	PSS	1.0
Protein	Urease	5.1
	BSA	4.9
	Cellulase	3.6

1.7.3 Covalent Binding

Covalent binding is the second main method of enzyme immobilization which is used to immobilize enzyme by binding a nonessential group of enzyme to the functional group of carriers via chemical bonds (**Figure 1-13**). The functional groups that can be used for covalent binding includes amino group, carboxyl group, thiol group, etc. [59]. Recently, functionalized Fe_3O_4 nanoparticles modified with chitosan were used as

carriers for the immobilization of cellulase [46]. Compared with the free cellulase, the immobilized cellulase exhibited higher operational stability over wider temperature and pH ranges and good superparamagnetism [46]. Qi *et al.* synthesized magnetic porous terpolymers which contained epoxy groups and used them to immobilize cellulase by forming covalent bonds between epoxy groups and cellulase [45]. Reusability was observed up to six recycles with 48% initial activity retained [45].

In some research, crosslinkers such as glutaraldehyde were used to form covalent bond in the presence/absence of solid support [59]. Besides forming covalent bonds, the crosslinker is also a spacer arm which can be used to avoid the steric hindrance and increase the specific activity [88, 89]. Li *et al.* investigated the immobilization of liposome-bound cellulase for the hydrolysis of insoluble cellulose [90]. The liposome-bound cellulase by glutaraldehyde was immobilized on chitosan beads [90]. The specific activity was 17% compared with the same amount of free cellulase, which was 10 times higher than that of the conventionally immobilized cellulase, and 80% initial activity retained after six recycles for the hydrolysis of CMC [90].

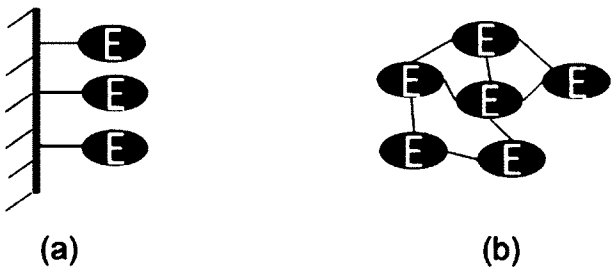

Figure 1-13: Covalent binding. (a) Covalent binding to carrier's surface, (b) Intermolecular crosslinking.

The main concern of this method is a major loss of immobilized enzyme activity due to the stable nature of the covalent bonds between the carriers and the cellulase

molecules. The decrease in activity is likely due to changes in the conformational structure of cellulase molecules and decrease in the degree of movement of the cellulase molecules [59]. The typical specific activity of immobilized cellulase by covalent binding is below 52% [44, 90, 91]. However, the stable covalent binding also leads to very high reusability of immobilized cellulase [44-46, 91]. This major advantage makes covalent binding more promising in industrial application.

CHAPTER 2

MATERIALS AND METHODS

2.1 Free Cellulase Assay

2.1.1 Chemicals

Cellulase (Accellerase 1500, Genencor Division) was purchased from Danisco US, Inc. Cellulase (Novozyme 188), cellulase (Cellulase from Trichoderma viride, 9 units/mg solid), cellulose (Sigmacell Cellulose, Type 20), carboxymethylcellulose sodium salt (CMC), sodium acetate trihydrate (ACS reagent), acetic acid ($\geq$ 99.7%), and sodium hydroxide (ACS reagent, $\geq$ 97.0%) were purchased from Sigma.

Figure 2-1 and **Figure 2-2** show the experiment setups for the hydrolysis of cellulose.

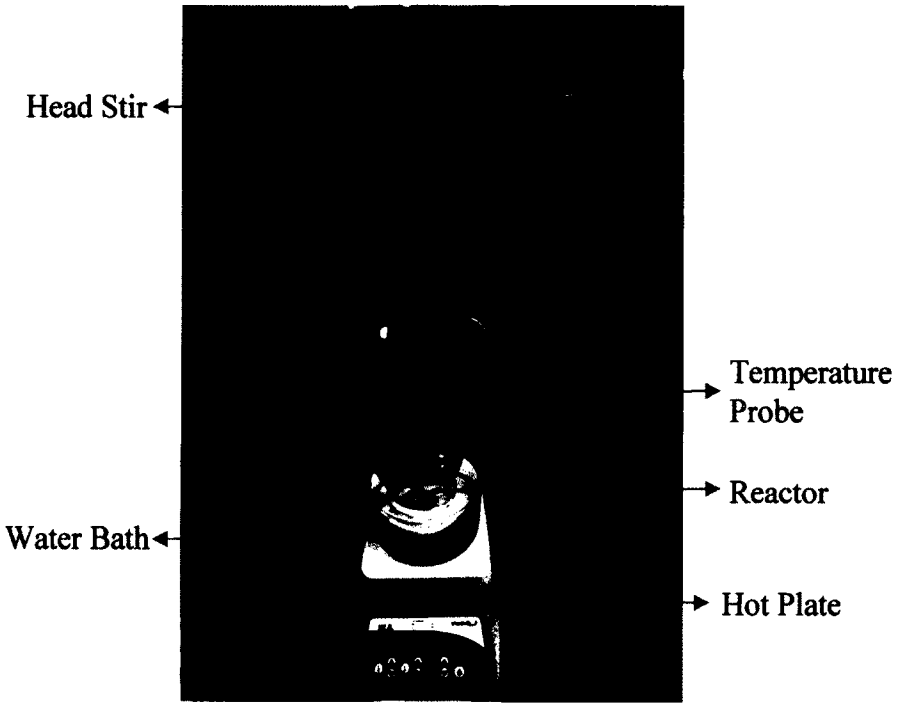

Figure 2-1: The 500 ml scale batch reactor.

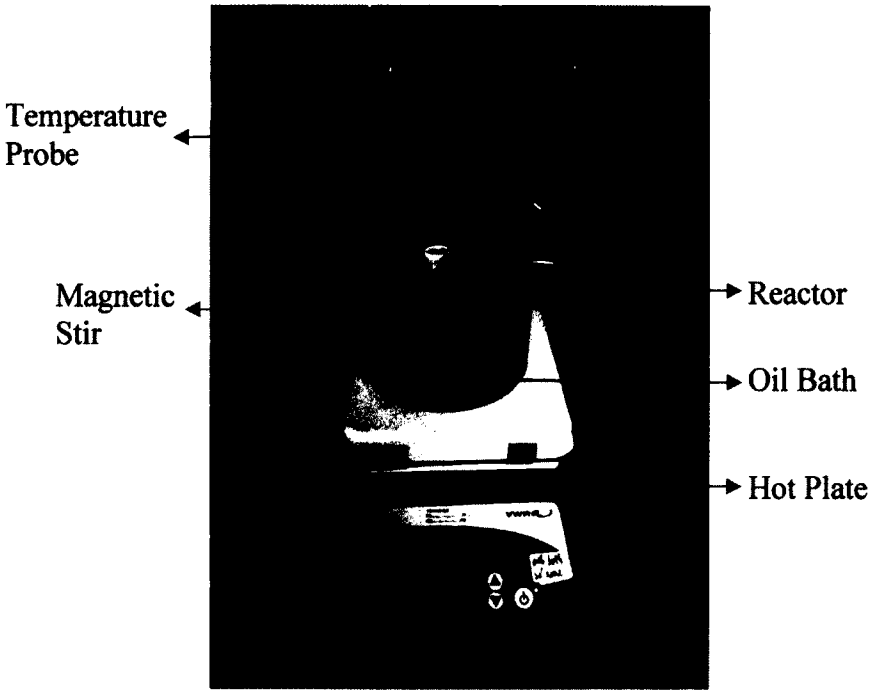

Figure 2-2: The 20 ml scale batch reactor.

2.1.2 Experimental Procedure

Free cellulase (either Novozyme 188, Accellerase 1500, or Trichoderma viride) was added to the cellulose solution (either cellulose type 20 or CMC). Hydrolysis reaction took place in either the 20 ml or 500 ml scale batch reactor (**Figure 2-1**, **Figure 2-2**). Samples were taken after a certain period of time and tested by the glucose assay.

2.1.3 Glucose Assay

Glucose analysis of the samples was tested by YSI 7100 MBS (Multiparameter Bioanalytical System from YSI Life Sciences) (**Figure 2-3**).

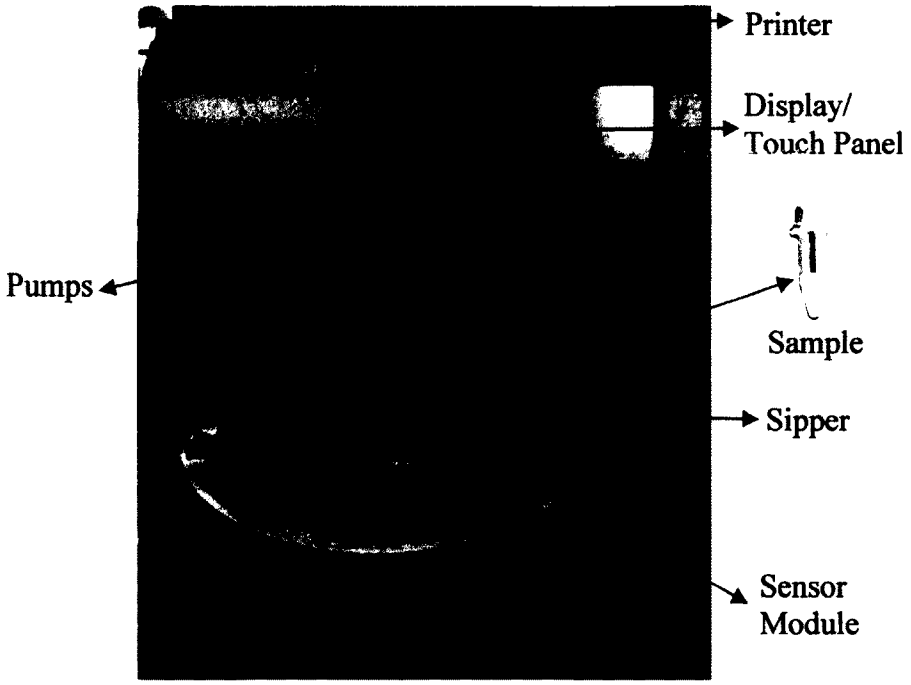

Figure 2-3: YSI 7100 MBS (Multiparameter Bioanalytical System).

2.1.3.1 *Chemicals for YSI 7100 MBS*

System buffer (YSI 2357), calibrator standard (YSI 7147 (1.8 g/L glucose)), membrane (YSI 2365 (Glucose Membrane)).

2.1.3.2 *Analysis procedure*

Sample was taken by the sipper. The sipper can be raised or lowered by one motor, and moved horizontally to its various positions (sample's position/sensor module's position) by another motor. The released sample by the sipper entered the sensor module and is stirred and diluted. The glucose in the sample diffused through a thin polycarbonate membrane which was coupled with an electrochemical probe and housed in a sensor module where sample delivery and flushing occurred. Once past the membrane, the glucose encountered an extremely thin layer of glucose oxidase which was immobilized on the membrane. There is where the following reaction occurs:

$$Glucose + O_2 \xrightarrow{glucose\ oxidase} H_2O_2 + DGluconoδLactone. \qquad \textbf{Eq. 2-1}$$

Hydrogen peroxide diffused toward the platinum anode in the probe assembly, and was electrochemically oxidized at the platinum anode of an electrochemical probe. This gave rise to the probe signal current, which was detected and compared with the calibrated current (1.80 g/L glucose calibrator standard was used for calibration). The sample size was 50 µL. This gave the glucose concentration in the sample. The precision was 0.02 g/L.

2.2 Layer-by-Layer Nano-Assembly Technology

2.2.1 Chemicals

Cellulase (Accellerase 1500, Genencor Division) was purchased from Danisco US, Inc. Cellulose (Sigmacell Cellulose, Type 20), carboxymethylcellulose sodium salt (CMC), Polyethylenimine (PEI, high molecular weight, MW 25,000, water free), poly (sodium 4-styrene-sulfonate) (PSS, MW 70,000), sodium acetate trihydrate (ACS

reagent), N-Hydroxysuccinimide (NHS, 98%), acetic acid (≥ 99.7%) were purchased from Sigma. 1-Ethyl-3-(3-dimethylaminopropyl) carbodiimide (EDC) was purchased from Thermo Scientific. Polystyrene beads were purchased from Crosman Airsoft.

2.2.2 QCM

Quartz Crystal Microbalance (QCM) was used to monitor the thickness of the coating films. PEI was prepared at a concentration of 2 mg/ml in 0.05 M acetate buffer at pH 7. PSS was prepared at a concentration of 2 mg/ml in DI water at pH 6. Cellulase was centrifuged at 10,000 rpm for 5 min and the suspension was diluted 10 times in 0.02 M acetate buffer at pH 5.7.

2.2.2.1 *Equipment*

QCM 200 Quartz Crystal Microbalance was purchased from Stanford Research Systems, Inc.

2.2.2.2 *Experimental procedure*

- Coating PEI: the QCM crystal oscillator was immersed into the PEI solution for 10 min.
- Washing and drying steps: the crystal oscillator was washed by DI water. Then it was dried by compressed air.
- Coating PSS: the QCM crystal oscillator was immersed into the PSS solution for 10 min.
- Washing and drying steps: the crystal oscillator was washed by DI water. Then it was dried by compressed air.

Then a complete PEI/PSS bilayer was formed. After 3-bilayer precursor layers, the cellulase solution was utilized instead of the PSS solution.

- Coating PEI: the QCM crystal oscillator was immersed into the PEI solution for 10 min.
- Washing and drying steps: the crystal oscillator was washed by DI water. Then it was dried by compressed air.
- Coating cellulase: the QCM crystal oscillator was immersed into the cellulase solution for 30 min.
- Washing and drying steps: the crystal oscillator was washed by DI water. Then it was dried by compressed air.

The process was repeated until the number of desired layer was achieved.

2.2.3 Immobilization on Polystyrene Beads

Immobilization carrier: polystyrene beads (**Figure 2-4**).

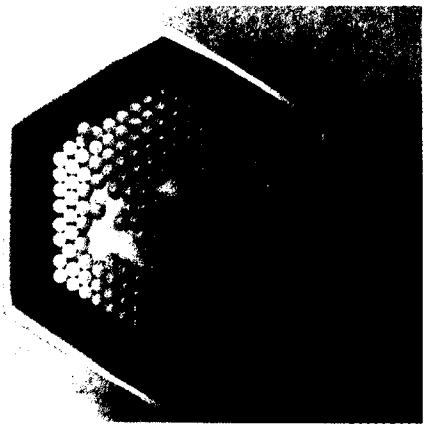

Figure 2-4: Polystyrene beads.

PEI was prepared at a concentration of 2 mg/ml in 0.05 M acetate buffer at pH 7. PSS was prepared at a concentration of 2 mg/ml in 0.05 M acetate buffer at pH 6.

Cellulase was centrifuged at 10,000 rpm for 5 min and the suspension was diluted 10 times in 0.02 M acetate buffer at pH 6.

2.2.3.1 *Experimental procedure*

- Pretreatment of the polystyrene beads: 6 mm diameter polystyrene beads were boiled in 5 g/L NaOH solution for 3 hours to increase the surface roughness. The pretreated beads were washed by DI water after boiling and dried by compressed air.
- Coating first PEI layer: for the first PEI layer, the pretreated polystyrene beads were immerged into PEI solution for 20 min.
- Washing and drying steps: the polystyrene beads were washed by DI water. Then they were dried by compressed air.
- Coating PSS layer: the polystyrene beads were immersed into the PSS solution for 10 min.
- Washing and drying steps: the polystyrene beads were washed by DI water. Then they were dried by compressed air.
- Coating PEI layer: For the rest PEI layer in precursor layers, the polystyrene beads were immersed into PEI solution for 10 min.
- Washing and drying steps: the polystyrene beads were washed by DI water. Then they were dried by compressed air.

After 3-bilayer precursor layers, cellulase solution was used instead of the PSS solution.

- Coating cellulase: the polystyrene beads were immersed into the cellulase solution for 20 min.

- Washing and drying steps: the polystyrene beads were washed by DI water. Then they were dried by compressed air.
- Coating PEI layer: the polystyrene beads were immersed into the PEI solution for 5 min.
- Washing and drying steps: the polystyrene beads were washed by DI water. Then they were dried by compressed air.

The process was repeated until the number of desired layers was achieved.

2.2.3.2 *Crosslinking of the immobilized polystyrene beads by LbL*

A mixture of 0.2 mM EDC and 0.5 mM NHS which was made in DI water was used to crosslink the immobilized cellulase after LbL coating. After immobilization of cellulase by LbL, the coated beads were immerged into the crosslinker for a certain of time. Then the coated beads were washed by DI water and dried by compressed air.

2.2.4 Hydrolysis of Cellulose by the Immobilized Polystyrene Beads

We prepared 10 g/L cellulose solution (cellulose type 20/CMC) in 0.05 M acetate buffer. The hydrolysis reaction was operated at 25°C in a certain pH environment. There were two volumes of cellulose solution, i.e. 100 ml and 250 ml. The hydrolysis of 100 ml and 250 ml cellulose solution was operated in a 100 ml batch reactor (**Figure 2-5**) and a 500 ml batch reactor (**Figure 2-1**), respectively. The masses of the immobilized polystyrene beads for hydrolysis of 100 ml and 250 ml cellulose solution were 27.4 g and 68.6 g, respectively. Samples were taken according to time and tested by the glucose analysis as described in Section 2.1.3. The first order rate (the linear slope of the

time-dependent curve) was applied to represent the enzymatic activity of the immobilized cellulase as described in **Eq. 2-2**.

$$\text{The first order rate} = \frac{\text{The produced glucose concentration } (\frac{mg}{ml})}{\text{Hydrolysis time (min)}}. \quad \textbf{Eq. 2-2}$$

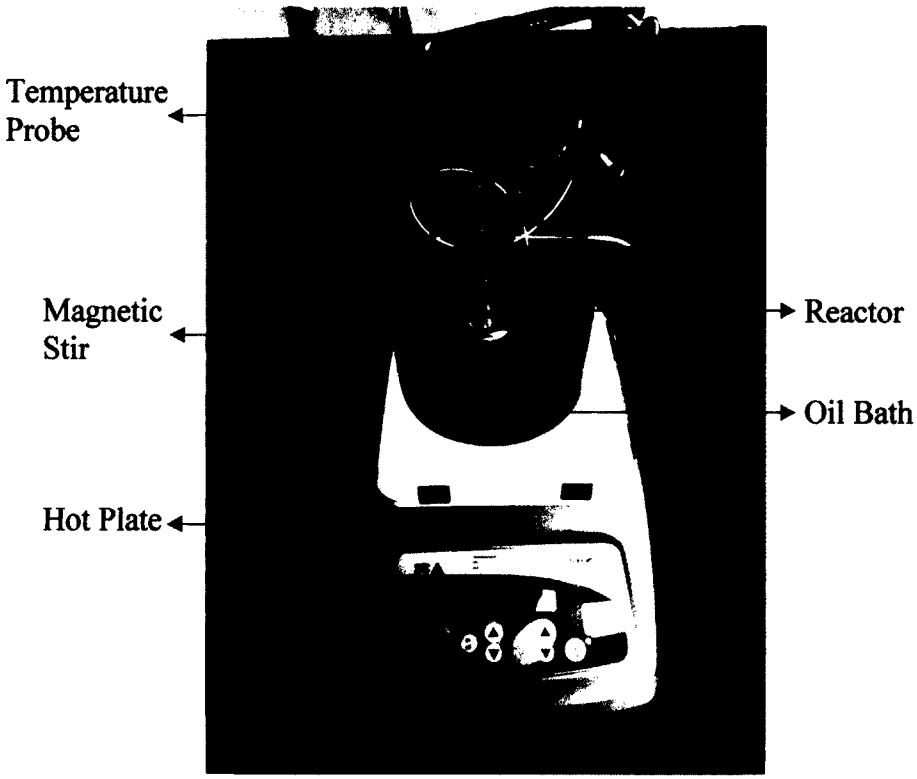

Figure 2-5: The 100 ml scale batch reactor.

2.2.5 Reusability of the Immobilized Cellulase

Reusability of the immobilized cellulase was studied by recycling the immobilized cellulase in a fresh cellulose solution under the same hydrolysis conditions as the first cycle. After each cycle, the immobilized cellulase was removed from the cellulose solution and washed by DI water. The first cycle was recognized as the control group, and its activity was defined as a relative activity of 100%.

2.3 Ca^{2+}-$Al(OH)_x$ Modification

2.3.1 Chemicals

Cellulase (Accellerase 1500, Genencor Division) was purchased from Danisco US, Inc. Cellulose (Sigmacell Cellulose, Type 20), carboxymethylcellulose sodium salt (CMC), sodium acetate trihydrate (ACS reagent), acetic acid (≥ 99.7%), sodium hydroxide (ACS reagent, ≥ 97.0%), Calcium chloride (anhydrous, ≥ 97%), Aluminum chloride hexahydrate (ReagentPlus, 99%), and molecular sieves (13X, 3.2 mm pellets) (**Figure 2-6**) were purchased from Sigma.

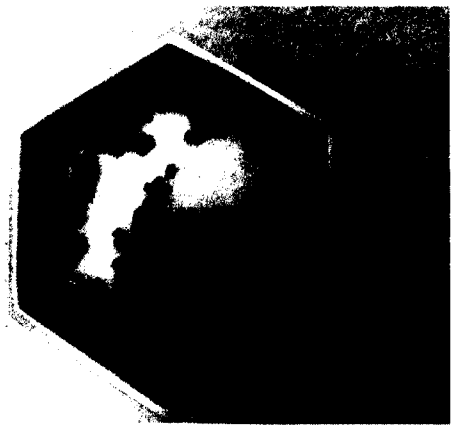

Figure 2-6: Molecular sieves (13X, 3.2 mm pellets).

One mol/L $AlCl_3$ solution and 0.5 mol/L $CaCl_2$ solution were made in DI water, respectively. We made a 0.5 M NaOH solution in DI water. Cellulase (Accellerase 1500) was diluted 10 times with DI water.

2.3.2 Experimental Procedure

- Pretreatment of the molecular sieves: the molecular sieves (pellets) were wet by DI water.

- Ca^{2+} homo-ionization: The wet molecular sieves (pellets) were immersed into 50 ml 0.5 mol/L $CaCl_2$ solution for 20 min to make a Ca^{2+} homo-ionized surface. Then washed by DI water several times.
- $Al(OH)_x$ modification: The modified molecular sieves (pellets) were immersed into 20 ml 1 mol/L $AlCl_3$ solution for 20 min. Then the pH of the solution (with molecular sieves in it) was adjusted to seven with 0.5 M NaOH solution. After filtering, the modified molecular sieves (pellets) were washed several times with DI water.
- Immobilization of cellulase: The modified molecular sieves (pellets) were immersed into 20 ml 10-time diluted cellulase solution for one hour. Then the immobilized cellulase was washed several times by DI water to remove the loose cellulase.

2.3.3 Hydrolysis of Cellulose by the Immobilized Molecular Sieves

We prepared a 10 g/L CMC solution in pH = 6 0.05 M acetate buffer. The hydrolysis reaction was operated at 25°C. We used 11.2 g immobilized molecular sieves for hydrolysis of 40 ml CMC solution. The hydrolysis reaction was operated in a 100 ml scale batch reactor (**Figure 2-5**). Samples were taken according to time and tested by the glucose analysis as described in Section 2.1.3. The first order rate (the linear slope of the time-dependent curve) was applied to represent the enzymatic activity of the immobilized cellulase as described in **Eq. 2-2**. The reusability of the immobilized cellulase was studied as described in Section 2.2.5.

2.4 Combination of LbL and Ca^{2+}-$Al(OH)_x$ Modification

2.4.1 Chemicals

Cellulase (Accellerase 1500, Genencor Division) from Danisco US, Inc. Cellulose (Sigmacell Cellulose, Type 20), carboxymethylcellulose sodium salt (CMC), sodium acetate trihydrate (ACS reagent), acetic acid (≥ 99.7%), Polyethylenimine (PEI, high molecular weight, MW 25,000, water free), poly(sodium 4-styrene-sulfonate) (PSS, MW 70,000), glutaraldehyde (GA) solution (grade I, 50%), sodium hydroxide (ACS reagent, ≥ 97.0%), Calcium chloride (anhydrous, ≥ 97%), Aluminum chloride hexahydrate (ReagentPlus, 99%), molecular sieves (13X, 3.2 mm pellets), and molecular sieves (13X, beads, 4-8 mesh) (**Figure 2-7**) were purchased from Sigma.

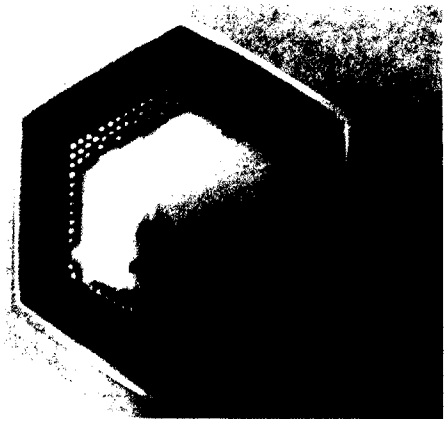

Figure 2-7: Molecular sieves (13X, beads, 4-8 mesh).

One mol/L $AlCl_3$ solution and 0.5 mol/L $CaCl_2$ solution were made in DI water, respectively. We made a 0.5 M NaOH solution in DI water. Cellulase (Accellerase 1500) was diluted 10 times with DI water. Two mg/ml PEI solution was made in DI water. Cellulase solution was diluted 10 times with DI water.

2.4.2 Experimental Procedure

- The molecular sieves (pellets) or molecular sieves (beads) were pretreated by Ca^{2+}-$Al(OH)_x$ modification as described in Section 2.3.2.
- Coating cellulase layer: the pretreated molecular sieves (pellets) or molecular sieves (beads) were immersed into the cellulase solution for one hour.
- Washing step: then the immobilized molecular sieves (pellets) or molecular sieves (beads) were washed by DI water five times.
- Coating PEI layer: the immobilized molecular sieves (pellets) or molecular sieves (beads) were immersed into PEI solution for 10 min.
- Washing step: then the immobilized molecular sieves (pellets) or molecular sieves (beads) were washed by DI water five times.

The coating processes were applied until the desired cellulase/PEI bilayers were achieved.

2.4.3 Hydrolysis of Cellulose by the Immobilized Molecular Sieves by Combination of LbL and Ca^{2+}-$Al(OH)_x$ Modification

Ten g/L CMC solution was prepared in pH = 6 0.05 M acetate buffer. The hydrolysis reaction was operated at 25°C. We used 11.2 g immobilized molecular sieves for hydrolysis of 40 ml CMC solution. The hydrolysis reaction was operated in a 100 ml scale batch reactor (**Figure 2-5**) and the packed bed reactor setup for hydrolysis of cellulose solution by the immobilized molecular sieves (**Figure 2-8**), respectively. The flow rate of the packed bed reactor was 100 ml/min. Samples were taken according to time and tested by the glucose analysis as described in Section 2.1.3. The first order rate (the linear slope of the time-dependent curve) was applied to represent the enzymatic

activity of the immobilized cellulase as described in **Eq. 2-2**. The reusability of the immobilized cellulase was studied as described in Section 2.2.5.

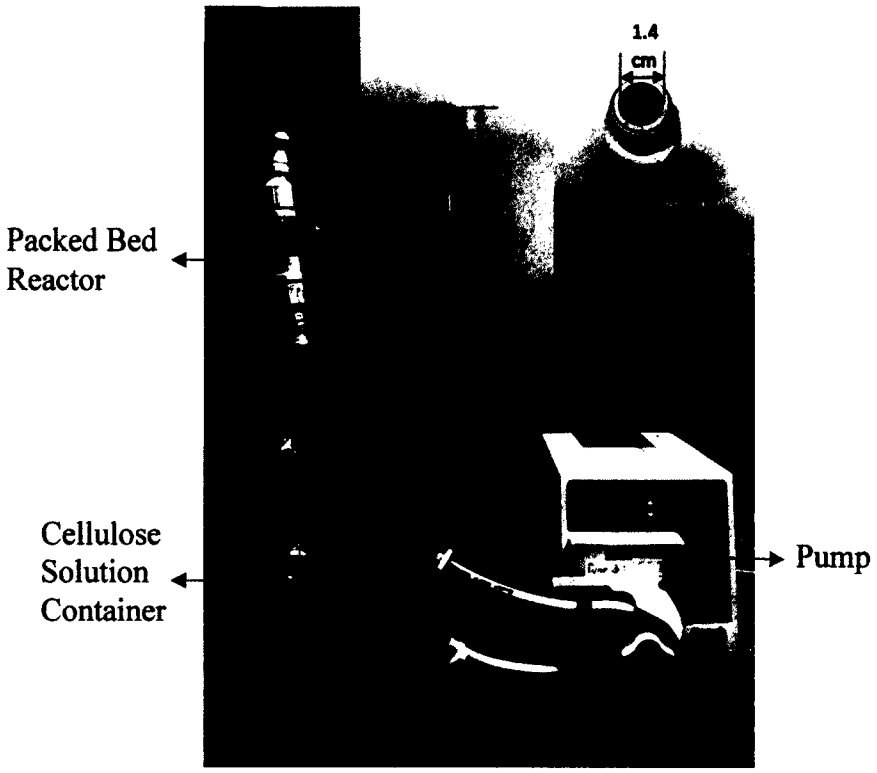

Figure 2-8: Packed bed reactor setup for hydrolysis of cellulose solution by immobilized molecular sieves.

Norprene tube (06402-17) (**Figure 2-9**) was purchased from Masterflex.

- Masterflex tubing size (L/S): 17 (6.4 mm inside diameter).
- Hose barb size: 6.4 mm.

Norprene tube (06404-14) (**Figure 2-9**) was purchased from Masterflex.

- Masterflex tubing size (L/S): 14 (1.6 mm inside diameter).
- Hose barb size: 1.6 mm.

Nylon tube (1025L06 01) (**Figure 2-9**) was purchased from Legris.

- Inside diameter: 4 mm.
- Outside diameter: 6 mm.

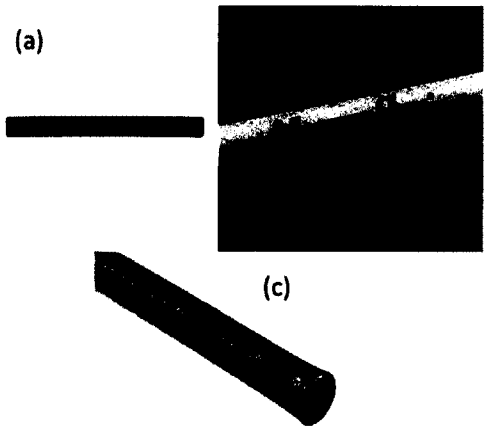

Figure 2-9: (a) Norprene tube (06404-14), (b) Norprene tube (06402-17), (c) Nylon tube (1025L06 01).

2.5 3-APTES Self-assembly Monolayer

2.5.1 Chemicals

Cellulase (Accellerase 1500, Genencor Division) was purchased from Danisco US, Inc. Silica-Amorphous (precipitated, pore size 150 Å), (3-Aminopropyl) triethoxy-silane (3-APTES,99%), toluene (anhydrous, 99.8%), glutaraldehyde (GA) solution (grade I, 50%), carboxymethylcellulose sodium salt (CMC), sodium acetate trihydrate (ACS reagent), cellulose (Sigmacell Cellulose, Type 20), solid-glass beads (3 mm diameter), and molecular sieves (13X, beads, 4-8 mesh) were purchased from Sigma.

2.5.2 Immobilization on Molecular Sieves (Beads)

Ten percent v/v 3-APTES was prepared in toluene, and 2% v/v glutaraldehyde solution was prepared in pH = 6 acetate buffer (50 mmol L^{-1}). Cellulase (Accellerase 1500) was diluted 10 times with DI water, and 11.2 g molecular sieves (beads) were used for one batch.

2.5.2.1 *Experimental procedure*

- 3-APTES modification: molecular sieves (beads) were immersed into 10% v/v 3-APTES solution for 10 min. Then the pretreated molecular sieves (beads) were washed by toluene five times to remove the residues.
- Glutaraldehyde crosslinking: the pretreated molecular sieves (beads) were immersed into 2% v/v glutaraldehyde solution for 5 min. Then the molecular sieves (beads) were washed by DI water five times.
- Cellulase immobilization: the pretreated molecular sieves (beads) were immersed into 10-time diluted cellulase solution for 24 hours. Then the molecular sieves (beads) were washed by DI water several times to remove the cellulase residue.

2.5.3 Immobilization on Glass Beads

Ten percent v/v 3-APTES was prepared in toluene, and 2% v/v glutaraldehyde solution was prepared in pH = 6 acetate buffer (50 mmol L^{-1}). Cellulase (Accellerase 1500) was diluted five times with DI water. The glass beads were washed by DI water and dried by compressed air. Two hundred and forty-seven glass beads (**Figure 2-10**) were used as immobilization carriers for one batch.

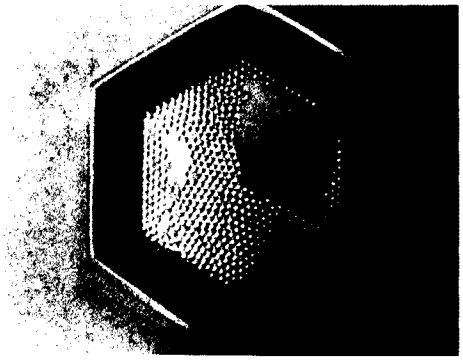

Figure 2-10: Glass beads.

2.5.3.1 *Experimental procedure*

- 3-APTES modification: glass beads were immersed into 10% v/v 3-APTES solution for 24 hours. Then the pretreated glass beads were washed by toluene five times to remove the residues and dried by compressed air.
- Glutaraldehyde crosslinking: the pretreated glass beads were immersed into 2% v/v glutaraldehyde solution for 30 min. Then the glass beads were washed by DI water five times and dried by compressed air.
- Cellulase immobilization: the pretreated glass beads were immersed into 10-time diluted cellulase solution for 24 hours. Then the glass beads were washed by DI water several times to remove the cellulase residue and dried by compressed air.

2.5.4 Immobilization on Silica Gel

Ten percent v/v 3-APTES was prepared in toluene, and 2% v/v glutaraldehyde solution was prepared in pH = 6 acetate buffer (50 mmol L^{-1}). Cellulase (Accellerase 1500) was diluted five times with DI water (17.5 mg protein/ml), and 0.06 g silica gel was used for one batch.

2.5.4.1 *Experimental procedure*

- 3-APTES modification: 0.06 g silica gel was incubated with 10% v/v 3-APTES prepared in toluene at 30°C for 24 hours in incubator shaker (Innova^{TM} 4000, New Brunswick Scientific) with 300 rpm shaking speed. The modified silica gel was followed by a washing step with 1.2 ml toluene for four-five times to remove the unbound 3-APTES. Then the modified silica gel was cured on a hot plated at 40°C for 24 hours. The modified silica gel is stable for months if sealed [92].

- Glutaraldehyde crosslinking: Glutaraldehyde was used as a crosslinker and a space arm between the 3-APTES layer and the cellulase layer. The 3-APTES modified silica gel was immersed into 2% v/v glutaraldehyde solution which was prepared with pH = 6 acetate buffer (50 mmol L-1) for 30 min at room temperature. After this step, an aldehyde terminated silica gel surface was formed. Then modified silica gel was washed by 1.2 ml DI water four-five times to remove the unbound glutaraldehyde.
- Cellulase immobilization: the modified silica gel was immersed into 1 ml of five-time diluted cellulase with DI water (17.5 mg protein/ml) for 24 hours at room temperature in incubator shaker with 300 rpm shaking speed. After remove the residue immobilization solution, the immobilized silica gel was washed five times with DI water. Only 0.1% of cellulase was detected in the supernate of the fifth wash suggesting that no further washes were required.

The incubator shaker utilized for immobilization of 3-APTES and cellulase was to make the silica gel uniformly distributed in the solution and kept a certain temperature. The cellulase solution after immobilization and the water waste were kept together in a 100 ml volumetric bottle for protein assay in order to determine the amount of immobilized cellulase. **Figure 2-11** shows the mechanism of immobilization with 3-APTES.

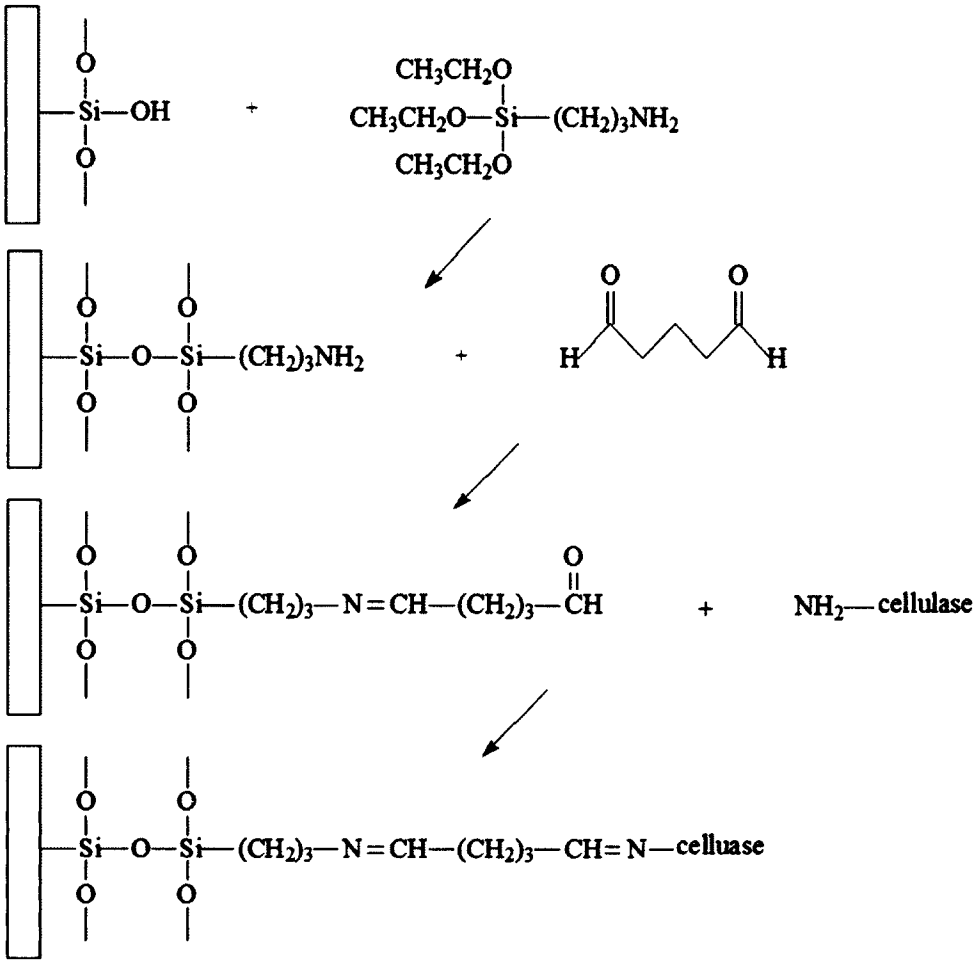

Figure 2-11: Mechanism of immobilization with 3-APTES.

2.5.4.2 *Impact of initial concentration of cellulase solution on the immobilized cellulase*

The activities of the immobilized cellulase from different time-diluted cellulase solutions for immobilization were tested. Silica gel was modified by 3-APTES and crosslinked by glutaraldehyde as described in Section 2.5.4.1. Then the pretreated silica gel was immerged in 20 X, 10 X, 5 X diluted and undiluted cellulase solution, respectively. The protein concentrations of the diluted cellulase solutions for immobilization measured by the flourescamine protein assay were 4.4, 8.8, 17.5, 87.5 mg/ml for 20 X, 10 X, 5 X diluted and undiluted cellulase solution, respectively.

The activity of the immobilized cellulase was determined by the CMC assay as stated in Section 2.5.7.

2.5.4.3 *Impact of temperature on immobilized cellulase*

The effect of temperature on the immobilized cellulase was examined in 10 g/L CMC solution in pH = 6 acetate buffer (50 mmol L^{-1}) by altering the reaction temperature to 20°C, 30°C, 40°C, 50°C, and 60°C. The cellulase was immobilized on the silica gel as described in Section 2.5.4.1. The initial concentration of cellulase solution for immobilization of silica gel was 17.5 mg/ml (five-time diluted). The highest activities of free and immobilized cellulase were considered as the control groups for each series of experiments, respectively, and defined 100% relative activity [45].

2.5.4.4 *Impact of pH on immobilized cellulase*

The effect of pH for hydrolysis of CMC on immobilized cellulase was examined by altering the acetate buffer to pH 4, 5, 6 in the CMC assay in Section 2.5.7. The immobilized cellulase was performed as stated in Section 2.5.4.1.

2.5.5 Hydrolysis of Cellulose by the Immobilized Molecular Sieves (Beads)

Ten g/L CMC solution was prepared in pH=6 0.05 M acetate buffer. The hydrolysis reaction was operated at 25°C. We used 11.2 g immobilized molecular sieves for hydrolysis of 40 ml CMC solution. The hydrolysis reaction was operated in the packed bed reactor setup for hydrolysis of cellulose solution by the immobilized molecular sieves (**Figure 2-8**). The flow rate of the packed bed reactor was 100 ml/min. Samples were taken according to time and tested by the glucose analysis as described in

Section 2.1.3. The first order rate (the linear slope of the time-dependent curve) was applied to represent the enzymatic activity of the immobilized cellulase as described in **Eq. 2-2**. The reusability of the immobilized cellulase was studied as described in Section 2.2.5.

2.5.6 Hydrolysis of Cellulose by the Immobilized Glass Beads

Ten g/L CMC solution was prepared in pH = 6 0.05 M acetate buffer. The hydrolysis reaction was operated at 25°C. Two hundred and forty-seven immobilized glass beads were used for hydrolysis of 10 ml CMC solution. The hydrolysis reaction was operated in the packed bed reactor setup for hydrolysis of the cellulose solution by the immobilized glass beads (**Figure 2-12**). The flow rate of the packed bed reactor was 6 ml/min. Samples were taken according to time and tested by the glucose analysis as described in Section 2.1.3. The first order rate (the linear slope of the time-dependent curve) was applied to represent the enzymatic activity of the immobilized cellulase as described in **Eq. 2-2**. The reusability of the immobilized cellulase was studied as described in Section 2.2.5.

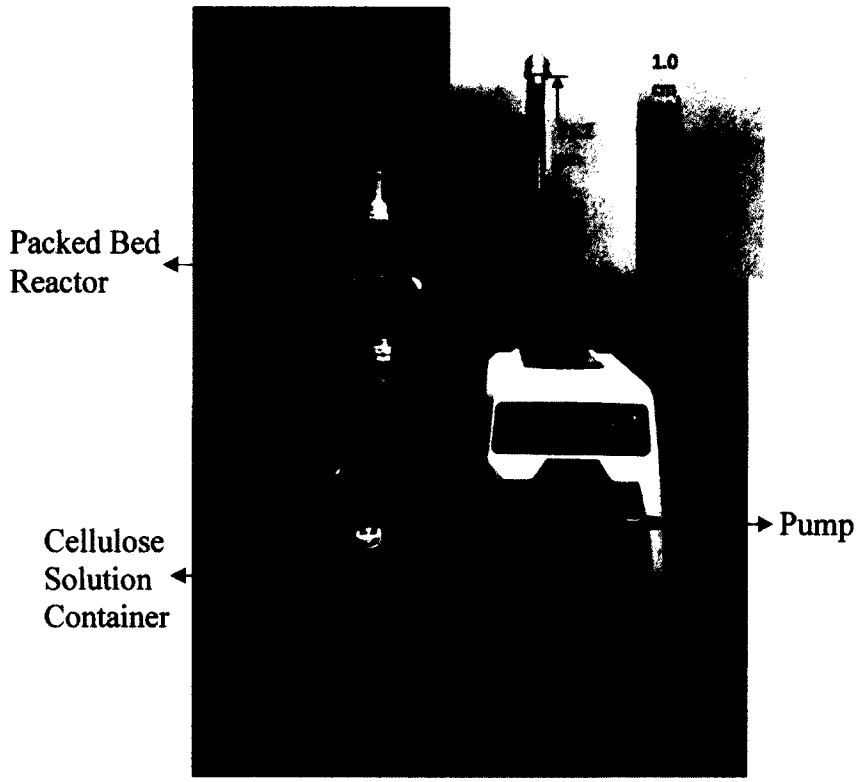

Figure 2-12: Packed bed reactor setup for hydrolysis of cellulose solution by immobilized glass beads.

Norprene tube (06404-14) (**Figure 2-13**) was purchased from Masterflex.

Figure 2-13: Norprene tube (06404-14)

- Masterflex tubing size (L/S): 14 (1.6 mm inside diameter).
- Hose barb size: 1.6 mm.

2.5.7 Hydrolysis of Cellulose by the Immobilized Silica Gel

Activities of the immobilized silica gel were determined by hydrolysis of 10 g/L CMC solution dissolved in pH = 6 acetate buffer (50 mmol L^{-1}). 0.06 g immobilized silica gel was immersed into a 10 ml CMC solution and stirred well in the reactor, which

maintained a temperature of 20°C in bath water. The hydrolysis reaction took place in a 20 ml scale batch reactor (**Figure 2-2**). Samples were taken after 1 hour, 2 hours, and 3 hours, which were centrifuged for 5 min at 10,000 rpm. The supernate was collected, and its glucose concentration was tested by the glucose analysis as described in Section 2.1.3. One unit of cellulase activity was defined as nmol glucose produced per minute. The reusability of the immobilized cellulase was studied as described in Section 2.2.5.

2.6 Protein Assay

2.6.1 Chemicals

Fluorescamine (≥ 98.0%, powder), toluene (anhydrous, 99.8%), and bovine serum albumin (BSA, ≥ 98.0%) were purchased from Sigma.

2.6.2 Equipment

LS 55 Fluorescence Spectrometer was purchased from PerkinElmer (**Figure 2-14**).

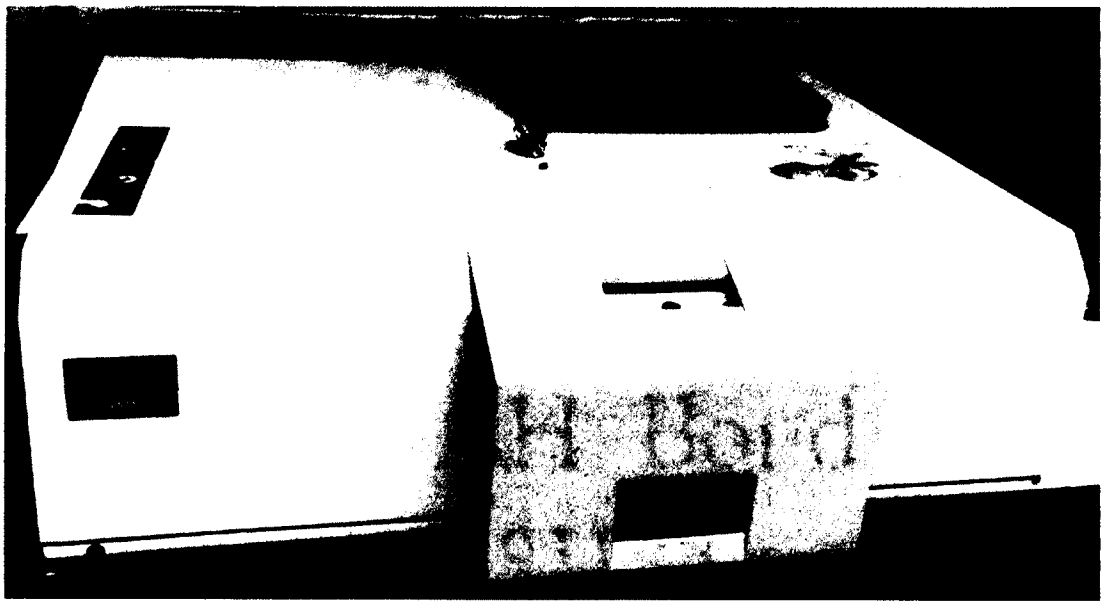

Figure 2-14: LS 55 Fluorescence Spectrometer.

Fluorescamine protein assay was used to determine the amount of immobilized cellulase, in which 5 mg/ml BSA stock was prepared for a standard curve. **Table 2-1** shows the standard curve. One ml of five-time diluted cellulase solution for immobilization was added into a 100 ml volumetric bottle, and diluted with DI water. Three ml of the diluted solution was used for protein assay. The samples were measured using fluorescence spectrometer at excitation wavelength 390 nm and emission wavelength 460 nm. The amount of immobilized cellulase was calculated by

$$Mass\ of\ the\ immobilized\ cellulase = C_i V_i - C_f V_f, \qquad \textbf{Eq. 2-3}$$

where C_i is the initial protein concentration, V_i the initial volume of cellulase solution, C_f the final protein concentration after immobilization, V_f the final volume of cellulase solution after immobilization (water washes included). The maximum percentage error of C_i and C_f ranged from 3% to 4%. The magnitude of the measured difference of enzyme mass before and after the immobilization step was 11% to 14%.

Table 2-1: Standard curve of fluorescamine protein assay.

Protein conc. [mg/ml]	BSA stock [ml]	Water [ml]	Fluorecamine [ml]	Incubation [min]
0	0	3.000	0.05	30
0.025	0.015	2.985	0.05	30
0.050	0.030	2.970	0.05	30
0.100	0.060	2.940	0.05	30
0.200	0.120	2.880	0.05	30
0.300	0.180	2.820	0.05	30

2.7 Scanning Electron Microscopy

Scanning Electron Microscopy (SEM) was applied to monitor the surface topography change before and after immobilization. For immobilized polystyrene beads

by LbL, samples were prepared by non-pretreated polystyrene beads, NaOH boiled polystyrene beads, and the 120-bilayer immobilized polystyrene beads as described in Section 2.2.3.1. The samples were tested by scanning electron microscope Hitachi S-4800.

2.8 Fourier Transform Infrared Spectroscopy

The Fourier Transform Infrared Spectroscopy (FTIR) was used for recording the chemical composition of the samples. The samples were prepared by 100% pure silica, 3-APTES modified silica, 3-APTES modified glutaraldehyde crosslinked silica gel, and cellulase immobilized silica gel as described in Section 2.5.4.1, respectively. The spectra were recorded at room temperature in the 400-4000 cm^{-1} range using Thermo Scientific NICOLET IR100 FT-IR Spectrometer (**Figure 2-15**).

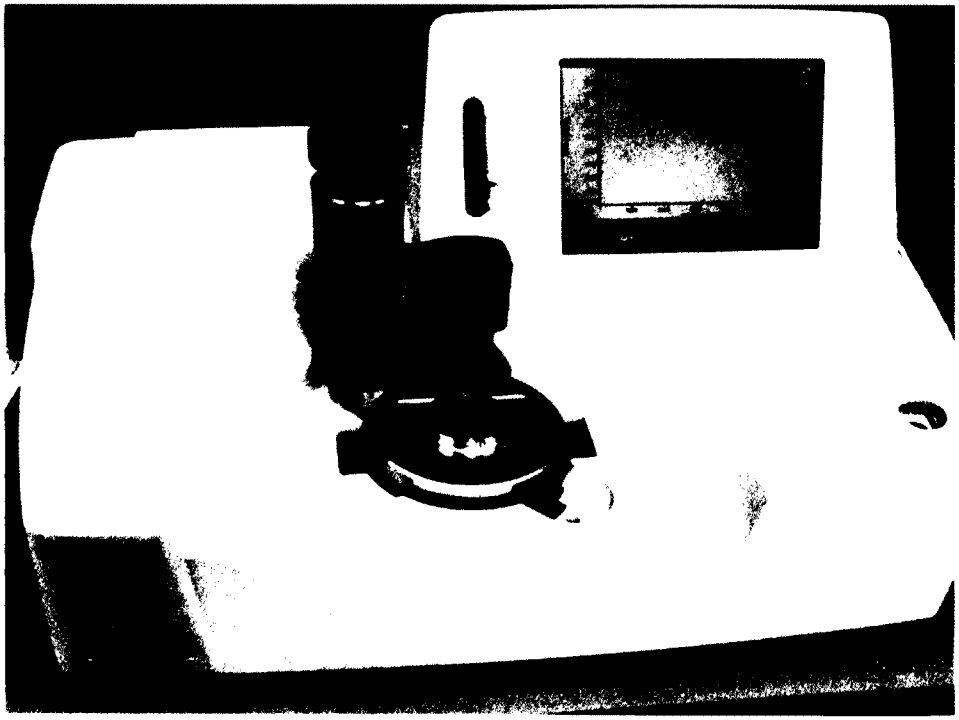

Figure 2-15: Thermo Scientific NICOLET IR100 FT-IR Spectrometer.

2.9 Nitrogen Adsorption/desorption Analysis

The pore size and pore volume were calculated by nitrogen adsorption and desorption utilizing the Barrett-Joyner-Halenda (BJH) method using NOVA 2000 High-Speed Surface Area & Pore Size Analyzer. The surface area was calculated by the Brunauer–Emmett–Teller (BET) method. The samples were prepared by 100% pure silica, 3-APTES modified silica, 3-APTES modified glutaraldehyde crosslinked silica gel as described in Section 2.5.4.1, respectively.

CHAPTER 3

RESULTS AND DISCUSSION

In this chapter, the results of immobilization of the cellulase by different immobilization techniques will be discussed in detail. The activity and reusability of the immobilized cellulase will be the purpose and focus of attention. For each immobilization technique, the key variables of both immobilization steps and hydrolysis of cellulose by the immobilized cellulase were studied.

3.1 Free Cellulase Assay

Three different kinds of cellulases were investigated in order to find the enzyme with the highest activity for immobilization. Free cellulase assay of Novozyme 188, Accellerase 1500 (uncentrifuged) and cellulase (Trichoderma viride) were tested under the same hydrolysis conditions. **Figure 3-1** shows the activities of three different cellulases (Novozyme 188, Accellerase 1500 and Trichoderma viride). The activity of cellulase (Novozyme 188) was much lower than the activities of cellulases (Accellerase 1500 and Trichoderma viride). The activity of cellulase (Trichoderma viride) was the same as the activity of cellulase (Accellerase 1500) until about 260 min. However, after 260 min, the activity of cellulase (Accellerase 1500) increased. The produced glucose yield by cellulase (Accellerase 1500) was larger than the one by cellulase (Trichoderma

viride). Because cellulase (Accellerase 1500) had the highest enzymatic activity and the largest produced glucose yield, it was chosen for immobilization of the following studies.

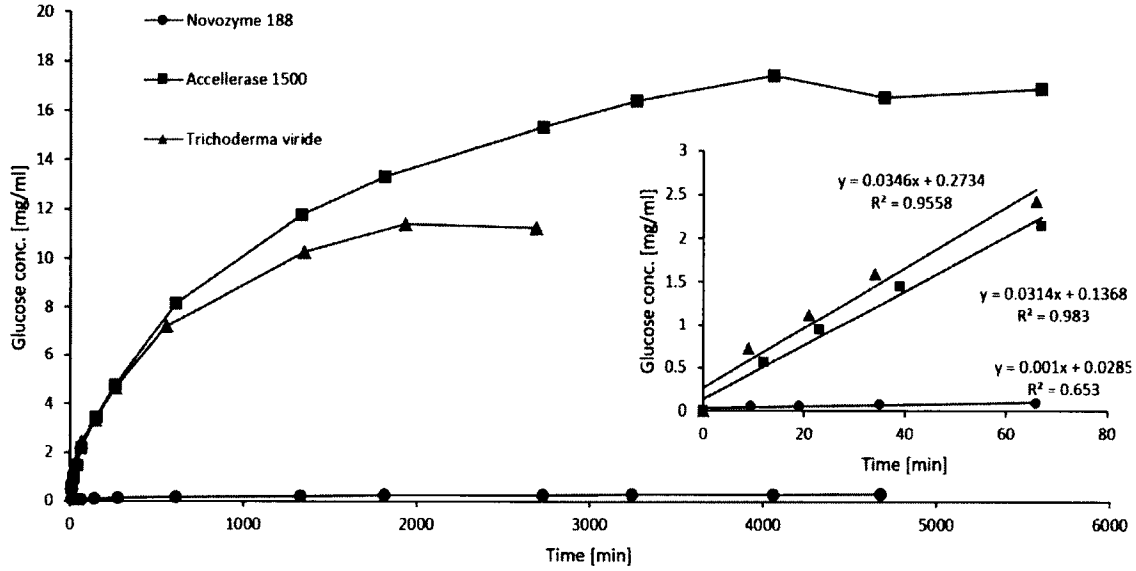

Figure 3-1: Activities of three different free cellulase (Novozyme 188, Accellerase 1500 and Trichoderma viride). Enzyme: Novozyme 188, 2 ml undiluted; Accellerase 1500, 2 ml undiluted (uncentrifuged); cellulase (Trichoderma viride), 500 mg. Cellulose solution: 250 ml cellulose (type 20), 5% (w/v) in pH = 5 0.05 M acetate buffer at 25°C.

In the following experiments, cellulase (Accellerase 1500) was centrifuged to remove the particles in the native cellulase solution, which did not contribute to the enzymatic activity but disturbed the protein assay. The supernatant was used for hydrolysis of cellulose or immobilization. **Figure 3-2** and **Figure 3-3** show the activities of the centrifuged and uncentrifuged free cellulase (Accellerase 1500) in 10 g/L pH = 6 CMC solution, respectively. The same enzymatic activities (first order rates) were observed.

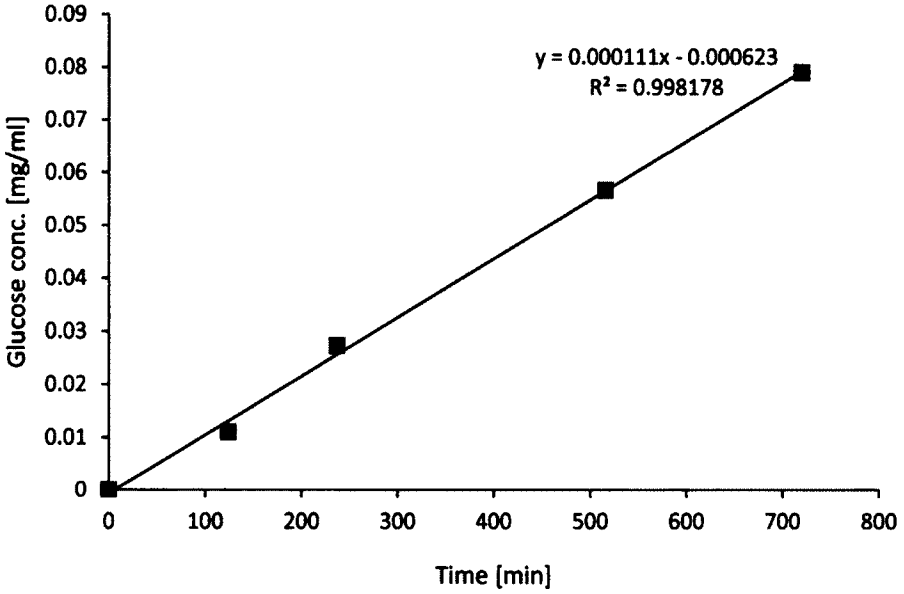

Figure 3-2: Activity of free cellulase (Accellerase 1500) in CMC solution. Enzyme: Accellerase 1500, 0.1 ml 500-time diluted cellulase (centrifuged). Cellulose solution: 10 ml CMC, 10 g/L in pH = 6 0.05 M acetate buffer at 20°C.

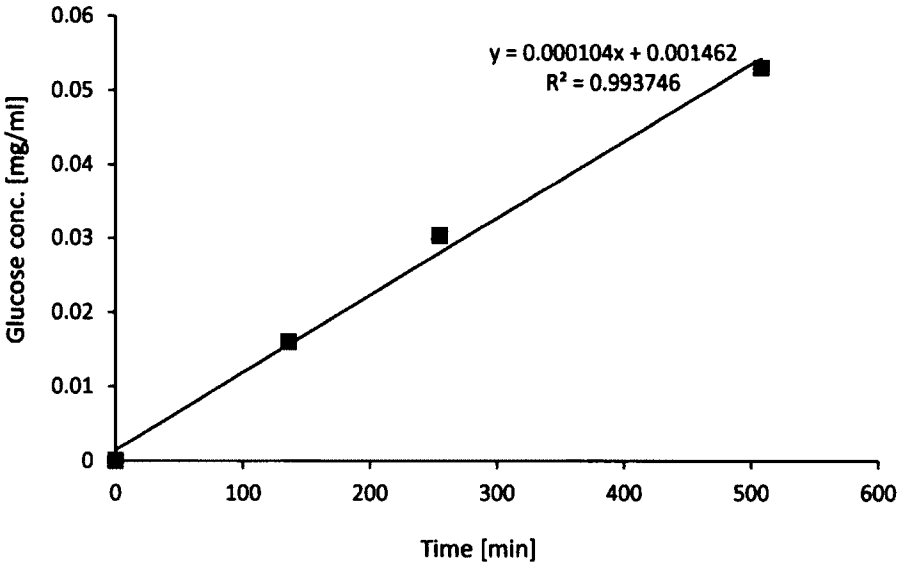

Figure 3-3: Activity of free cellulase (Accellerase 1500) in CMC solution. Enzyme: Accellerase 1500, 0.1 ml 500-time diluted cellulase (uncentrifuged). Cellulose solution: 10 ml CMC, 10 g/L in pH = 6 0.05 M acetate buffer at 20°C.

3.2 Results from the Immobilized Cellulase by Layer-by-Layer Nano-Assembly (LbL)

Layer-by-Layer Nano-Assembly was the first immobilization technique that was studied for immobilization of cellulase. It was widely reported for immobilization of enzymes such as glucose oxidase, glucoamylase, and lysozyme [79]. The main advantage of LbL was that the activity of the immobilized enzyme increased with the number of enzyme layers [85]. Also, the mobility of the immobilized cellulase molecules between layers improved the enzyme denaturation during immobilization, which was commonly found in other immobilization techniques [79]. These advantages of LbL make it very promising for immobilization of cellulase.

3.2.1 Characterization of the Immobilized Cellulase

SEM and QCM were applied to characterize the immobilized cellulase by LbL. QCM was applied to measure the mass change on the crystal resonator during the immobilization steps. **Figure 3-4** shows that the coated mass linearly increased according to the number of bilayers. During the PEI/PSS precursor layer, about 0.85-1.48 $\mu g/cm^2$ material was coated for each PEI/PSS bilayer. After changing PSS to a cellulase solution, about 0.88-1.96 $\mu g/cm^2$ cellulase was coated after each bilayer.

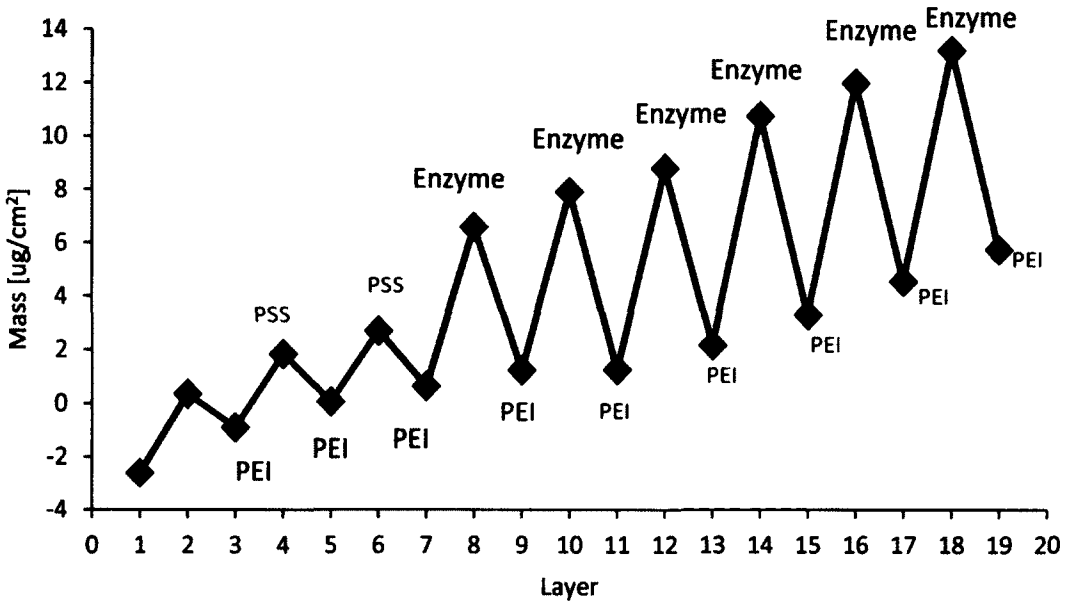

Figure 3-4: QCM results of the immobilized cellulase by Layer-by-Layer Nano-Assembly. [$(PEI/PSS)_3$+$(PEI/Cellulase)_5$]. The precursor layers and the enzyme layers were coated as described in Section 2.2.2.

SEM imaging was applied to monitor the surface topography change before and after the immobilization. **Figure 3-5** shows that the surface of the polystyrene beads is rough after 3 hours of NaOH boiling, which increases the surface area for immobilization. After coating 120 PEI/cellulase bilayers, the surface became smoother than the uncoated one. It indicated that PEI and cellulase were successfully coated onto the surface of the polystyrene beads.

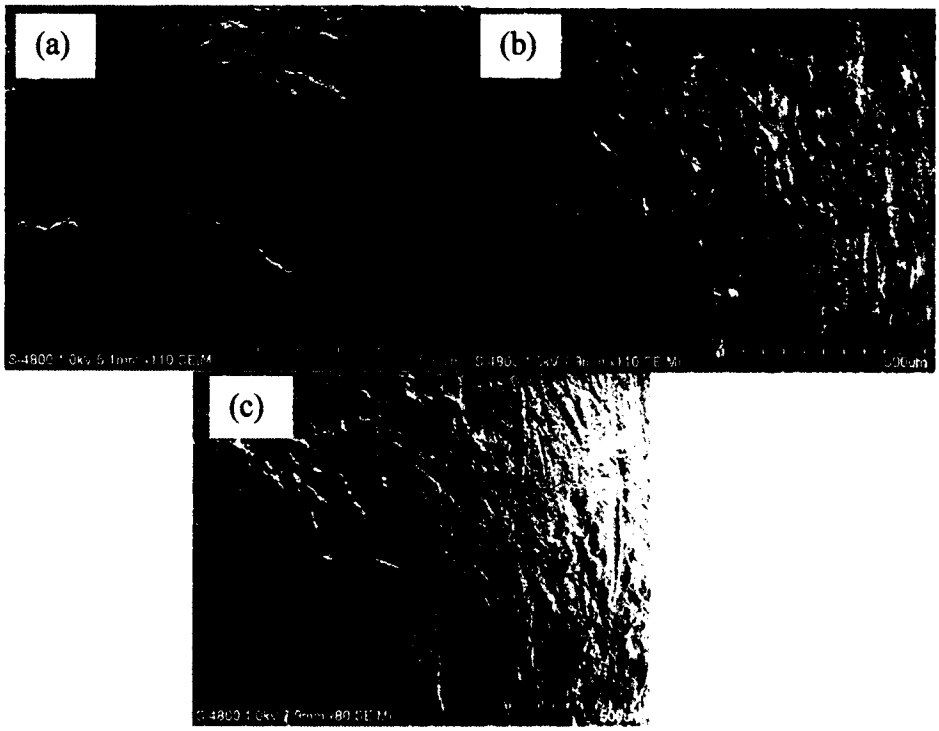

Figure 3-5: SEM images of polystyrene beads before and after immobilization. (a) Polystyrene beads before NaOH boiling. (b) Polystyrene beads after 3 hours of NaOH boiling. (c) Polystyrene beads with 120 bilayers of cellulase. Cellulase was immobilized onto the polystyrene beads as described in Section 2.2.3.

3.2.2 Hydrolysis of Crystalline Cellulose (Type 20) by the Immobilized Cellulase

After adjusting the pH condition for coating by the QCM technology, the LbL technique was applied for the immobilization of cellulase on polystyrene beads. The activity of the immobilized cellulase was tested by hydrolysis of the cellulose solution. Efforts were focused on increasing the activity and reusability of the immobilized cellulase.

3.2.2.1 *Impact of the cellulase bilayers on the activity of the immobilized cellulase*

The activity of the immobilized cellulase by LbL was tested by hydrolysis of a 10 g/L cellulose (type 20) solution in pH 6 acetate buffer (50 $mmol^{-1}$). The first order

rate (the linear slope of the time-dependent curve) was applied to represent the enzymatic activity of the immobilized cellulase as shown in **Figure 3-6**. **Figure 3-6** shows that the activity of the 5-bilayer immobilized cellulase is 11.2 times larger than one of the 3-bilayer immobilized cellulase, which indicates that the activity of the immobilized cellulase by LbL increases with the number of the cellulase bilayers.

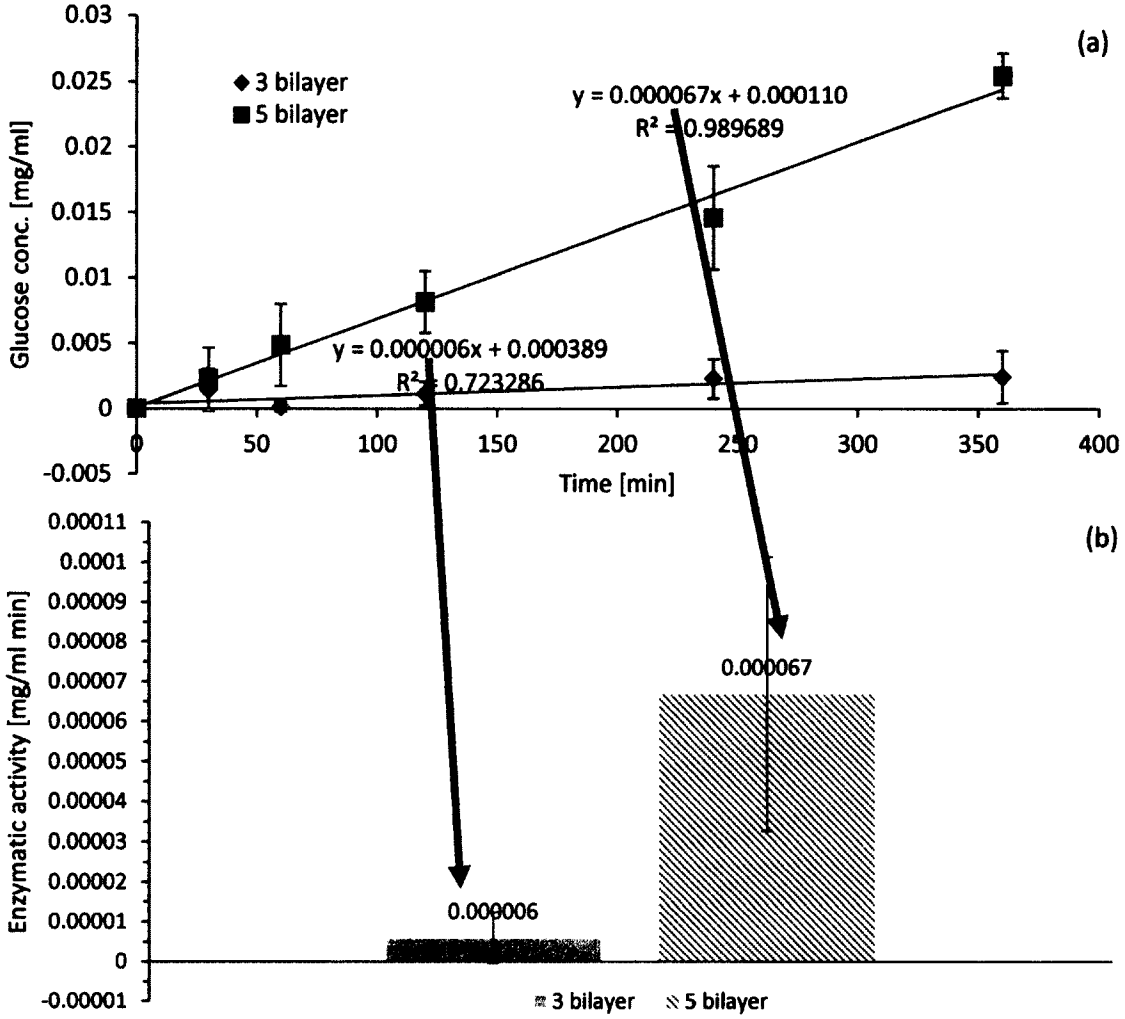

Figure 3-6: Activity of 3-bilayer and 5-bilayer immobilized cellulase on polystyrene beads by LbL. (a) Time-dependent curves, (b) Enzymatic activity. $[(PEI/PSS)_3+(PEI/Cellulase)_x]$ x = 3 or 5. Cellulase was immobilized onto the polystyrene beads as described in Section 2.2.3. Hydrolysis by 27.4 g immobilized cellulase was applied in a 100 ml 10 g/L pH 6 cellulose (type 20) solution at room temperature (25°C) as described in Section 2.2.4.

However, the enzyme desorption problem was observed for the immobilized cellulase by LbL. In order to test the immobilized cellulase desorption, the immobilized cellulase was removed from the cellulose (type 20) solution after 14 hours. The cellulose solution was kept in the water bath, and samples were taken at determined intervals of time. **Figure 3-7** depicts that for both 5-bilayer and 10-bilayer immobilized cellulase, the produced glucose concentration increased without the immobilized cellulase. A possible reason was that there was desorbed cellulase in the reactor which contributed to the hydrolysis activity. This would also explain why the activity of the 5-bilayer was larger than one of the 10-bilayer at the sample point of 14 hours (**Figure 3-7**): the desorbed cellulase of 5-bilayer contributed more hydrolysis activity than the 10-bilayer one.

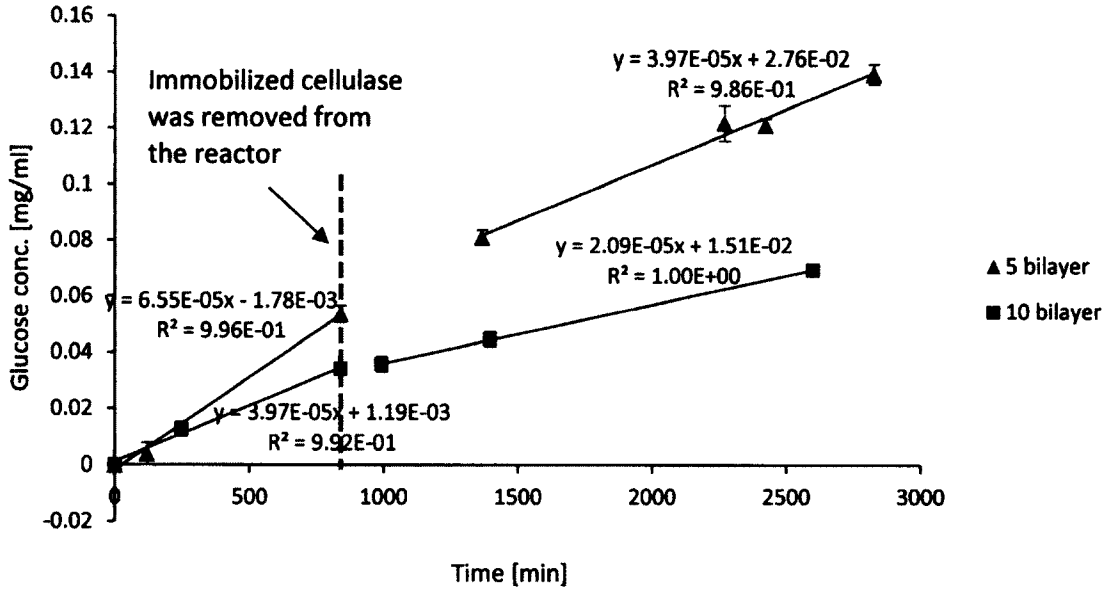

Figure 3-7: Activity of the 5-bilayer and 10-bilayer immobilized. Cellulose was hydrolyzed by the immobilized cellulase for 14 hours. Then the immobilized cellulase was removed from the reactor. The cellulose solution was kept in the water bath, and samples were taken at determined intervals of time. $[(PEI/PSS)_3+(PEI/Cellulase)_x]$ x = 5 or 10. Cellulase was immobilized onto the polystyrene beads as described in Section 2.2.3. Hydrolysis by 27.4 g immobilized cellulase was applied in a 100 ml 10 g/L pH 6 cellulose (type 20) solution at room temperature (25°C) as described in Section 2.2.4.

The reusability of the immobilized cellulase by LbL was tested. After the first batch, the immobilized cellulase was removed from the cellulose solution and washed several times with DI water. Then the immobilized cellulase was immersed in the fresh cellulose solution. Unfortunately, no detectable produced glucose was observed on the 5th day (6000 min). Possible reasons were that first, the immobilized cellulase was desorbed in the hydrolysis and washing steps; second, the cellulose particles would not penetrate into the deep enzyme layers.

3.2.2.2 *Impact of the choice of the terminated layer*

Experiments were conducted to reduce the desorption of cellulase that was observed in the previous section. A PEI layer or PEI/PSS bilayer was applied after the terminal cellulase layer as a sealing layer. **Figure 3-8** shows that the activity of the immobilized cellulase dramatically decreased after applying a sealing layer. Although desorption of the enzyme was not observed, the bioavailability of the enzyme to the cellulose (type 20) particle was prohibitively low. The catalyst beads were filtered and tested using the same initial conditions. No detectible glucose concentration was measured for the second cycle of experiments on the 6th day (8000 min).

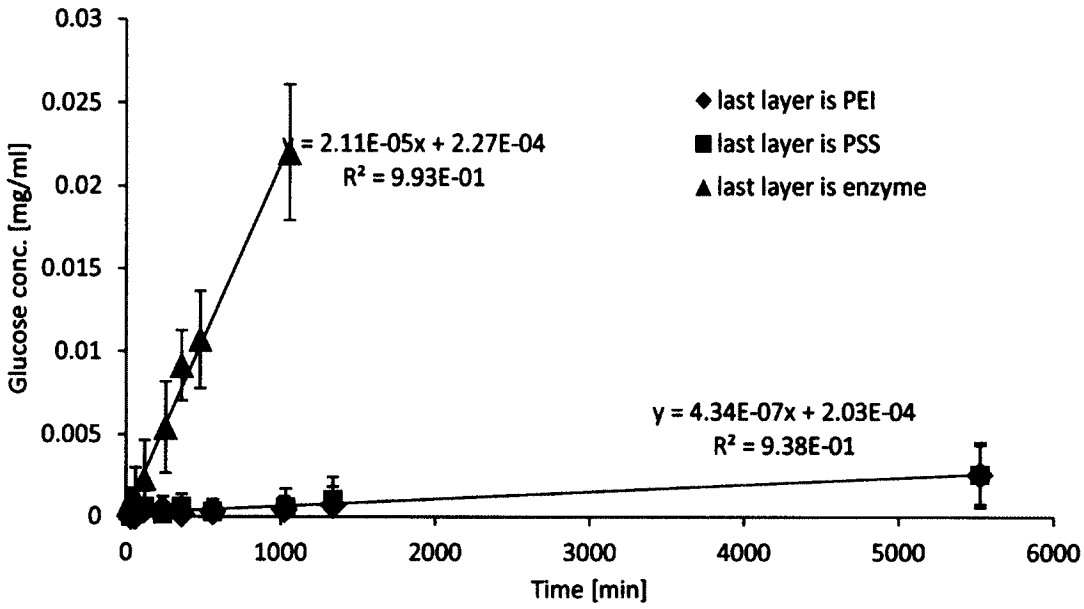

Figure 3-8: Activity of the immobilized cellulase with PEI, PSS or cellulase as a terminated layer. $[(PEI/PSS)_4+(PEI/Cellulase)_5+PEI$ or PEI/PSS]. Cellulase was immobilized onto the polystyrene beads as described in Section 2.2.3. Hydrolysis by 68.6 g immobilized cellulase was applied in 250 ml 10 g/L pH 6 cellulose (type 20) solution at room temperature (25°C) as described in Section 2.2.4.

3.2.2.3 *Impact of crosslinking on the immobilized cellulase*

Crosslinking was another method tested for the purposes of reducing the desorption of the immobilized cellulase. By intermolecular crosslinking, the enzyme desorption was expected to be improved. However, because the crosslinking also reduced the mobility of the cellulase molecules, the enzymatic activity might be decreased. **Figure 3-9** and **Figure 3-10** show the results. **Figure 3-9** shows that only 9% initial activity is retained after 10 min of crosslinking and 7% initial activity is retained after 20 min of crosslinking. A lighter crosslinking (3 min of crosslinking with 1/10 concentration of the crosslinker) was applied, but the result did not improve. **Figure 3-10** shows that the reusability of the immobilized cellulase with crosslinking. The second cycle's activity of the immobilized cellulase was only 11% compared with the first cycle.

The results from **Figure 3-9** and **Figure 3-10** confirmed that while the crosslinker strengthened the bonding condition of the immobilized cellulase, it also decreased the activity of the immobilized cellulase. Therefore, considering the activity loss of the immobilized cellulase, crosslinking was not suitable for the immobilized cellulase by LbL.

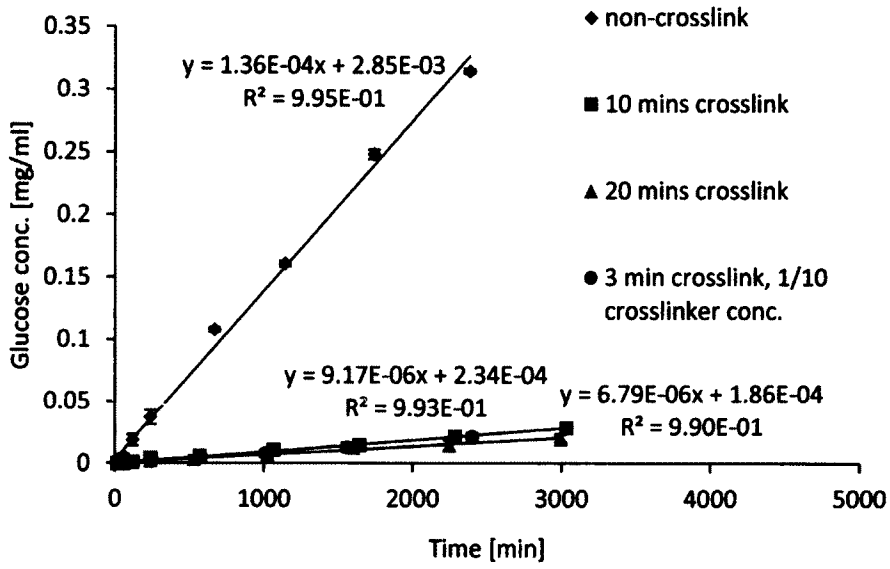

Figure 3-9: Impact of crosslinking on the activity of the immobilized beads. $[(PEI/PSS)_4+(PEI/Cellulase)_5+crosslinker]$. Cellulase was immobilized and crosslinked onto the polystyrene beads as described in Section 2.2.3. Hydrolysis by 68.6 g immobilized cellulase was applied in 250 ml 10 g/L pH 5 cellulose (type 20) solution at room temperature (25°C) as described in Section 2.2.4.

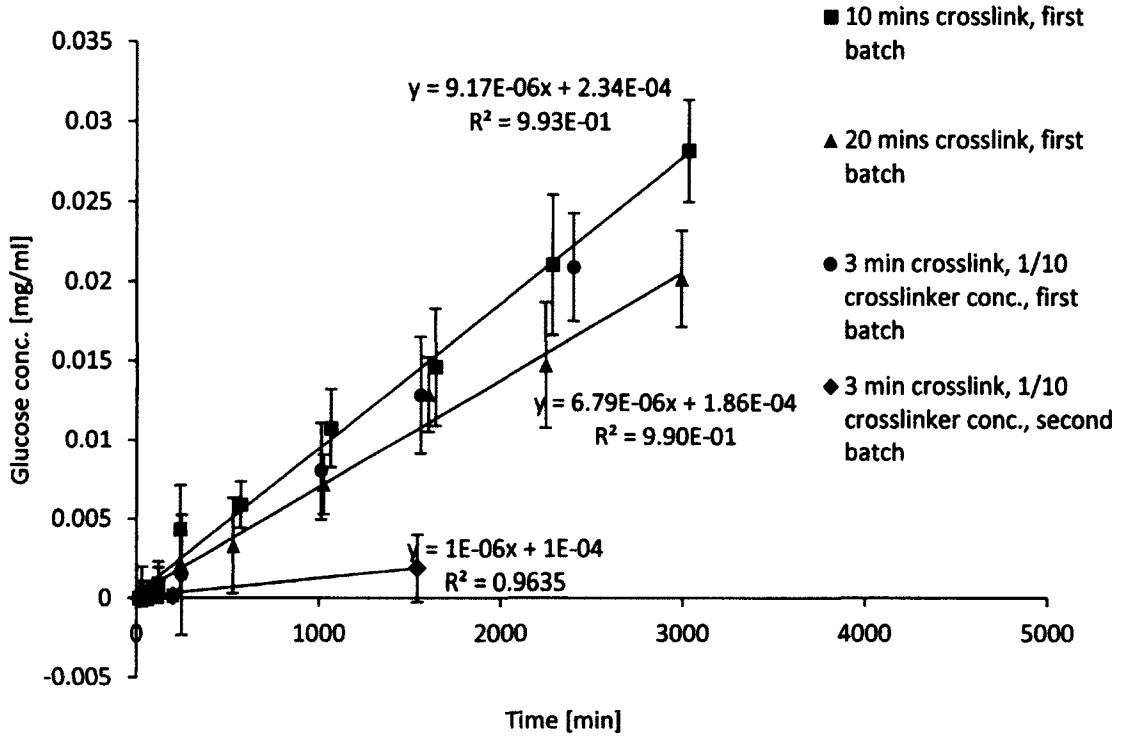

Figure 3-10: Activity and reusability of the immobilized beads with crosslinking. [$(PEI/PSS)_4$+$(PEI/Cellulase)_5$+crosslinker]. Cellulase was immobilized and crosslinked onto the polystyrene beads as described in Section 2.2.3. Hydrolysis by 68.6 g immobilized cellulase was applied in a 250 ml 10 g/L pH 5 cellulose (type 20) solution at room temperature (25°C) as described in Section 2.2.4.

3.2.3 Hydrolysis of CMC by the Immobilized Cellulase

The produced glucose concentration of hydrolysis of cellulose (type 20) by the immobilized cellulase was low. **Figure 3-8** shows that the produced glucose concentration of hydrolysis of cellulose (type 20) after 6 hours was just 0.009 mg/ml. When a sealing layer was applied to the immobilized cellulase, the produced glucose concentration further decreased to 0.003 mg/ml even after 90 hours, which was close to the detectable limitation. Besides the low enzymatic activity of the hydrolysis reaction by the cellulase enzyme, the mass transfer and penetration problems had a significant effect. In order to get a better understanding of the immobilization technique (what made the

enzyme desorption; how to improve the reusability; and how to improve the activity.), a soluble cellulose, CMC, was used instead of cellulose (type 20) to minimize the mass transfer and penetration problem. Thus, the enzymatic activity of the immobilized cellulase was increased using CMC as a substrate for hydrolysis.

3.2.3.1 *Comparison enzymatic activity of the immobilized cellulase for crystalline cellulose (type 20) with CMC*

As shown in **Figure 3-11**, the activity of the immobilized cellulase in the CMC solution was about 7.9 times larger than the one in the cellulose (type 20) solution. After 240 min of hydrolysis of CMC, the produced glucose concentration by the immobilized cellulase was 0.041 mg/ml, which was 20 times larger than the one in the hydrolysis of the cellulose (type 20) (0.002 mg/ml).

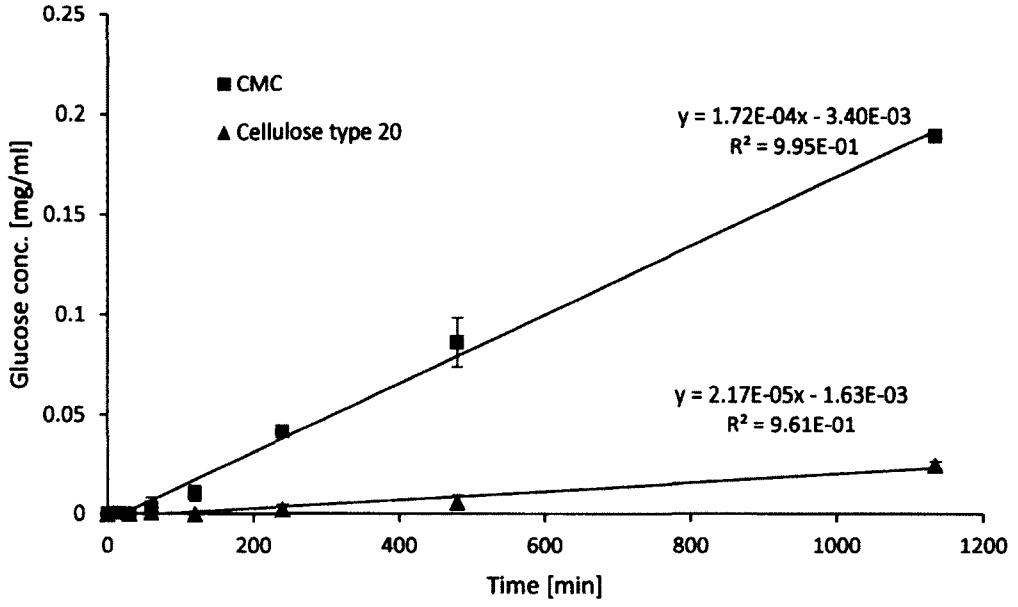

Figure 3-11: Activity of the immobilized cellulase in CMC/cellulose (type 20). $[(PEI/PSS)_5+(PEI/cellulase)_5+PEI]$. Cellulase was immobilized onto the polystyrene beads as described in Section 2.2.3. Hydrolysis by 27.4 g immobilized cellulase was applied in a 100 ml 10 g/L pH 6 CMC/cellulose (type 20) solution at room temperature (25°C) as described in Section 2.2.4.

3.2.3.2 *Reusability of the immobilized cellulase*

The reusability of the immobilized cellulase by LbL with a PEI sealing layer was also observed for hydrolysis of the CMC solution. **Figure 3-12** shows that the activity of the second cycle was 2.06E-05 mg/(ml min), which is 12% compared with the first cycle. A possible reason for low reusability was the immobilized cellulase loss during hydrolysis of CMC and the washing steps between cycles.

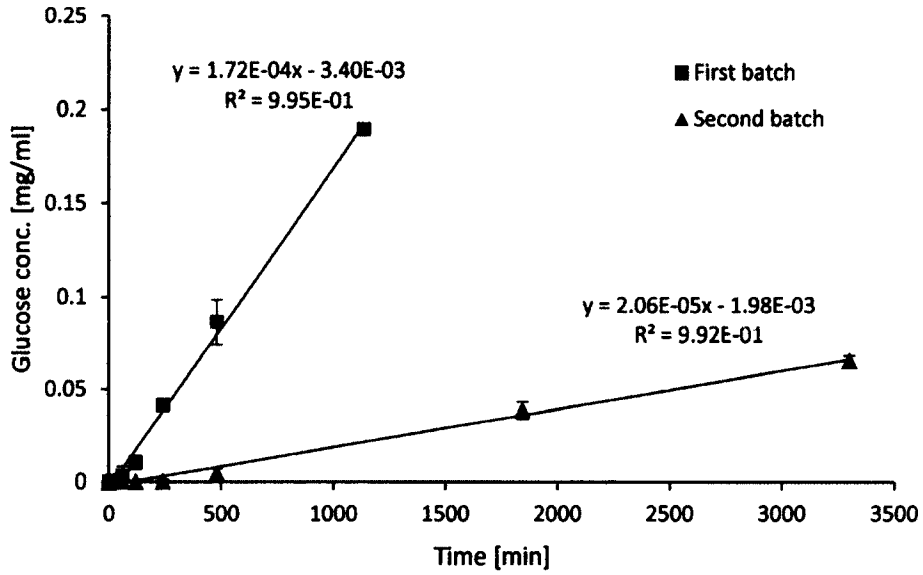

Figure 3-12: Reusability of the immobilized cellulase by LbL in CMC. $[(PEI/PSS)_5+(PEI/cellulase)_5+PEI]$. Cellulase was immobilized onto the polystyrene beads as described in Section 2.2.3. Hydrolysis by 27.4 g immobilized cellulase was applied in a 100 ml 10 g/L pH 6 CMC solution at 25°C as described in Section 2.2.4.

3.2.3.3 *Impact of the choice of the terminated layer*

The activity of the immobilized cellulase by LbL with different terminated layers was tested in the CMC solution. A PEI layer was applied after the terminal cellulase layer as a sealing layer. The results are shown in **Figure 3-13**. In the results for cellulose (type 20) solution, the activity of the immobilized cellulase with cellulase as a terminated layer was higher than the one with a PEI layer as a terminated layer. From the QCM result in

Figure 3-4, it can be demonstrated that for each cellulase layer, the immobilized cellulase stripped off during the next PEI coating process. Therefore, the mass of the immobilized cellulase with cellulase as a terminated layer was larger than the one with PEI as a terminated layer. Thus, the activity of the immobilized cellulase with cellulase as a terminated layer was higher than the one with PEI as a terminated layer.

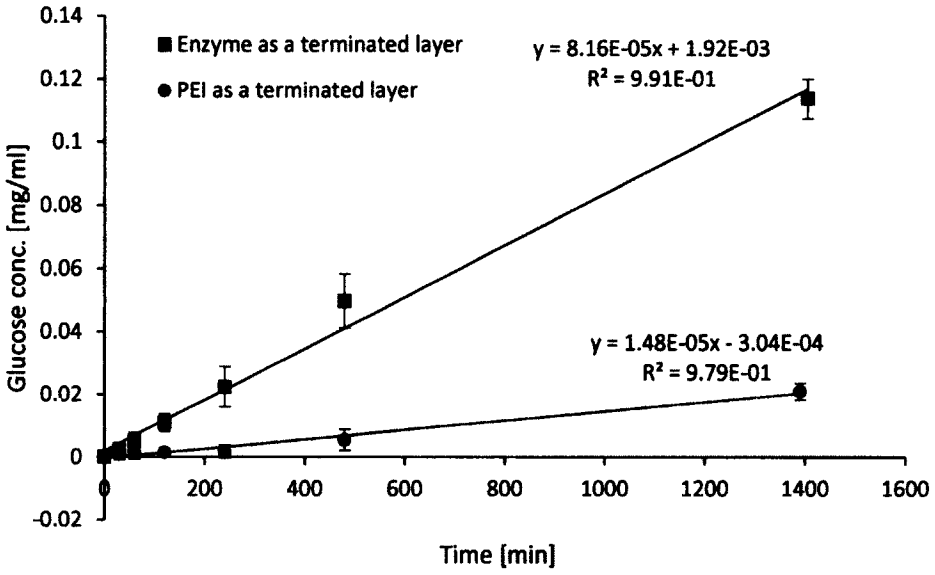

Figure 3-13: Activity of the immobilized cellulase with PEI or cellulase as a terminated layer. [$(PEI/PSS)_5$+$(PEI/Cellulase)_5$+PEI]. Cellulase was immobilized onto the polystyrene beads as described in Section 2.2.3. Hydrolysis by 27.4 g immobilized cellulase was applied in a 100 ml 10 g/L pH 7 CMC solution at 25°C as described in Section 2.2.4.

The impact of the PEI sealing layer on the activity and reusability of the immobilized cellulase by LbL was tested in the CMC solution. Unlike hydrolysis in the cellulose (type 20) solution, hydrolysis in the CMC solution by the immobilized cellulase minimized the penetration problem. **Figure 3-14** and **Figure 3-15** show the activities of the first and second cycles. In the first cycle, the immobilized cellulase was removed from the CMC solution after 2 hours. The CMC solution was kept in bath water, and the

samples were taken at determined time intervals. **Figure 3-14** shows that for both immobilized cellulase with/without a sealing layer, the produced glucose concentration increased without the immobilized cellulase. It indicated that there was cellulase desorbed during hydrolysis of CMC for both immobilized cellulase with/without a PEI sealing layer. **Figure 3-14** shows that the first cycle's activity of the immobilized cellulase with a PEI sealing layer was smaller than the one without the PEI sealing layer. However, **Figure 3-15** depicts the second cycle's activity of the immobilized cellulase showing the opposite. It indicated that although using PEI as a terminated layer decreased the initial activity of the immobilized cellulase, it improved the cellulase desorption problem. Thus, using a PEI sealing layer improved the reusability.

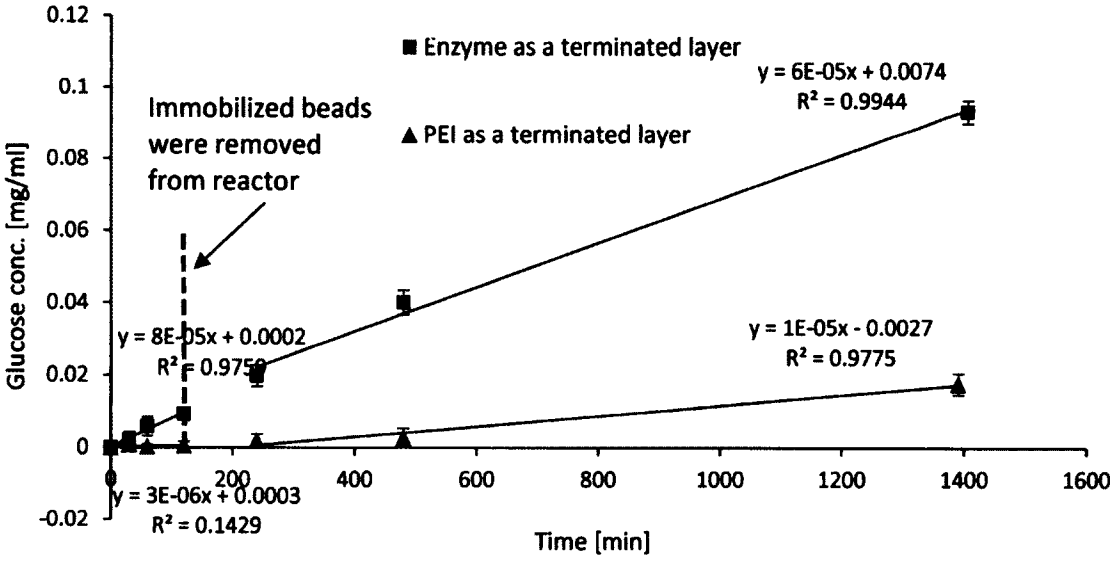

Figure 3-14: Activity of the immobilized cellulase with PEI or cellulase as a terminated and the impact of enzyme desorption. First batch. The immobilized beads were removed from the reactor after 2 hours. The CMC solution was kept in the water bath, and samples were taken at determined time intervals. Immobilization carriers: polystyrene beads 27.4 g. $[(PEI/PSS)_5+(PEI/Cellulase)_5+PEI]$. Cellulase was immobilized onto the polystyrene beads as described in Section 2.2.3. Hydrolysis by 27.4 g immobilized cellulase was applied in 100 ml 10 g/L pH 7 CMC solution at 25°C as described in Section 2.2.4.

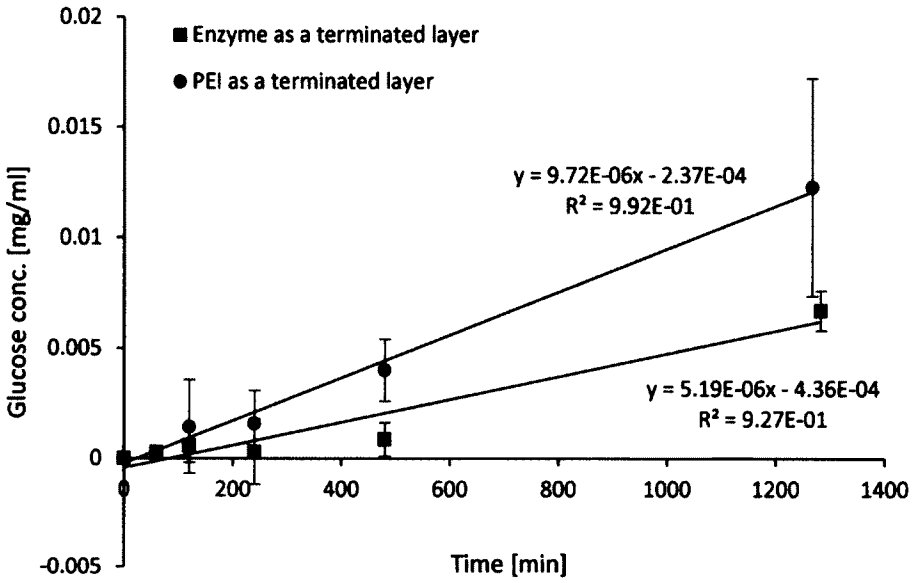

Figure 3-15: Activity and reusability of the immobilized cellulase with PEI or cellulase as a terminated layer in CMC. Second batch. $[(PEI/PSS)_5+(PEI/Cellulase)_5+PEI]$. Cellulase was immobilized onto the polystyrene beads as described in Section 2.2.3. Hydrolysis by 27.4 g immobilized cellulase was applied in a 100 ml 10 g/L pH 7 CMC solution at 25°C as described in Section 2.2.4.

3.2.4 Summary for Hydrolysis of Cellulose by the Immobilized Cellulase Using LbL

Table 3-1 shows the results for hydrolysis of cellulose by the immobilized cellulase using LbL. The initial activity of the immobilized cellulase did not increase with the number of cellulase layers. Enzyme desorption was observed during the hydrolysis of cellulose, which was the possible reason that there was no or low reusability for the immobilized cellulase. Applying crosslinking dramatically denatured the initial activity of the immobilized cellulase by 15-20 folds, yet rarely improved the reusability. A PEI sealing layer slightly improved the reusability of the immobilized cellulase for hydrolysis of CMC, but it was not working for the hydrolysis of cellulose (type 20). A possible reason was that the cellulose (type 20) molecules would not penetrate into the deep layers. It was also the possible reason that the initial activity of the immobilized cellulase

did not increase with the number of enzyme layers. Therefore, according to our study, these negative results limits the application of LbL for the immobilization of cellulase.

Table 3-1: Summary for hydrolysis of cellulose by the immobilized cellulase using LbL.

Immobilization conditions		Amount of immobilization carriers (g)	Cellulose	Volume of cellulose solution (ml)	pH of cellulose solution	Initial activity (mg/ml min)	Activity for the second batch (mg/ml min)
Non-crosslinking	3-bilayer	27.4	Cellulose (type 20)	100	6	6.00E-06	NA
	5-bilayer	27.4	Cellulose (type 20)	100	6	6.70E-05	NA
	5-bilayer	27.4	CMC	100	6	1.72E-04	2.06E-05
	5-bilayer	27.4	CMC	100	7	8.16E-05	5.19E-06
	5-bilayer	68.6	Cellulose (type 20)	250	5	1.36E-04	NA
	10-bilayer	27.4	Cellulose (type 20)	100	6	3.97E-05	NA
	PEI sealing layer	68.6	Cellulose (type 20)	250	6	4.34E-07	NA
	PEI sealing layer	27.4	CMC	100	7	1.48E-05	9.72E-06
	PEI/PSS sealing layer	68.6	Cellulose (type 20)	250	6	4.34E-07	NA
Crosslinking, 5-bilayer	20 min	68.6	Cellulose (type 20)	250	5	6.79E-06	NA
	10 min	68.6	Cellulose (type 20)	250	5	9.17E-06	NA
	3 min, 1/10 crosslinker conc.	68.6	Cellulose (type 20)	250	5	8.74E-06	1.00E-06

3.3 Results from the Immobilized Cellulase by Ca^{2+}-homoionized and $Al(OH)_x$ Coating Technique on Molecular Sieves (Pellets)

Ca^{2+}-homoionized and $Al(OH)_x$ pretreatment was the second immobilization technique that was investigated on molecular sieves. This immobilization technique combined physical adsorption and entrapment. After Ca^{2+}-homoionization, the positive surface charge of the molecular sieves increases. Because the cellulase molecules have a negative charge, the interaction between the cellulase molecules and the immobilization

carrier is significantly improved. The purpose for $Al(OH)_x$ pretreatment is to coat an $Al(OH)_x$ gel film outside the immobilization carriers to provide additional surface area for cellulase immobilization. **Figure 3-16** shows the results.

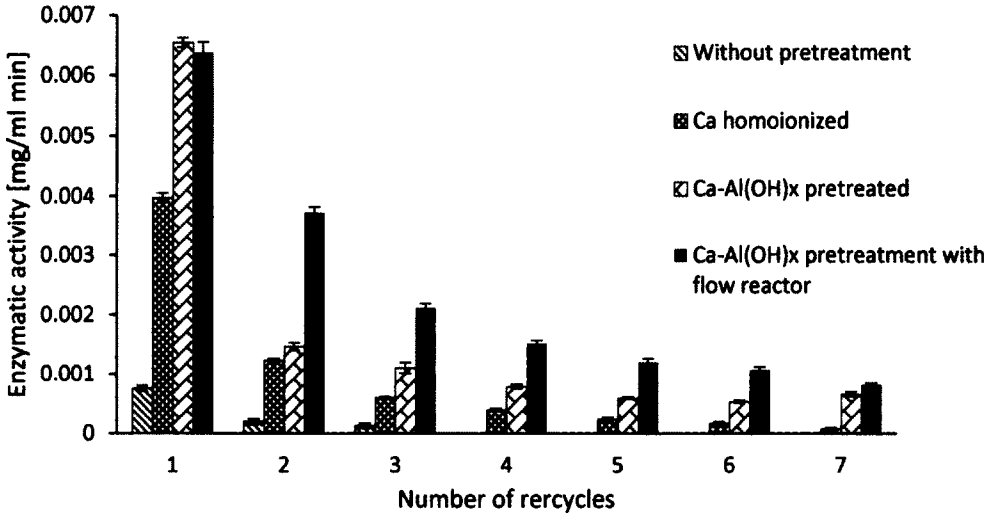

Figure 3-16: Activity and reusability of the immobilized cellulase on molecular sieves (pellets) by Ca^{2+}-Al(OH) modification. Cellulase was immobilized onto molecular sieves (pellets) as described in Section 2.3.2. Hydrolysis reaction was applied as described in Section 2.3.3. The flow rate of the packed bed reactor was 100 ml/min.

3.3.1 Effect of Ca^{2+} Homo-ionized Pretreatment on Molecular Sieves (Pellets)

Porous molecular sieves (pellets) were used for the immobilization of cellulase. The activity of the immobilized cellulase was tested by hydrolysis of 1% w/v CMC solution in pH 6 acetate buffer at room temperature. Reusability of the immobilized cellulase was observed.

The homo-ionizing Ca^{2+} had a significant effect on the activity of the immobilized cellulase. **Figure 3-16** shows that the initial activity of the immobilized cellulase with Ca^{2+} homo-ionization was five times higher than the one without Ca^{2+} homo-ionization. A possible reason was that after Ca^{2+} homo-ionization, the positive surface charge

increased and thus increased the amount of the cellulase (which had a negative charge) immobilization. The reusability of the immobilized cellulase was barely improved after Ca^{2+} homo-ionization. The second and third cycles' activities of the immobilized cellulase without Ca^{2+} homo-ionization were 26% and 17% of the initial activity, respectively. In comparison, the second and third cycles' activities of the immobilized cellulase with Ca^{2+} homo-ionization were 31% and 15% of the initial activity, respectively.

3.3.2 Effect of Ca^{2+} Homo-ionized and $Al(OH)_x$ Coating Pretreatment on Molecular Sieves (Pellets)

The positive impact of $Al(OH)_x$ coating on the Ca^{2+} homo-ionized molecular sieves (pellets) was significant. **Figure 3-16** shows that the initial activity of the immobilized cellulase with $Al(OH)_x$ is 1.6 times larger than the one without $Al(OH)_x$ coating. However, the reusability barely improved. The second and third cycles' activities of the immobilized cellulase with $Al(OH)_x$ coating were 22% and 17% of the initial activity, respectively. In comparison, the second and third cycles' activities of the immobilized cellulase without $Al(OH)_x$ coating were 31% and 15% of the initial activity, respectively. Enzyme desorption was observed during the hydrolysis and washing steps, which was the possible reason for low reusability. Besides, the immobilized molecular sieves were observed to be abraded during the hydrolysis, while they were stirred in the reactor.

A packed bed reactor (**Figure 2-8**) was designed and used for the hydrolysis of the CMC solution by the immobilized cellulase (molecular sieves) instead of the batch reactor in order to minimize the abrasion. It significantly improved the reusability of the immobilized cellulase. The activity of the second cycle retained 58% initial activity in

a packed bed reactor by contrast with 22% initial activity retained in a batch reactor (**Figure 3-16**). The close-packing of the immobilized molecular sieves in the packed bed reactor may have improved the abrasion among the immobilized molecular sieves and thus saved the immobilized cellulase. Therefore, the reusability of the immobilized cellulase on molecular sieves (pellets) was improved by using a packed bed reactor. However, enzyme desorption was still observed during the hydrolysis of the CMC solution. The cellulose solution container was removed from the packed bed reactor setup after 1 hour, and it was stirred at 300 rpm by a magnetic stirrer. A sample was taken after 14 hours and 45 min. The produced glucose concentration increased from 0.065 mg/ml to 0.392 mg/ml, which indicated that the desorbed cellulase existed in the reactor.

3.4 Results from the Immobilized Cellulase by Combination of Ca^{2+}-$Al(OH)_x$ Modification and LbL on Molecular Sieves

Because relatively high initial activity but low reusability of the immobilized cellulase by Ca^{2+}-$Al(OH)_x$ modification technique were observed, LbL technique was applied after Ca^{2+}-$Al(OH)_x$ pretreatment to improve the reusability of the immobilized cellulase. The influence of a different number of enzyme layers was investigated for both activity and reusability of the immobilized cellulase.

3.4.1 Activity and Reusability of the Immobilized Cellulase

LbL immobilization technique was used after the Ca^{2+}-$Al(OH)_x$ pretreatment. There were two kinds of immobilization carriers used for the immobilization of cellulase, i.e. molecular sieves (pellets) and molecular sieves (beads). For three cellulase bilayers, the initial activity of the immobilized molecular sieves (pellets) was 1.9 times higher than

one of the immobilized molecular sieves (beads) (**Figure 3-17**). This was probably because the surface area (per mass) of the molecular sieves (pellets) was larger than one of the molecular sieves (beads). Therefore, the mass of the immobilized cellulase on the molecular sieves (pellets) was larger.

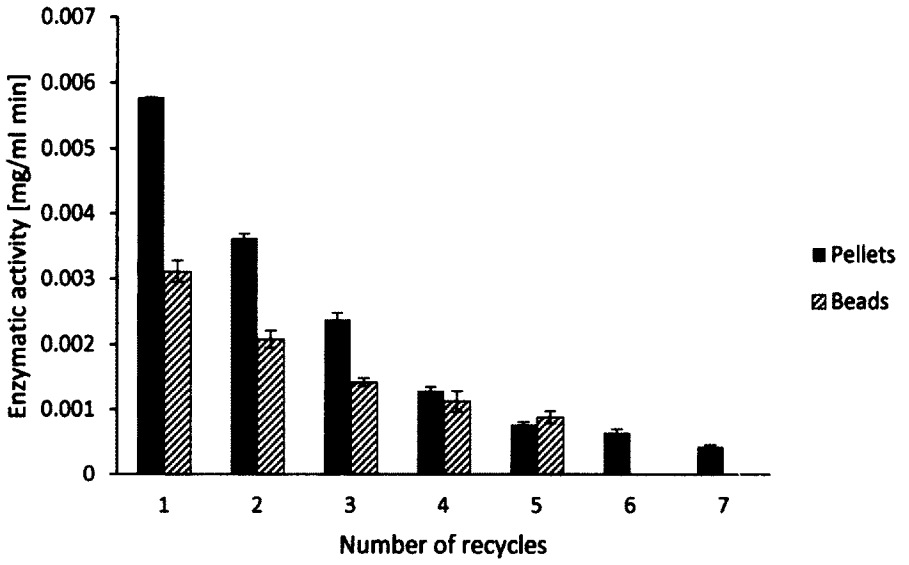

Figure 3-17: Impact of different immobilization carriers (molecular sieve pellets or beads) on the activity and reusability of the 3-bilayer immobilized cellulase by combination of LbL and Ca^{2+}-$Al(OH)_x$ modification. Cellulase was immobilized onto molecular sieves (pellets or beads) as described in Section 2.4.2. Hydrolysis reaction was applied as described in Section 2.4.3.The flow rate of the packed bed reactor was 100 ml/min.

The difference between the reusabilities of the immobilized molecular sieves (pellets) and molecular sieves (beads) was observed. The immobilized molecular sieves (pellets) had 63% initial activity retained for the second recycle while the immobilized molecular sieves (beads) had 67% initial activity retained for the same recycle (**Figure 3-17**). However, from the 4^{th} recycle, the activity of the immobilized molecular sieves (beads) was almost the same as one of the immobilized molecular sieves (pellets), even if the initial activity of the immobilized molecular sieves (pellets) was 1.9 times higher. It

indicated that by using molecular sieves (beads), the reusability of the immobilized cellulase improved.

3.4.2 Effect of Different Number of Cellulase Bilayers

Reusability of the immobilized cellulase was significantly improved by increasing the number of cellulase layers. **Figure 3-18** shows that the 6^{th} recycle's activity of the 15-bilayer immobilized cellulase was 0.0011 mg/(ml min), which was 75% of the initial activity. Compared with direct immobilization of cellulase on the Ca^{2+}-$Al(OH)_x$ pretreated molecular sieves (beads), the PEI layer protected cellulase molecules from desorption from the pores of the molecular sieves (beads). This effect increased with the number of cellulase bilayers, but also led to an activity decrease of the immobilized cellulase because the PEI layer partially blocked the pores. Therefore, the initial activity of the immobilized molecular sieves (beads) with 15 cellulase bilayers was 46% compared with one of the immobilized molecular sieves (beads) with three cellulase bilayers (**Figure 3-18**).

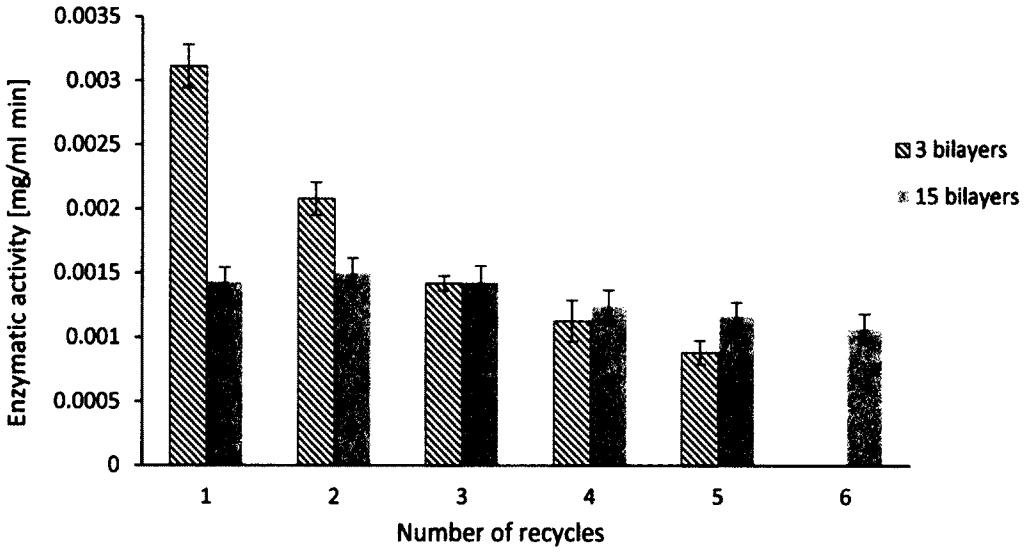

Figure 3-18: Activity and reusability of the 3-bilayer/15-bilayer immobilized cellulase by combination of LbL and Ca^{2+}-$Al(OH)_x$ modification on molecular sieves (beads). Cellulase was immobilized onto molecular sieves (beads) as described in Section 2.4.2. Hydrolysis reaction was applied as described in Section 2.4.3. The flow rate of the packed bed reactor was 100 ml/min.

3.4.3 Effect of Crosslinking After Cellulase Immobilization

Glutaraldehyde was used as a crosslinker after LbL coating on the Ca^{2+}-$Al(OH)_x$ pretreated molecular sieves (beads). The two aldehyde groups can react with amino groups in cellulase molecules and restrict their movement, therefore decreasing the immobilized cellulase desorption from the molecular sieves. **Figure 3-19** shows the results. The initial activity of the immobilized cellulase with crosslinking was 0.0009 mg/(ml min), which was only 29% of the activity of the 3-bilayer immobilized cellulase (**Figure 3-19**). The reusability was not improved by crosslinking. For the immobilized cellulase with crosslinking, 56% initial activity was retained for the 2nd recycle. In comparison, for the immobilized cellulase without crosslinking, 68% initial activity was retained for the 2nd recycle.

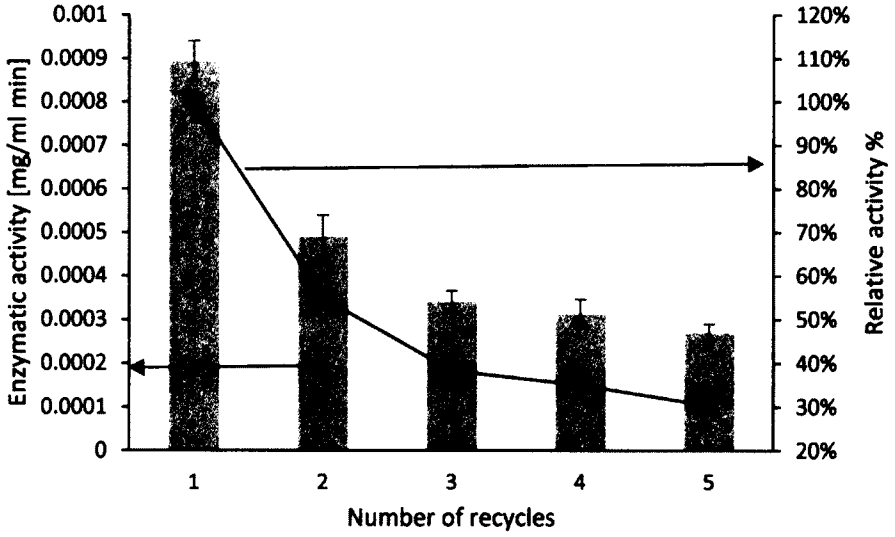

Figure 3-19: Activity and reusability of crosslinking 2-bilayer immobilized cellulase by combination of LbL and Ca^{2+}-$Al(OH)_x$ modification on molecular sieves (beads). [Enzyme (1 hour) + PEI (10 min)]$_2$ + Crosslinker (2 hours). Crosslinker: 2% (v/v) glutaraldehyde in DI water. Cellulase was immobilized onto molecular sieves (beads) as described in Section 2.4.2. Hydrolysis reaction was applied as described in Section 2.4.3. The flow rate of the packed bed reactor was 100 ml/min.

3.4.4 Summary for the Hydrolysis of the CMC by the Immobilized Cellulase Using Combination of Ca^{2+}-$Al(OH)_x$ and LbL

Table 3-2 shows the results for the hydrolysis of the CMC by the immobilized cellulase using combination of Ca^{2+}-$Al(OH)_x$ and LbL.

Table 3-2: Summary for hydrolysis of CMC by the immobilized cellulase using combination of Ca^{2+}-$Al(OH)_x$ and LbL.

Immobilization techniques	Immobilization carriers	Initial activity (mg/ml min)	Reusability, relative activity %			
			Second batch	Third batch	Fourth batch	Fifth batch
3-bilayer	pellets	0.0058	62%	41%	22%	14%
3-bilayer	beads	0.0031	68%	45%	35%	29%
15-bilayer	beads	0.0014	107%	100%	86%	86%
2-bilayer, crosslinking	beads	0.0009	56%	33%	33%	33%

3.5 Results from the Immobilized Cellulase Using 3-APTES Self-assembly Monolayer Technique

3-APTES self-assembly monolayer technique was the third immobilization technique that was investigated. Since the enzyme layer is the terminated layer, there is no penetration problem for the cellulose molecules to interact with the immobilized cellulase during hydrolysis, greatly improving the initial activity. Also, because the cellulase molecules are covalently bound to the modified immobilization carriers, there is little enzyme desorption during the hydrolysis reaction. Thus, the reusability of the immobilized cellulase will be improved.

3.5.1 Immobilization of Cellulase on Molecular Sieves (Beads)

Immobilization of cellulase on molecular sieves (beads) modified by 3-APTES and GA was investigated. GA crosslinking after 3-APTES modification played a significant role in immobilization of cellulase. **Figure 3-20** shows that both the initial activity and the reusability of the immobilized cellulase are dramatically improved after GA crosslinking. The initial activity of the immobilized cellulase by 3-APTES and GA modification was 1.5 times higher than the one with just 3-APTES modification. The 2^{nd} batch's activity of the immobilized cellulase by 3-APTES and GA was 6.3 times higher than the one with just 3-APTES. The use of GA worked not only as a crosslinker, but also as a spacer arm which decreased the steric hindrance and thus increased the initial activity.

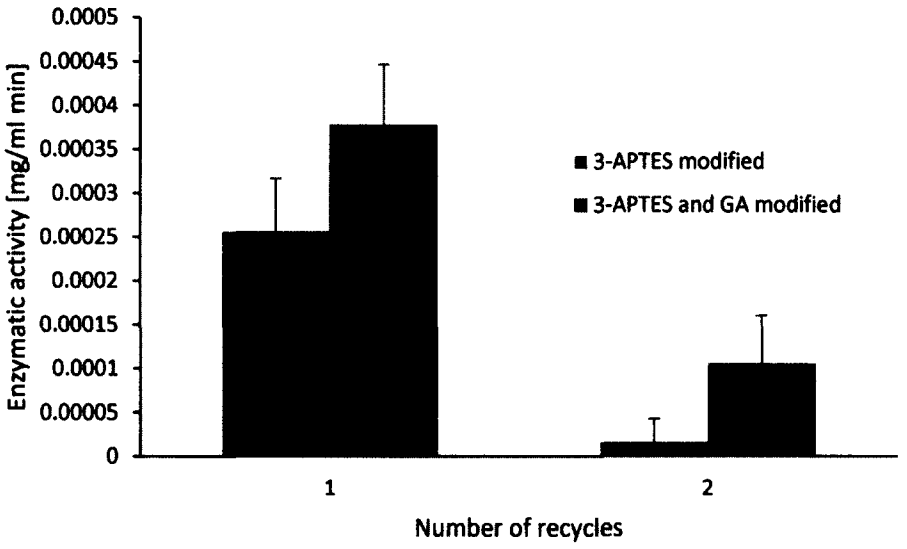

Figure 3-20: Impact of glutaraldehyde crosslinking after 3-APTES modification on immobilized molecular sieves (beads). Enzyme: Accellerase 1500, 10-time diluted.

Figure 3-21 shows the activity and the reusability of the immobilized cellulase using 3-APTES and GA modification pretreatment. The activity of the sixth cycle retained 71% initial activity.

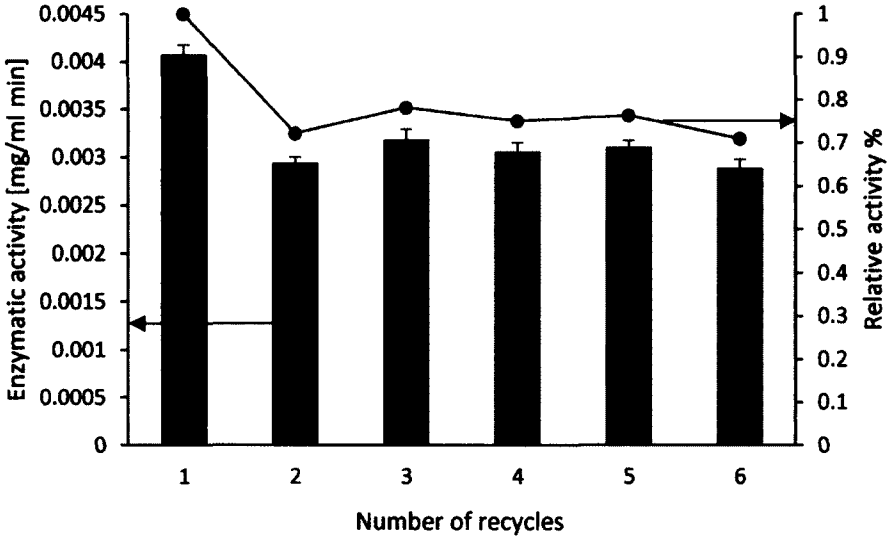

Figure 3-21: Activity and reusability of the immobilized cellulase on molecular sieves (beads) by 3-APTES and glutaraldehyde modification. Enzyme: Accellerase 1500, undiluted.

3.5.2 Immobilization of Cellulase on Glass Beads

Glass beads (3 mm diameter) were chosen for the immobilization of cellulase instead of molecular sieves. Because of the poor structural strength of the molecular sieves, the immobilized molecular sieves abraded during the hydrolysis reaction, which lowered reusability (**Figure 3-22**). In contrast, glass beads had high structural strength and the surface was chemically suitable for 3-APTES modification.

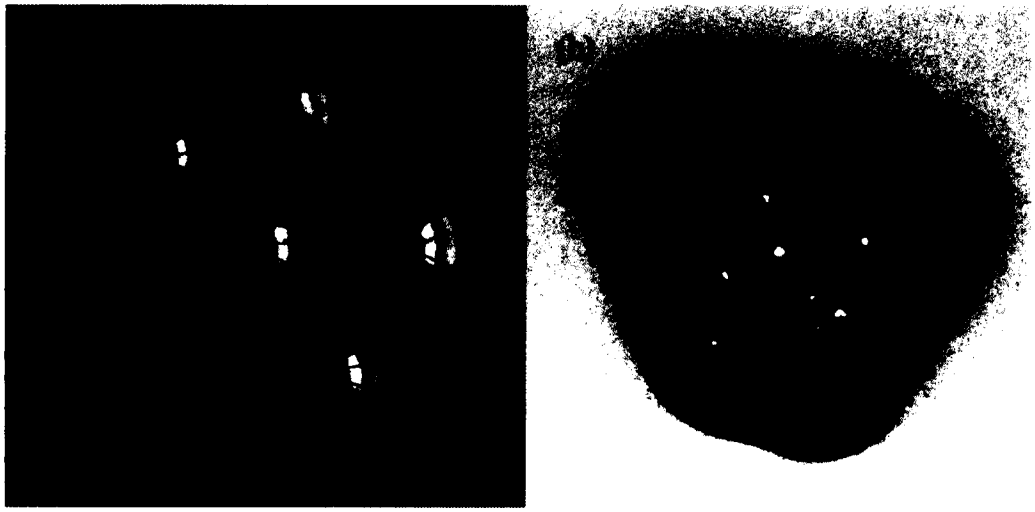

Figure 3-22: (a) whole molecular sieves; (b) Abraded molecular sieves.

The activity of the immobilized cellulase was determined by hydrolysis of the CMC in pH 6 acetate buffer solution (50 $mmol^{-1}$) using a packed bed reactor. **Figure 3-23** shows the activity and reusability of the immobilized cellulase with a 5-time diluted cellulase solution. **Figure 3-24** shows the time-dependent curve of the produced glucose by the immobilized cellulase. The produced glucose by the immobilized cellulase on the glass beads was low because of the limited surface area of the glass beads, which led to a small amount of the immobilized cellulase.

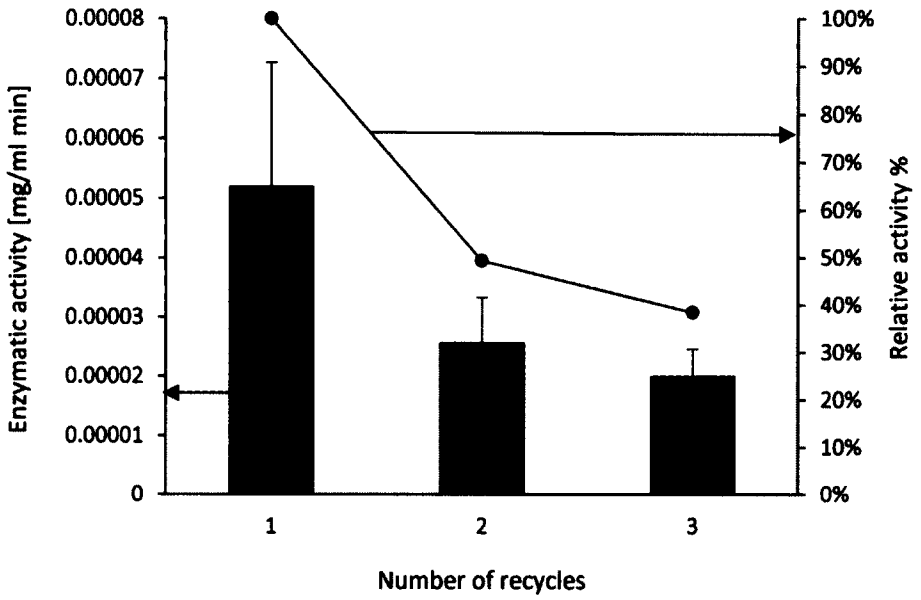

Figure 3-23: Activity and reusability of the immobilized cellulase by 3-APTES and glutaraldehyde modification on glass beads.

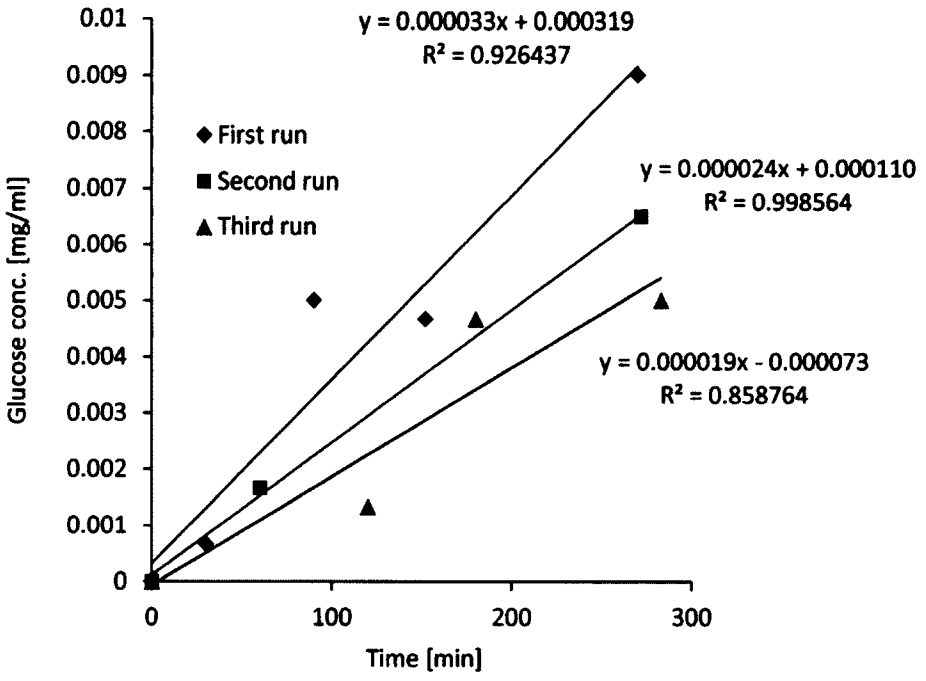

Figure 3-24: Time-dependent curve of the produced glucose by the immobilized cellulase on glass beads.

3.5.3 Immobilization of Cellulase on Silica Gel

Silica gel has been widely used for the immobilization of enzymes. Compared with the molecular sieves and the glass beads, it had advantages of both high structural strength and large surface area. Other advantages included low cost, chemical stability in an acid environment, good dispersion in the solution and chemically suitable for 3-APTES modification, which made it promising for immobilization using 3-APTES self-assembly monolayer technique.

3.5.3.1 *Nitrogen adsorption/desorption analysis and enzyme loading of the modified silica gel*

Nitrogen adsorption/desorption analysis was used to characterize the porous structure of the immobilization carrier. **Figure 3-25** shows the nitrogen adsorption/desorption isotherms for silica gel; 3-APTES modified silica gel, and glutaraldehyde-crosslinked 3-APTES modified silica gel. According to IUPAC classification, they can be classified as Type IV isotherms with H_2 hysteresis loops, which are characteristic of mesoporous materials with a cage-like structure [93]. **Figure 3-26** shows the pore size distributions which are calculated from nitrogen desorption branch by the Barrett-Joyner-Halenda (BJH) method. It can be seen that the pore size of silica gel decreases from 10.6-16.2 nm to 7.7-10.6 nm after 3-APTES and glutaraldehyde pretreatment. **Table 3-3** shows the summary of the pore volume and surface area. The pore volume of pretreated silica gel was 0.6 cm^3/g, calculated by the BJH method. The (Brunauer–Emmett–Teller) BET surface area of pretreated silica gel was 175.5 m^2/g. The immobilized cellulase on glutaraldehyde crosslinked 3-APTES modified silica gel was 18.8 mg protein (cellulase)/g silica gel.

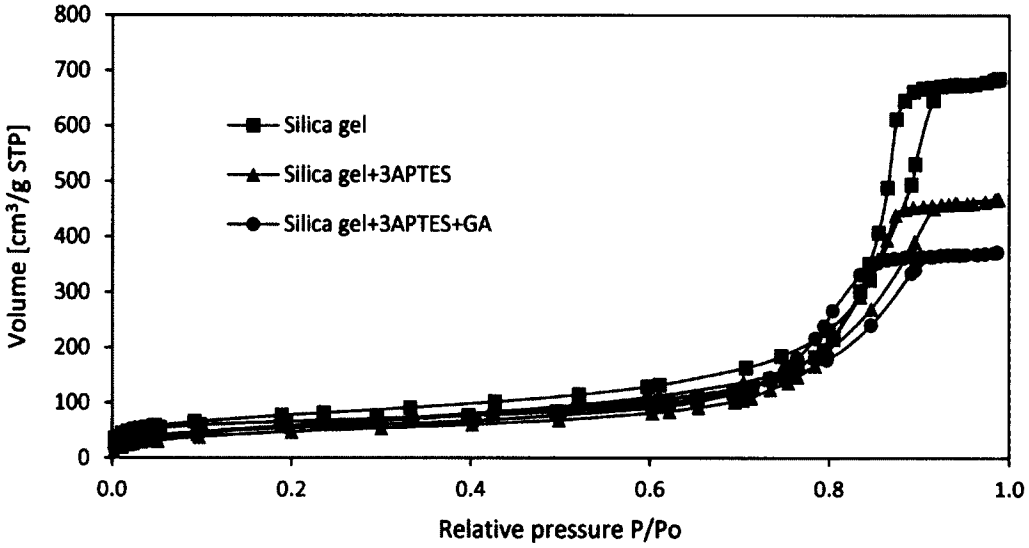

Figure 3-25: Nitrogen adsorption/desorption isotherms of silica gel, 3-APTES modified silica gel, and glutaraldehyde-crosslinked 3-APTES modified silica gel.

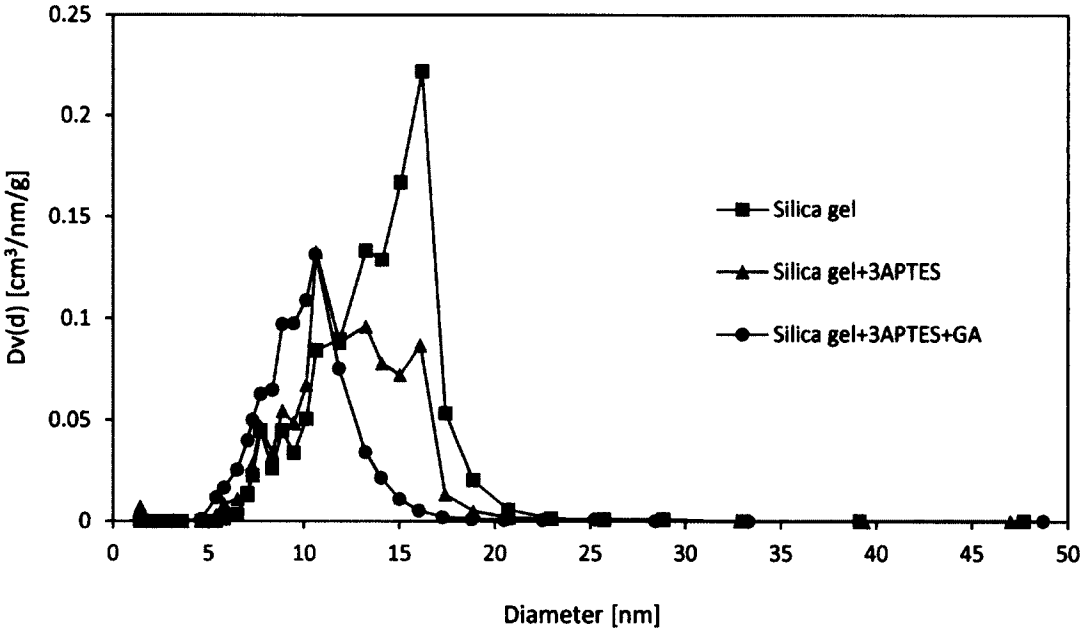

Figure 3-26: Pore size distribution obtained from nitrogen desorption branch by the BJH method.

Table 3-3: Properties of silica gel after immobilization steps.

	BET surface area [m^2/g]	Pore volume [cm^3/g]
Silica gel	251.9	1.15
Silica gel+3APTES	159.9	0.78
Silica gel+3APTES+GA	175.5	0.60

3.5.3.2 *Characterization of immobilized cellulase by FTIR analysis*

The Fourier Transform Infrared (FTIR) spectra of silica gel, 3-APTES modified silica gel, 3-APTES modified glutaraldehyde crosslinked silica gel, and cellulase immobilized silica gel are given in **Figure 3-27**. For silica gel, the Si-O-Si asymmetric stretching vibration at 1000-1250 cm^{-1}, OH bending vibration at 800 cm^{-1} appeared [92, 94]. After 3-APTES modification, a new band at 2917 cm^{-1} represented C-H stretching vibration [92]. The new peaks at 1563 cm^{-1} and 1489 cm^{-1} were attributed to the formation of an amine bicarbonate salt ($-NH_3^+(HCO_3)^-$) because of drying 3-APTES modified silica gel at room environment [92]. The new peak at 1644 cm^{-1} appeared after glutaraldehyde crosslinking suggested imine bond (C=N) vibration, which was formed between the glutaraldehyde and the 3-APTES layer [95, 96]. After cellulase immobilization, the characteristic bands of the protein at 1645 cm^{-1} and 1539 cm^{-1} associated with C=N vibration at 1644 cm^{-1} appeared in the spectrum [46]. The broad band at 3400 cm^{-1} after the immobilization of cellulase was due to association intermolecular bonds from O-H stretching vibration with N-H stretching vibration in the cellulase molecules, which confirmed the successful immobilization of cellulase onto the pretreated silica gel [97].

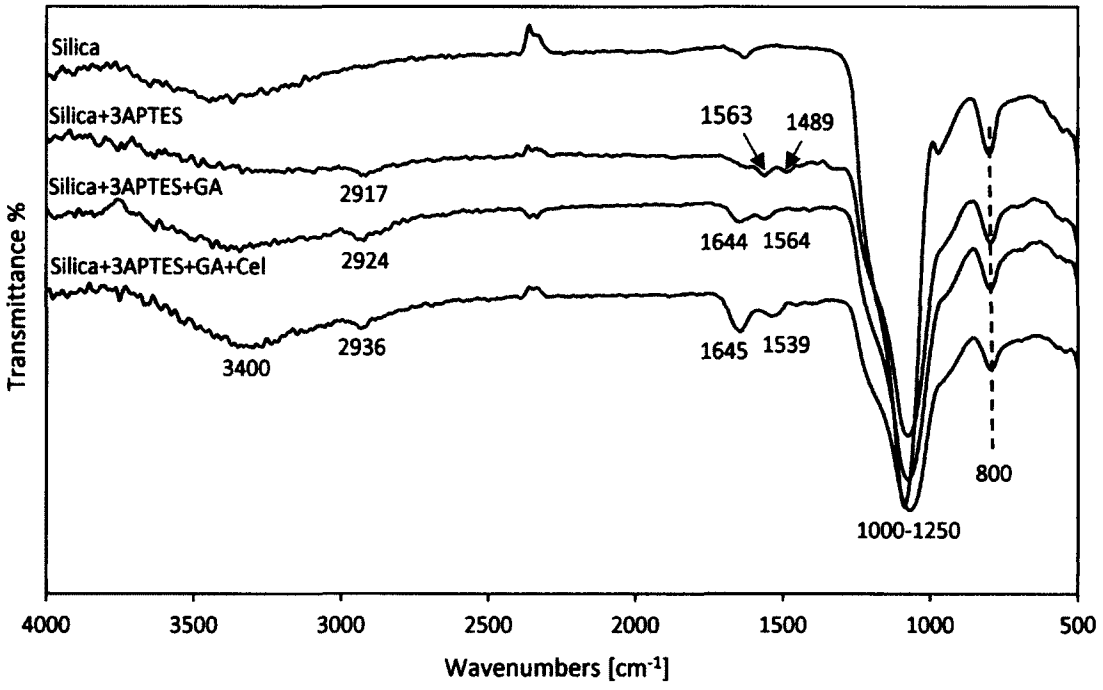

Figure 3-27: FTIR spectra of silica gel, 3-APTES modified silica gel, 3-APTES modified glutaraldehyde crosslinked silica gel, and immobilized cellulase.

3.5.3.3 *Modification of immobilization steps*

In the immobilization process, the factors that affected the activity of the immobilized cellulase included the saturation and the thickness of the 3-APTES layer. 3-APTES exhibited a fast adsorption on silica gel surface. The monolayer of 3-APTES reached equilibrium within minutes on the silica gel surface [98]. Organic solvent (toluene) was chosen for 3-APTES in order to control further adsorption and the hydrolysis of 3-APTES [92]. The activity of the immobilized cellulase was observed no change for 20-24 hours' immobilization of 3-APTES in toluene. Therefore, 24 hours was sufficient time for 3-APTES to saturate the silica gel surface.

The curing process after 3-APTES immobilization has a significant impact on the activity of the immobilized cellulase as shown in **Figure 3-28**. The activity of the immobilized cellulase after curing was 1.7 times higher than a similar experiment without

curing. The curing process in air environment can cause hydrolysis and possible oligomerization of 3-APTES immobilized. The oligomerization can decrease the thickness of the 3-APTES layer and minimize the changes of pore size of the silica gel [98]. Therefore, curing will increase the cellulase loading on the modified silica gel, and increase the overall activity of the immobilized cellulase.

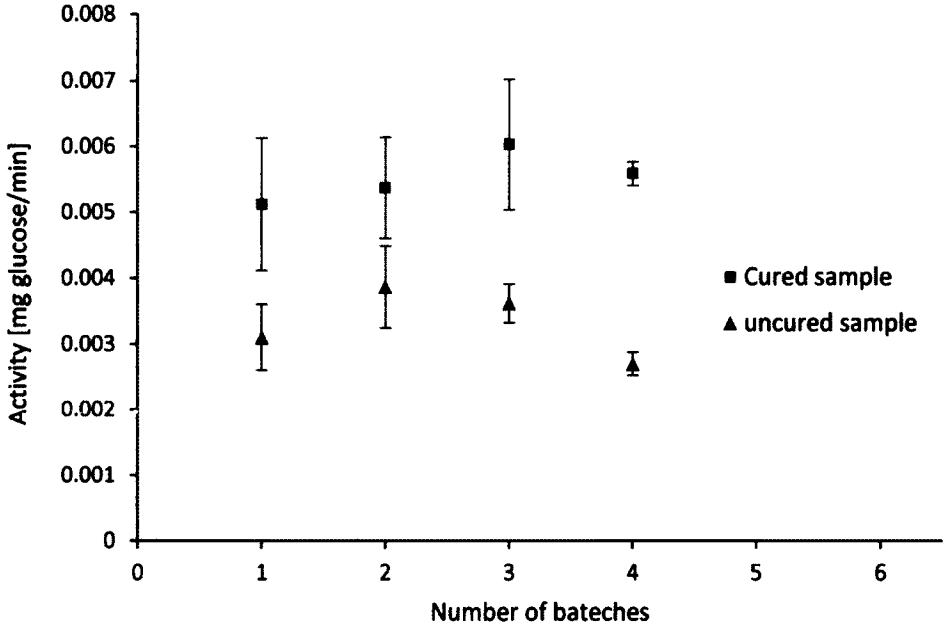

Figure 3-28: Effect of curing process after 3-APTES modification on the activity of the immobilized cellulase.

3.5.3.4 *Effect of initial concentration of cellulase solution on immobilized cellulase*

Figure 3-29 shows the results of enzymatic activity vs. the protein concentration of the cellulase solution for immobilization. The non-linear increasing curve trend is due to the Langmuir adsorption isotherm, as well as the mass transfer of produced glucose and CMC. This figure suggests that although the undiluted cellulase solution for immobilization would produce the highest absolute activity, the efficiency in the utilization of the enzyme is higher at lower dilutions due to losses at the immobilization

step (consuming more enzyme) and the hydrolysis step (low mass transfer coefficient caused by cellulase immobilized deep in the pores). Therefore, the optimal dilution of the cellulase solution for immobilization appears to be five. The reusability of the immobilized cellulase by different protein concentrations of cellulase solution is shown in **Figure 3-30**. The activity does not change after four batches of hydrolysis of CMC. This indicates that all the cellulase is firmly immobilized on the silica gel surface, and it is independent of the protein concentration of the cellulase solution for immobilization.

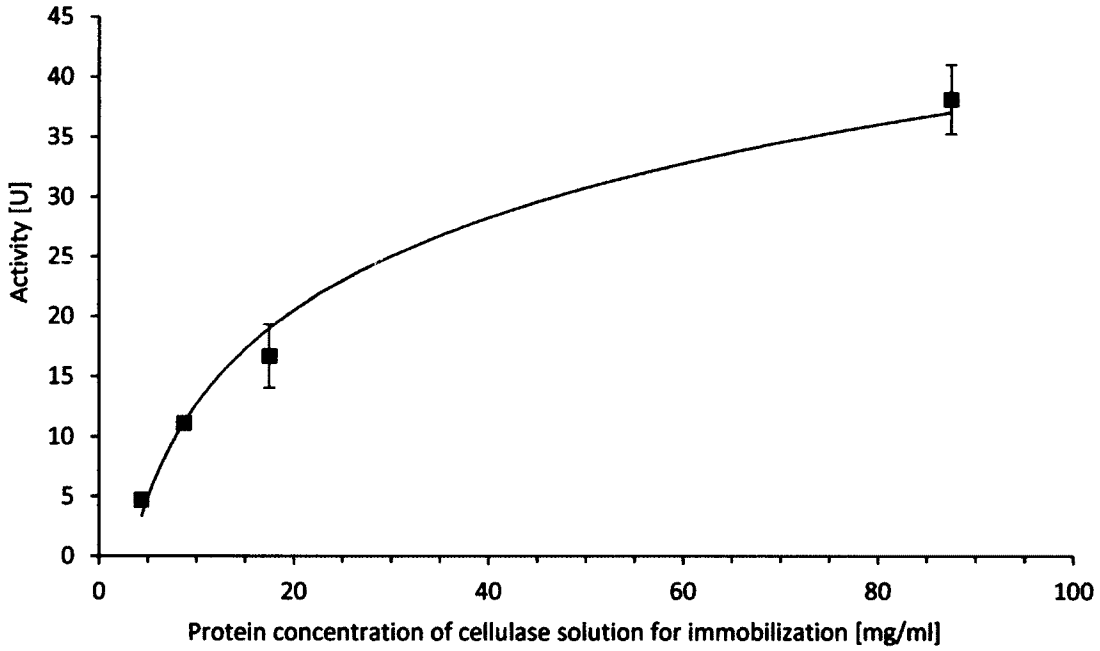

Figure 3-29: Activity vs. protein conc. of cellulase solution for immobilization.

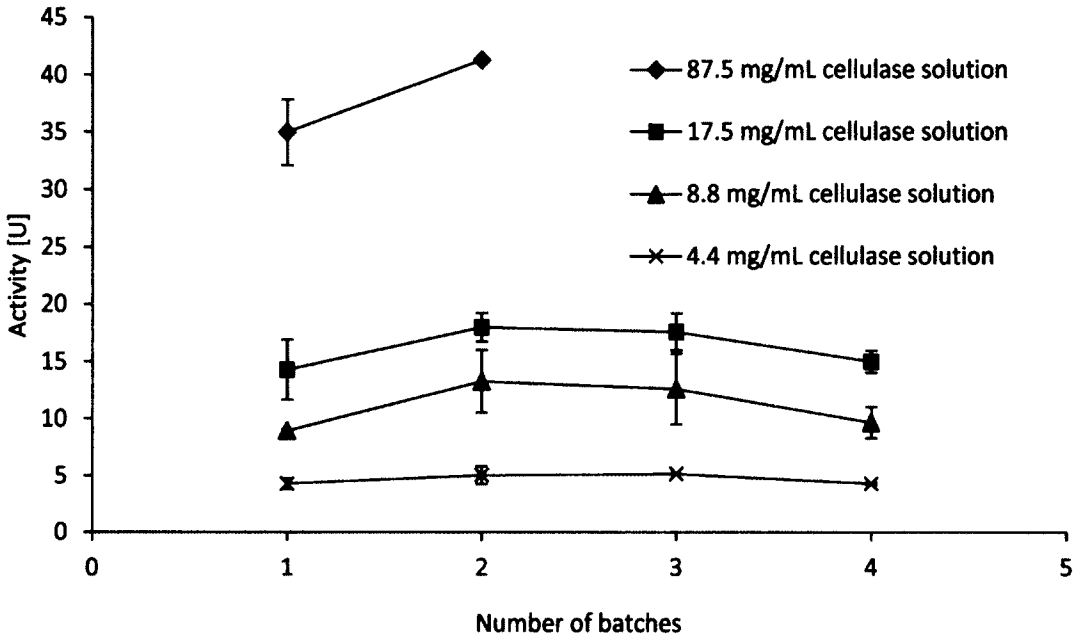

Figure 3-30: Effect of initial concentration of cellulase solution on the immobilized cellulase.

3.5.3.5 *Activity of the immobilized cellulase*

Cellulase was immobilized on 3-APTES and glutaraldehyde pretreated silica gel surfaces as described. The activity was determined by testing the produced glucose in a 10 g/L CMC solution dissolved in 10 ml pH = 6 acetate buffer (50 mmol L^{-1}) at 20°C. One unit of cellulase activity was defined as nmol glucose produced per minute. The activity of immobilized cellulase using 3-APTES and glutaraldehyde pretreatment is 474 ± 20 U per unit gram of immobilized silica gel. The activity of unit enzyme mass of immobilized cellulase is 24 ± 6 U/mg, while the one of the free cellulase is 352 ± 43 U/mg. That is: the specific activity of immobilized cellulase is 7 ± 2% compared with the similar amount of free cellulase. The denaturation of the immobilized cellulase was due to the decrease in degree of movement of the cellulase molecules after covalent binding, which was commonly found in the studies of immobilization of enzyme [99].

3.5.3.6 *Effect of temperature on the immobilized cellulase*

Temperature is an important factor for hydrolysis reaction by enzymes. The activities of the free and immobilized cellulase at different temperatures are shown in **Figure 3-31**. The results show that the activities of both the free and immobilized cellulase have the same trend: the activity increases from 20°C to 50°C and deceases after 50°C, which is consistent with many other studies [100, 101]. The immobilized cellulase on modified silica gel exhibited better relative enzymatic activity than free cellulase below 50°C. Compared with free cellulase, an increase of 18%-27% relative activity was observed for immobilized cellulase from 20°C to 40°C, respectively.

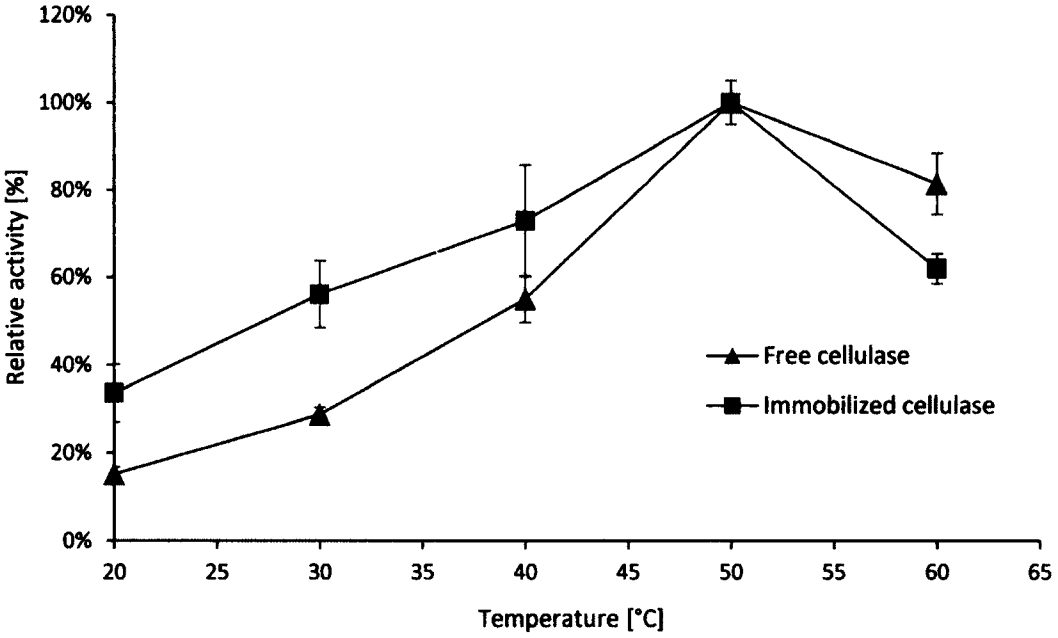

Figure 3-31: Activity of the immobilized and free cellulase according to temperatures for hydrolysis of CMC.

Reusability of immobilized cellulase was performed at 40°C, 50°C, and 60°C, since the activities of both immobilized cellulase and free cellulase in this range exhibited peak area in **Figure 3-32**. **Figure 3-32** shows that the activities decrease to 24% and

59% of the initial activities for the third batch at 50°C and the second batch at 60°C, respectively. At 40°C, 66.5% of the initial activity was retained after three recycles. And the specific activity of the immobilized cellulase at 40°C was larger than the one at 50°C and 60°C after three recycles. The possible reason is that the immobilized cellulase at high temperature, i.e., 50°C and 60°C, appears to denature relatively rapidly. Other researchers also observed the same thermal effect [91, 102]. **Figure 3-33** clearly shows that the produced glucose concentration linearly increases at 20°C to 40°C for at least 2 hours; however, it rapidly reaches its plateau at 50°C. This behavior is even more obvious at 60°C, at which the glucose concentration reaches its plateau at 30 min. Therefore, although the initial activity at 50°C is the highest, 40°C appears to be the optimal temperature for hydrolysis of CMC using immobilized cellulase.

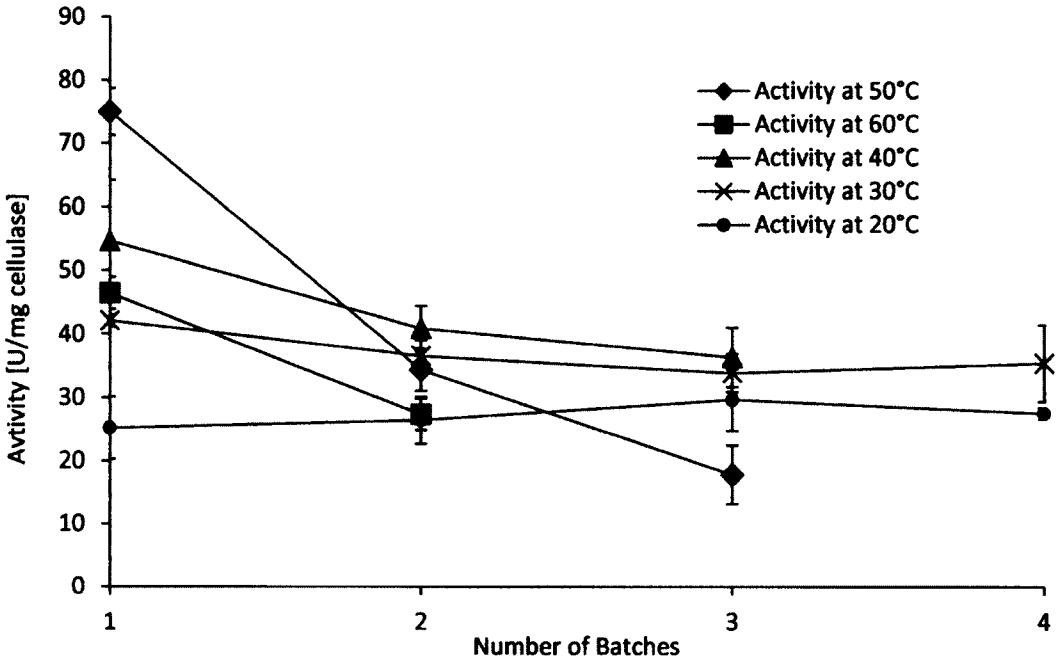

Figure 3-32: Reusability of the immobilized cellulase at different temperatures.

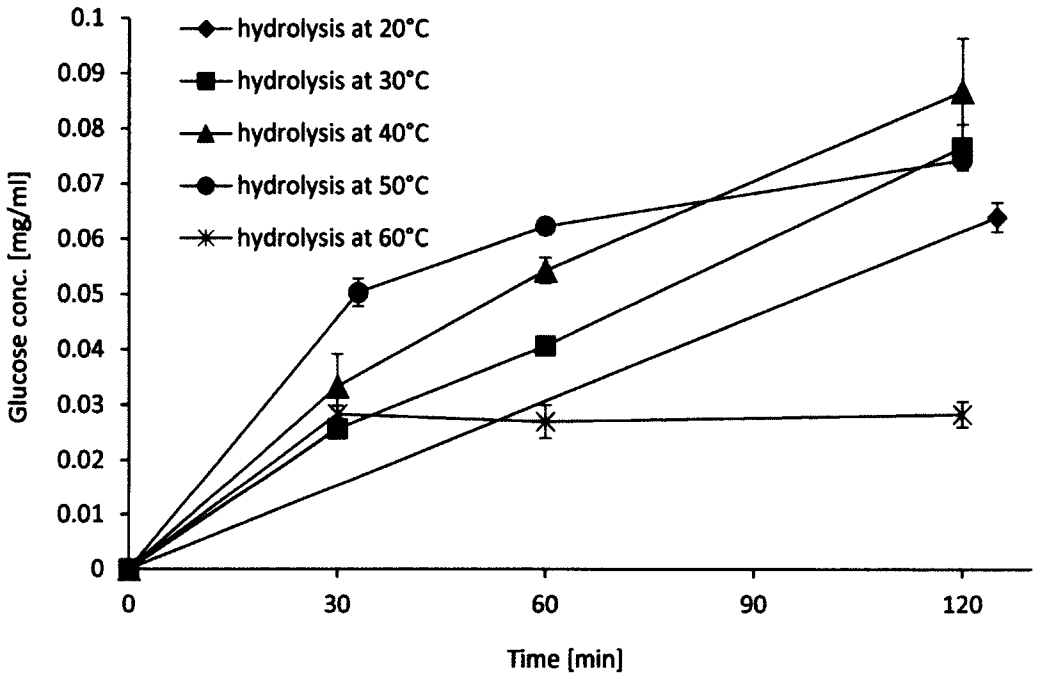

Figure 3-33: Time-dependent curve of the immobilized cellulase.

3.5.3.7 *Effect of pH on immobilized cellulase*

The pH for hydrolysis of CMC solution was also studied. The 17.5 mg/ml cellulase solution in DI water was used for immobilization. The CMC solution was prepared in pH 4, 5, 6 acetate buffer (50 mmol L^{-1}) respectively for hydrolysis at 20°C. **Figure 3-34** shows the results. The activity of the immobilized cellulase reached highest at pH 5, which was about four times higher than the one at pH 6 for the first cycle. However, the reusability at pH 5 was low. The activity of the third cycle rapidly decreased to 58% compared to the first cycle. The reusability at pH 4 was even worse. Only 14% activity retained after the fifth batch. The possible reason was that the enzyme rapidly desorbs at pH 4 and 5. Thus, the high activity for the first batch was due to the free cellulase in the CMC solution, since the specific activity of the immobilized cellulase was only 7% compared to the same amount of the free cellulase. Therefore, considering

the reusability, although the cellulase was slightly activated at pH 4 and 5, pH 6 was the optimal pH for hydrolysis of CMC.

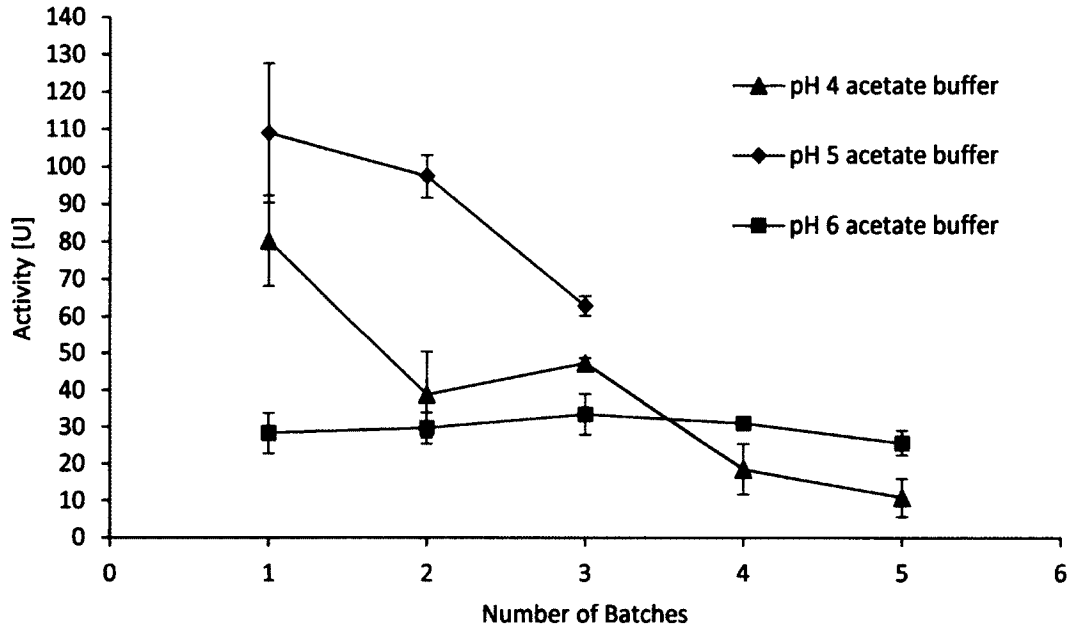

Figure 3-34: Reusability vs. pH for hydrolysis of CMC solution.

3.5.3.8 *Comparison enzymatic activity of the immobilized cellulase for crystalline cellulose (type 20) with the one of CMC*

The activity of the immobilized cellulase in cellulose (type 20) solution was tested. **Figure 3-35** shows that the activity of the immobilized cellulase in cellulose (type 20) solution is only 27% compared with the activity in CMC solution. This was because the insoluble cellulose (type 20) decreased the mass transfer between the cellulose particles and the immobilized cellulase.

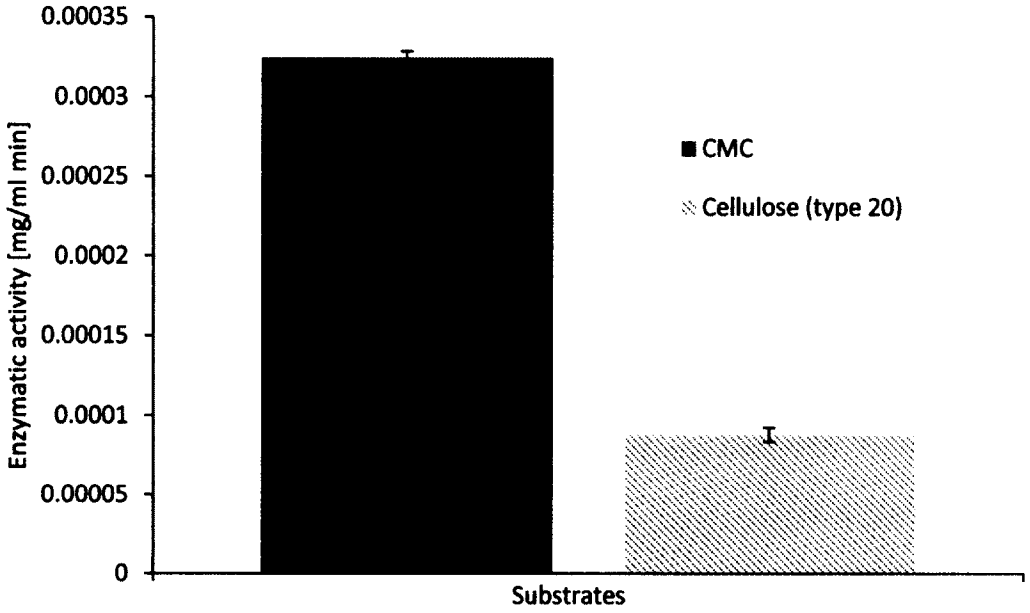

Figure 3-35: Activity of the immobilized cellulase by 3-APTES and glutaraldehyde modification on CMC vs. microcrystal cellulose (type 20). Enzyme for immobilization: Accellerase 1500, five-time diluted in DI water. Cellulose solution: 10 ml CMC or cellulose (type 20), 10 g/L in pH = 6 0.05 M acetate buffer at 20°C.

3.5.3.9 *Comparison of glucose yield by free cellulase with immobilized cellulase*

In order to compare the produced glucose yield by the free cellulase and the immobilized cellulase, hydrolysis of CMC solution under the same reaction conditions was applied. **Figure 3-36** shows that until 5000 min (slowly reaching plateau), the amount of the produced glucose by the free cellulase and the immobilized cellulase are 0.798 mg/ml and 0.374 mg/ml, respectively; that is, the produced glucose yield by the immobilized cellulase is 47% compared with the glucose yield produced by the free cellulase. Considering the excellent reusability of the immobilized cellulase (the activity retained 82% of the initial activity for the 7^{th} cycle), the immobilized cellulase provides an economical approach to produce glucose by hydrolysis of cellulose.

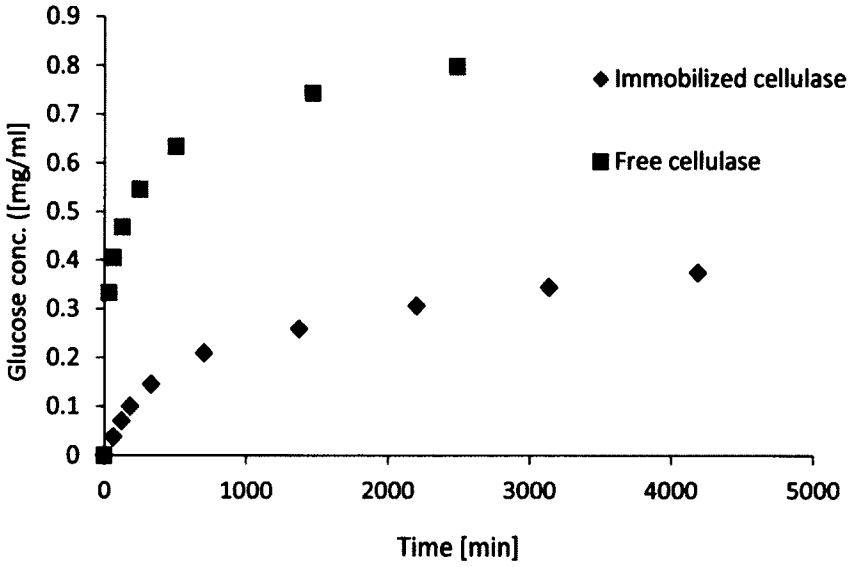

Figure 3-36: Activity of the immobilized cellulase and the free cellulase. Hydrolysis conditions: 0.2 ml 10-time diluted free cellulase (Accellerase 1500); 0.06 g immobilized silica gel as described in Section 2.5.4.1.

3.5.3.10 *Kinetic study on immobilized cellulase*

The kinetic study of the immobilized cellulase was investigated by using varying concentrations of CMC solution. **Figure 3-37** shows that the initial activity of the immobilized cellulase increases with the concentration of CMC solution until 6 g/L. After 6 g/L, the initial activity reached a plateau and slightly decreases with the increasing CMC concentration. It was because of the inhibition of the high concentration CMC on the cellulase enzyme, which was also found in other's research [103].

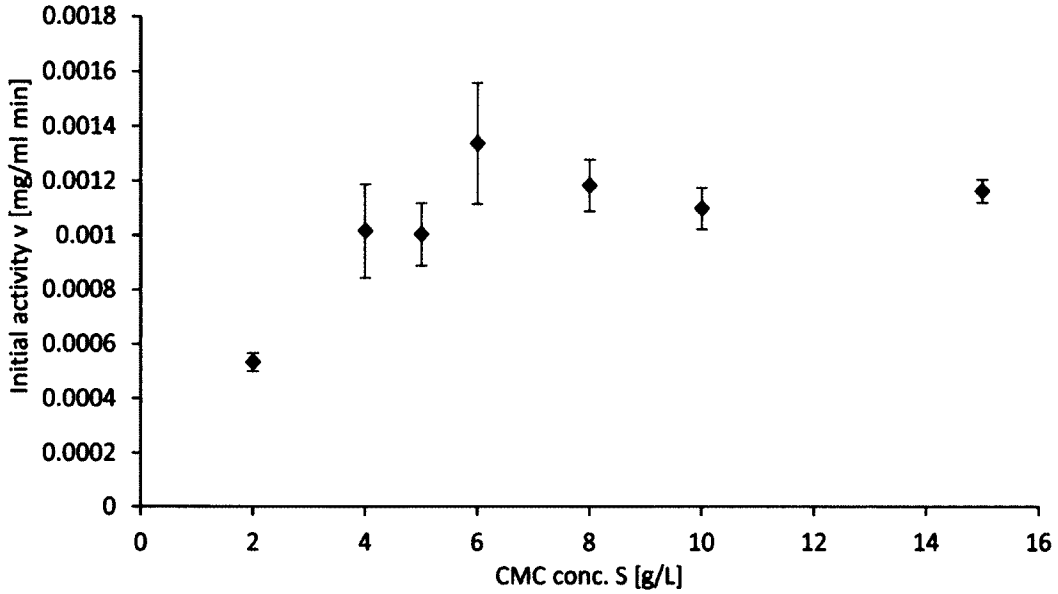

Figure 3-37: Activity of the immobilized cellulase with respect to CMC concentration. Cellulase was immobilized on silica gel as described in Section 2.5.4. Hydrolysis by the immobilized cellulase was applied in a 10 ml 2-10 g/L CMC in pH = 6 0.05 M acetate buffer at 20°C.

Michaelis-Menten kinetic derivation was used for monitor the rate of hydrolysis reaction with respect to the substrate concentration (**Eq. 3-1**). The K_m and V_{max} values were obtained by Hanes-Woolf plot (**Figure 3-38**). - K_m is the x-axis intercept of the trend line while $1/V_{max}$ is the slope of the trend line. The K_m value and V_{max} value are 1.5 g/L and 0.0013 mg/(ml min), respectively. The small K_m value suggested a high affinity of the CMC for the immobilized cellulase. **Eq. 3-1** is the Michaelis-Menten equation and **Eq. 3-2** is the Hanes-Woolf equation:

$$v = \frac{V_{max}[S]}{K_m + [S]}, \qquad \textbf{Eq. 3-1}$$

$$\frac{[S]}{v} = \frac{[S]}{V_{max}} + \frac{K_m}{V_{max}}, \qquad \textbf{Eq. 3-2}$$

v = the initial reaction rate

[S] = the substrate concentration

V_{max} is the maximal rate

K_m is the Michaelis constant (half-maximal rate).

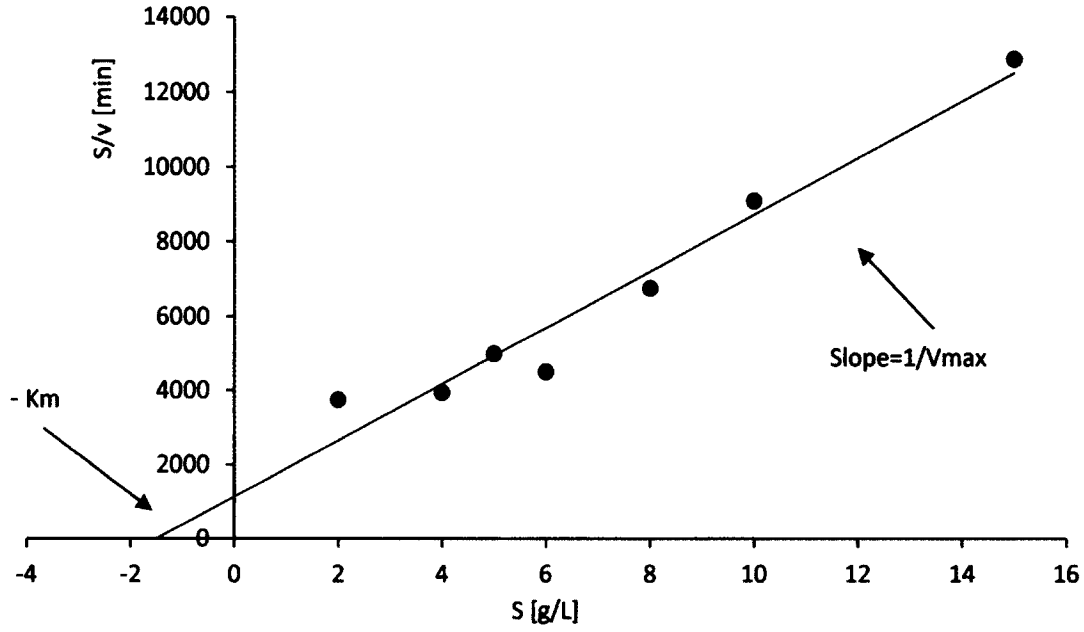

Figure 3-38: Hanes-Woolf plot of the activity of the immobilized cellulase respect to the CMC concentration.

3.5.3.11 *Reusability of the immobilized cellulase*

Reusability is an important issue for immobilized cellulase in industrial application [104-106]. The reusability of immobilized cellulase on modified silica gel was shown in **Figure 3-39**. The relative activity of the immobilized cellulase retained 100%- 82% initial activity from 1st to 7th cycle, 60%-48% from 8th to 13th cycle, and 36%-23% from 14th to 26th, respectively. In comparison, the immobilized cellulase was applied to the hydrolyzed CMC solution 3 hours for each cycle, which is longer than previously reported [39, 45, 47, 49, 91, 107-109]. The immobilized cellulase exhibits remarkable reusability up to 13 recycles. **Table 3-4** shows the comparison of reusability with other studies. Cellulase entrapped in a MeTMOS/TMOS (3:1 molar ratio) made

sol-gel matrix can be reused six times with 20% initial activity retained [110]. N.M. Mubarak *et al.* reported that cellulase immobilized on acid pretreated MWCNTs by physical adsorption retained 26% initial activity for the 8th recycle [39]. In another study, 55% initial activity was retained after four recycles when cellulase covalently bonded to the magnetic graphene nanoparticles [108]. Cellulase immobilized on magnetic nanoparticles via covalent binding can be reused six recycles with 40% initial activity retained [107]. The possible reasons of activity loss after each cycle might be immobilized enzyme loss during separation and washing processes after each cycle, enzyme denaturation, and enzyme leak (desorption) [46].

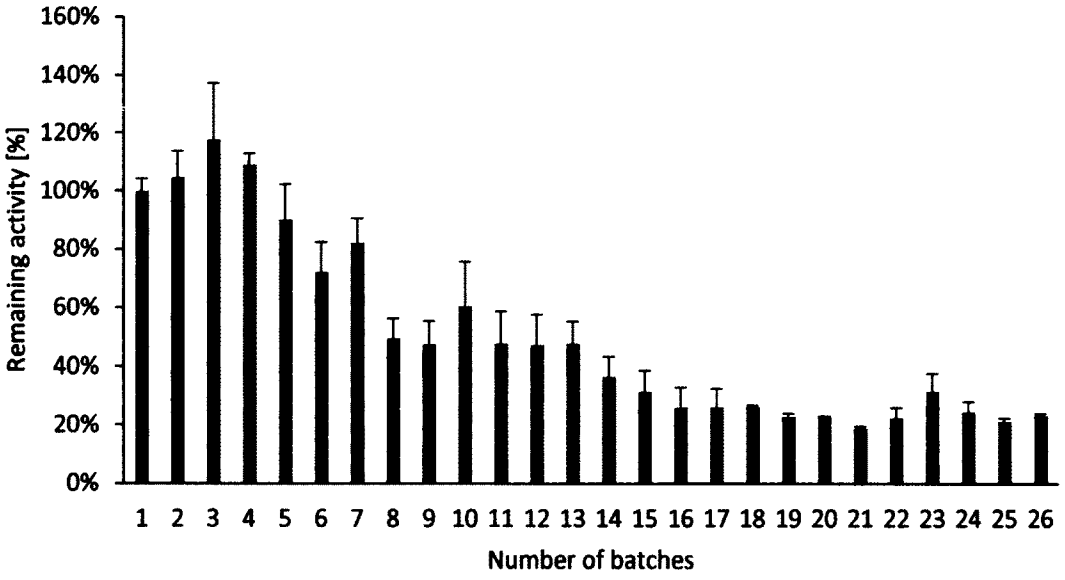

Figure 3-39: Reusability of immobilized cellulase according to batches.

Table 3-4: Cellulase immobilization carriers, techniques, and reusability of the current work and other researches.

Immobilization carrier	Immobilization technique	Reusability			Refs
		Recycles	Time for each cycle	Residual activity	
Sol-gel matrix	Sol-gel entrapment	6	24 hr	20%	[110]
Sodium alginate gel beads	Sol-gel entrapment and crosslinking	7	N/A	58.37%	[91]
Functionalized multiwall carbon nanotubes	Physical adsorption	8	30 min	26%	[39]
Ultrafine Eri silk microparticles	Physical adsorption	8	10 min	50%	[109]
Magnetic porous terpolymers	Covalent binding	6	30 min	48.2%	[45]
Magnetic graphene nanoplatelets	Covalent binding	4	1 hr	55%	[108]
Magnetic nanoparticles	Covalent binding	6	30 min	40%	[107]
Modified silica gel	Covalent binding	10	3 hr	60%	Current work

Enzyme leak (desorption) is a crucial issue for the immobilization of enzyme, and it was observed by many researchers for the immobilization of cellulase [46, 62, 99, 110]. Sandy Budi *et al.* found that up to 7% of immobilized cellulase was desorbed from silica in citrate buffer after 14 days' storage at 4°C [62]. Compared with cellulase leak in buffer solution (in washing and storage processes), it is expected that desorption during the hydrolysis of CMC would be more severe, since the binding between immobilized cellulase and CMC provide another driving force to pull the cellulase off the immobilized carrier. The cellulase leak (desorption) in the hydrolysis of the CMC can make the measured activity and reusability of the immobilized cellulase inaccurate [46]. Because free cellulase is more active than immobilized cellulase, a small amount of cellulase leaked (desorbed) would result in a high enzyme activity. Linear enzyme activity loss of immobilized cellulase was observed according to the number of recycles in many prior

studies, which suggests leaked (desorbed) cellulase strongly contributed to the activity and the lack of reusability of immobilized cellulase [39, 45, 91, 110]. In order to test the enzyme leak (desorption) of immobilized cellulase during the hydrolysis of CMC, the immobilized cellulase was centrifuged from the CMC solution after 6 hours and then the reactor was kept running. **Figure 3-40** depicts that for the hydrolysis of CMC by the immobilized silica gel in 8.8 mg/ml cellulase solution and 4.4 mg/ml cellulase solution, the produced glucose concentration never increased after centrifuging the immobilized silica gel. This strongly indicates that there is no enzyme desorption during the hydrolysis of CMC regardless of the protein concentration of the cellulase solution for immobilization. This was likely due to the entrapment of cellulase molecule in the silica gel pore structure and the strong covalent bond between the cellulase molecule and the silica gel surface, which make the specific activity low but maximize reusability.

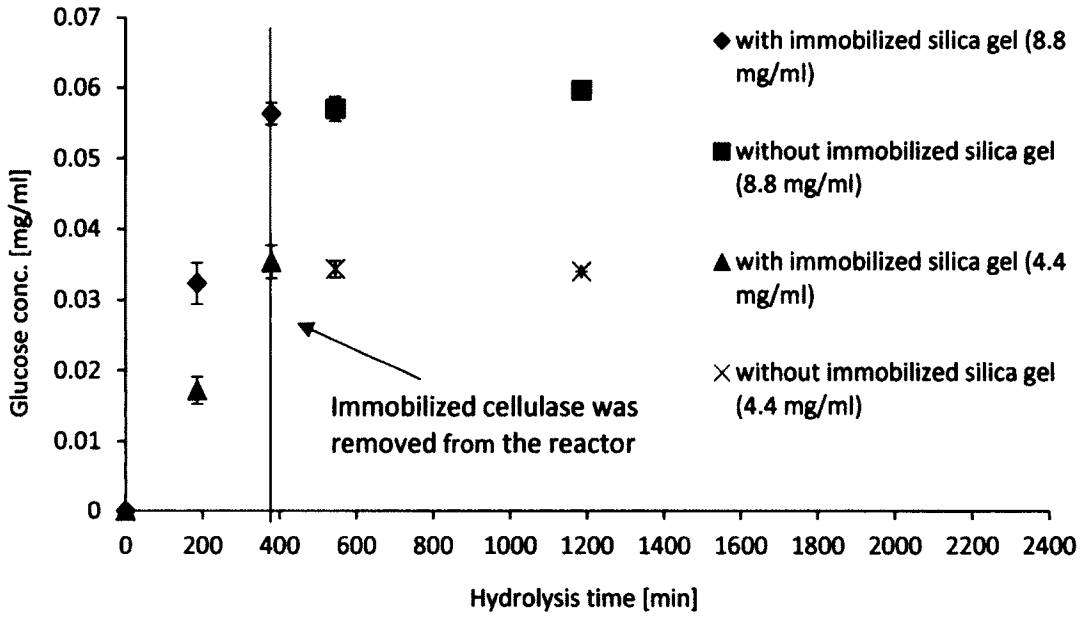

Figure 3-40: Hydrolysis time vs. produced glucose concentrations.

Since there was no enzyme leak from the immobilized silica gel, the activity loss could be attributed to denaturation of the immobilized cellulase. The immobilized cellulase exhibited three stages of activity loss in reusability, i.e., the first stage which was from 1st to 7th cycle (the activity retained 100%-82%), the second stage which was from 8th to 13th cycle (the activity retained 60%-48%), and the third stage which was from 14th to 26th cycle (the activity retained 36%-23%). A possible explanation of this behavior is that the immobilized cellulase outside the pores of silica gel was denatured after the first stage, while the one near the pores of silica gel was denatured after the second stage. The porous structure of the silica gel lowered the biological activity of the immobilized cellulase. However it also likely protected the cellulase molecules immobilized in the pores from the conformational structure shifting [111]. Therefore, the activity of immobilized cellulase remained stable after the 13th cycle. This is also confirmed by **Figure 3-41**, which shows that the activity of immobilized cellulase barely decreases after 5th day up to 14th days (from 14th cycle to 26th cycle).

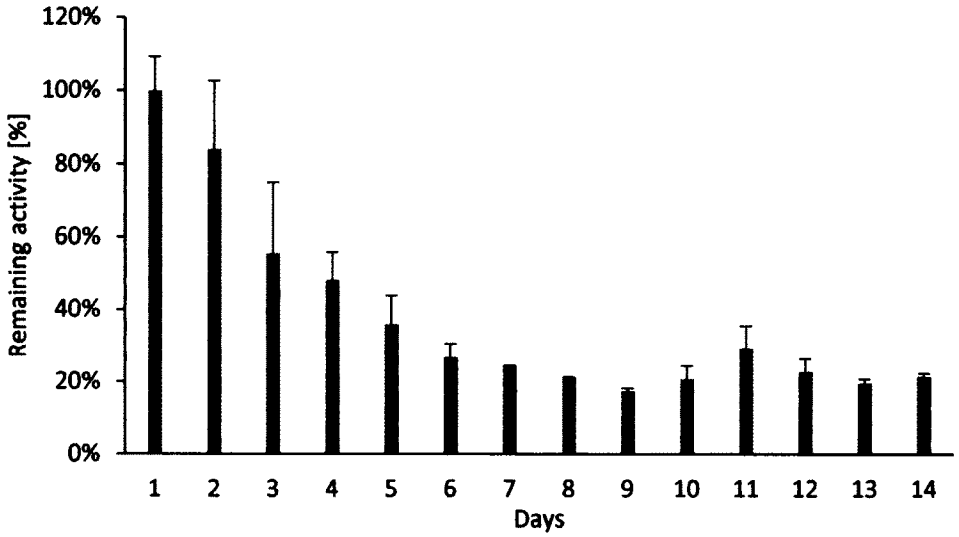

Figure 3-41: Reusability of immobilized cellulase according to days.

The storage stability of an enzyme is another important factor that limit its applications. The immobilized silica gel was operated first batch and then washed by DI water. After centrifuging and removing supernatant, the deposition (immobilized silica gel) was sealed and kept at 4°C in the refrigerator for 38 days. The second activity experiment was performed after the 38 day incubation period and the immobilized enzyme on the silica gel still retained 92.4% of its initial activity.

3.6 Comparison of the Activities of the Immobilized Cellulases by Four Different Immobilization Techniques

The activities of the immobilized cellulase by four different immobilization techniques were compared. Ten-time diluted cellulase solution (Accellerase 1500) was used for immobilization of the immobilization carriers. The mass of the immobilized cellulase for LbL was calculated by the QCM results as shown in **Figure 3-4**. The mass of the immobilized cellulase for 3-APTES self-assembly monolayer was tested by the protein assay as describe in Section 2.6.

- LbL: Hydrolysis of 100 ml 10 g/L CMC solution by 27.2 g immobilized polystyrene beads was operated in pH = 6 0.05 M acetate buffer at 25°C.
- Ca^{2+}-$Al(OH)_x$ modification: Hydrolysis of 40 ml 10 g/L CMC solution by 11.2 g immobilized molecular sieves (pellets) was operated in pH = 6 0.05 M acetate buffer at 25°C.
- Ca^{2+}-$Al(OH)_x$ modification & LbL: Hydrolysis of 40 ml 10 g/L CMC solution by 11.2 g immobilized molecular sieves (beads) was operated in pH = 6 0.05 M acetate buffer at 25°C.

- 3-APTES self-assembly monolayer: Hydrolysis of 10 ml 10 g/L CMC solution by 0.06 g immobilized silica gel was operated in pH = 6 0.05 M acetate buffer at 20°C.

One unit of cellulase activity was defined as nmol glucose produced per minute. **Table 3-5** shows these results. The initial activities of the immobilized cellulase by LbL, Ca^{2+}-$Al(OH)_x$ and Ca^{2+}-$Al(OH)_x$ & LbL were much higher than the activity of the immobilized cellulase by 3-APTES self-assembly monolayer. A possible reason was that the free enzyme desorbed from the immobilization carriers. The specific activity of the immobilized cellulase by LbL was 267 U per enzyme mass, which was very close to the specific activity of the free cellulase (352 U per enzyme mass). A combination of the fact that desorbed enzyme was observed, it suggested that the desorbed enzyme contributed to the enzymatic activity. The immobilized silica gel had the highest activity per unit mass immobilization carriers and the enzyme loading. A possible reason was that silica gel had the higher surface area per volume. The immobilized silica gel had the best reusability, which was due to the strong covalent bonding between the cellulase molecules and the immobilization carrier's surface.

Table 3-5: Comparison of the activities of the immobilized cellulases by four different immobilization techniques.

Immobilization techniques	Immobilization carriers	Enzyme loading (mg/g)	Initial activity (produced glucose mg/min)	Activity per unit mass immobilization carriers (U/g)	Activity per enzyme mass (U)	Reusability, relative activity for the 2nd recycle (%)
LbL	Polystyrene beads	0.013	0.0172	4	267	12%
Ca-Al(OH)	Molecular sieves (pellets)	NA	0.25532	127	NA	58%
Ca-Al(OH) & LbL	Molecular sieves (beads)	NA	0.12456	62	NA	67%
3-APTES and GA	Silica gel	12.207	0.00164	152	12	103%

CHAPTER 4

CONCLUSION AND FUTURE WORK

4.1 Conclusion

In this project, immobilization of cellulase was explored for reuse to reduce bioethanol production cost in commercial scale reactors. Four different enzyme immobilization methods, i.e. LbL, Ca^{2+}-$Al(OH)_x$ modification, combination of Ca^{2+}-$Al(OH)_x$ modification & LbL, and 3-APTES self-assembly monolayer, were studied. Four different materials were applied as immobilization carriers, including polystyrene beads, molecular sieves, glass beads, and silica gel.

For LbL technique, polystyrene beads were used as immobilization carriers. QCM results showed that the mass of the immobilized cellulase increased with the number of cellulase layers. The results from hydrolysis of cellulose showed that the activity of the immobilized cellulase increased with the number of the cellulase layers up to five cellulase layers. Further increasing the number of the cellulase layers lowered the activity of the immobilized cellulase. Enzyme desorption was observed during hydrolysis of cellulose by the immobilized cellulase. Sealing layers (PEI or PEI/PSS layers) or crosslinking was applied after the final cellulase layer to protect the immobilized cellulase from stripping off. However, the initial activity of the immobilized cellulase dramatically decreased and low reusability was observed.

For Ca^{2+}-$Al(OH)_x$ modification method, molecular sieves were used as immobilization carriers. After Ca^{2+}-$Al(OH)_x$ modification, the activity of the immobilized cellulase increased 8.7 times compared with the activity of the immobilized cellulase on non-Ca^{2+}-$Al(OH)_x$ pretreated molecular sieves. The reusability of the immobilized cellulase was observed. The second cycle's activity of the immobilized cellulase by Ca^{2+}-$Al(OH)_x$ modification method retained 58% initial activity in the packed bed reactor.

LbL technique was applied after Ca^{2+}-$Al(OH)_x$ modification method. The reusability increased with the number of enzyme bilayers. Great reusability of the 15-bilayer immobilized cellulase on Ca^{2+}-$Al(OH)_x$ pretreated molecular sieves (beads) was observed. The 6^{th} recycle's activity was 75% of its initial activity. By contrast, the 6^{th} recycle's activity of the directly immobilized cellulase on the Ca^{2+}-$Al(OH)_x$ modified molecular sieves was 17% of its initial activity. However, the initial activity of the immobilized cellulase decreased with the number of enzyme layers. Crosslinking dramatically decreased the initial activity, yet rarely improved the reusability of the immobilized cellulase.

For 3-APTES self-assembly monolayer method, molecular sieves (beads), glass beads and silica gel were used as immobilization carriers. The immobilized cellulase on silica gel showed the best results. Multiple reuses were observed up to 26 recycles and 14 days. No cellulase desorption was observed during the hydrolysis of the CMC solution at the optimized conditions of pH 6 acetate buffer (50 mmol L^{-1}). The influence of pH and temperature on hydrolysis of CMC by the immobilized cellulase was studied. The optimal temperature for hydrolysis of CMC was 40°C. The best reusability of the

immobilized cellulase appeared in hydrolysis of CMC in pH 6 buffer solution. The glucose yield of the immobilized cellulase was 47% compared with the free cellulase. Considering the excellent reusability of the immobilized cellulase, the immobilized cellulase by 3-APTES self-assembly monolayer technique provides a promising approach to reduce the cost of glucose production.

4.2 Future Work

In this work, the immobilization of cellulase by 3-APTES self-assembly monolayer method was demonstrated to be effective at both maintaining initial activity and retaining activity over a larger number of reuse cycles. Other covalent bonding techniques might be studied to reduce the impact of specific enzyme activity by immobilization. Longer linkers might reduce steric hindrances; cross-linkers might be able to identify target specific regions of the enzyme that minimize activity loss. Further kinetic study of the immobilized cellulase is needed. Michaelis-Menten equation only shows the substrate's affinity and the maximal rate of the immobilized cellulase. However, it lacks details of the reaction, such as inhibitions (glucose inhibition and CMC inhibition), influence of pH and temperature on enzymatic rates of hydrolysis, and mass transfer limitation. It also cannot be used to predict the produced glucose profile during hydrolysis of CMC.

The separation of the immobilized enzyme from the cellulose slurry in a commercial environment is a future opportunity. The CMC used in the majority of studies allowed the use of simple filtration to separate the enzyme immobilized on carriers such as polystyrene beads, molecular sieves, glass beads and silica gel. Density

differences may allow centrifugation to be effective. However other forces such as functionalization with magnetic particles might be beneficial.

BIBLIOGRAPHY

1. BP statistical review of world Energy. 2014.

2. National Research Council (U.S.), Review of the research strategy for biomass-derived transportation fuels. 1999, National Academies Press: Washington, D.C.

3. Nigam, P.S. and A. Singh, Production of liquid biofuels from renewable resources. Progress in Energy and Combustion Science, 2011. **37**(1): p. 52-68.

4. Mabee, W.E. and J.N. Saddler, Bioethanol from lignocellulosics: Status and perspectives in Canada. Bioresource Technology, 2010. **101**(13): p. 4806-13.

5. Tosa, T., *et al.*, Studies on continuous enzyme reactions. I. Screening of carriers for preparation of water-insoluble aminoacylase. Enzymologia, 1966. **31**(4): p. 214-224.

6. Brena, B.M. and F. Batista-Viera, Immobilization of enzymes, in Methods in biotechnology: Immobilization of enzymes and cells, J.M. Guisan, Editor. 2006, Humana Press. p. 15-30.

7. Guibault, G.G., J.M. Kauffmann, and G.J. Patriarche, Immobilized enzyme electrodes as biosensors, in Protein immobilization: Fundamentals and applications, R.F. Taylor, Editor. 1991, Marcel Dekker: New York, NT. p. 209-262.

8. Taylor, R.F., Immobilized antibody and receptor based biosensors, in Protein immobilization: Fundamentals and applications, R.F. Taylor, Editor. 1991, Marcel Dekker: New York, NY. p. 263-303.

9. Wyman, C., *et al.*, Hydrolysis of cellulose and hemicellulose, in polysaccharides: Structural diversity and functional versatility, S. Dumitriu, Editor. 2004, CRC Press.

10. Varrot, A., *et al.*, Structural basis for ligand binding and processivity in cellobiohydrolase Cel6A from humicola insolens. Structure, 2003. **11**(7): p. 855-864.

11. Brown, R.M., Cellulose structure and biosynthesis: What is in store for the 21st century? Journal of Polymer Science Part A: Polymer Chemistry, 2004. **42**(3): p. 487-495.

12. O'Sullivan, A.C., Cellulose: the structure slowly unravels. Cellulose, 1997. **4**(3): p. 173-207.

13. [cited 2015 12/5]; Available from: http://en.wikipedia.org/wiki/Cellulose#mediaviewer/File:Cellulose_strand.svg

14. Brown, C.J. and A.A. Houghton, The chemical and physical properties of carboxymethylcellulose and its salts. Journal of the Society of Chemical Industry, 1941. **60**(10): p. 254-258.

15. [cited 2015 12/4]; Available from: http://www.sigmaaldrich.com/catalog/substance/sodiumcarboxymethylcellulose12345900432411?lang=en&region=US.

16. Henrissat, B., T.T. Teeri, and R.A.J. Warren, A scheme for designating enzymes that hydrolyse the polysaccharides in the cell walls of plants. FEBS Letters, 1998. **425**(2): p. 352-354.

17. Boisset, C., *et al.*, Imaging the enzymatic digestion of bacterial cellulose ribbons reveals the endo character of the cellobiohydrolase Cel6A from humicola insolens and its mode of synergy with cellobiohydrolase Cel7A. Applied and Environmental Microbiology, 2000. **66**(4): p. 1444-1452.

18. Lynd, L.R., *et al.*, Microbial cellulose utilization: Fundamentals and biotechnology. Microbiology and Molecular Biology Reviews, 2002. **66**(3): p. 506-577.

19. Khademi, S., *et al.*, Structure of an endoglucanase from termite, nasutitermes takasagoensis. Acta Crystallographica Section D: Biological Crystallography, 2003. **58**(Pt 4): p. 653-659.

20. Davies, G. and B. Henrissat, Structures and mechanisms of glycosyl hydrolases. Structure, 1995. **3**(9): p. 853-859.

21. Rouvinen, J., *et al.*, Three-dimensional structure of cellobiohydrolase II from Trichoderma reesei. Science, 1990. **249**(4967): p. 380-386.

22. Divne, C., *et al.*, The three-dimensional crystal structure of the catalytic core of cellobiohydrolase I from Trichoderma reesei. Science, 1994. **265**(5171): p. 524-528.

23. Nidetzky, B., *et al.*, Cellulose hydrolysis by the cellulases from Trichoderma reesei: a new model for synergistic interaction. Biochemical Journal, 1994. **298**(3): p. 705-710.

24. Harjunpaa, V., *et al.*, Cello-oligosaccharide hydrolysis by cellobiohydrolase II from Trichoderma reesei. association and rate constants derived from an analysis of progress curves. European Journal of Biochemistry, 1996. **240**(3): p. 584-591.

25. Teeri, T.T., Crystalline cellulose degradation: new insight into the function of cellobiohydrolases. Trends in Biotechnology, 1997. **15**(5): p. 160-167.

26. Divne, C., *et al.*, High-resolution crystal structures reveal how a cellulose chain is bound in the 50 Å long tunnel of cellobiohydrolase I from Trichoderma reesei. Journal of Molecular Biology, 1998. **275**(2): p. 309-25.

27. Duff, S.J.B. and W.D. Murray, Bioconversion of forest products industry waste cellulosics to fuel ethanol: A review. Bioresource Technology, 1996. **55**(1): p. 1-33.

28. Tolan, J.S. and B. Foody, Cellulase from submerged fermentation. Advances in Biochemical Engineering/Biotechnology, 1999. **65**: p. 41-67.

29. Jeng, W.Y., *et al.*, Structural and functional analysis of three beta-glucosidases from bacterium Clostridium cellulovorans, fungus Trichoderma reesei and termite Neotermes koshunensis. Journal of Structural Biology, 2011. **173**(1): p. 46-56.

30. Trevan, M., Techniques of immobilization, in Immobilized enzymes: An introduction and applications in biotechnology, M. Trevan, Editor. 1980, Wiley: Chichester-New York. p. 1-9.

31. Brodelius, P. and K. Mosbach, Immobilization techniques for cells/organelles, in Methods in enzymology, K. Mosbach, Editor. 1987, Academic Press: London. p. 173-454.

32. Buchholz, K. and J. Klein, Characterization of immobilized biocatalysts, in Methods in enzymology, K. Mosbach, Editor. 1987, Academic Press: London. p. 3-30.

33. Cabral, J.M.S. and J.F. Kennedy, Covalent and coordination immobilization of proteins, in Protein immobilization: Fundamentals and applications, R.F. Taylor, Editor. 1991, Marcel Dekker: New York, NY. p. 73-138.

34. Ravi Kumar, M.N.V., A review of chitin and chitosan applications. Reactive and Functional Polymers, 2000. **46**(1): p. 1-27.

35. El-Ghaffar, M.A.A. and M.S. Hashem, Chitosan and its amino acids condensation adducts as reactive natural polymer supports for cellulase immobilization. Carbohydrate Polymers, 2010. **81**(3): p. 507-516.

36. Darias, R. and R. Villalonga, Functional stabilization of cellulase by covalent modification with chitosan. Journal of Chemical Technology & Biotechnology, 2001. **76**(5): p. 489-493.

37. Overney, G., W. Zhong, and D. Tomanek, Structural rigidity and low frequency vibrational modes of long carbon tubules. Zeitschrift fur Physik D Atoms, Molecules and Clusters, 1993. **27**(1): p. 93-96.

38. Panchakarla, L.S. and A. Govindaraj, Covalent and non-covalent functionalization and solubilization of double-walled carbon nanotubes in nonpolar and aqueous media. Journal of Chemical Sciences, 2009. **120**(6): p. 607-611.

39. Mubarak, N.M., *et al.*, Immobilization of cellulase enzyme on functionalized multiwall carbon nanotubes. Journal of Molecular Catalysis B: Enzymatic, 2014. **107**: p. 124-131.

40. Lei, Z. and Q. Jiang, Synthesis and properties of immobilized pectinase onto the macroporous polyacrylamide microspheres. Journal of Agricultural Food Chemistry, 2011. **59**(6): p. 2592-2599.

41. Li, Y., *et al.*, Pore size of macroporous polystyrene microspheres affects lipase immobilization. Journal of Molecular Catalysis B: Enzymatic, 2010. **66**(1-2): p. 182-189.

42. Xu, J., *et al.*, Characterization of direct cellulase immobilization with superparamagnetic nanoparticles. Biocatalysis and Biotransformation, 2011. **29**(2-3): p. 71-76.

43. Zhang, W., *et al.*, Increase in stability of cellulase immobilized on functionalized magnetic nanospheres. Journal of Magnetism and Magnetic Materials, 2015. **375**: p. 117-123.

44. Li, S.-K., *et al.*, Simple and efficient synthesis of copper(II)-modified uniform magnetic Fe_3O_4@SiO_2 core/shell microspheres for immobilization of cellulase. Journal of Nanoparticle Research, 2013. **15**(11).

45. Qi, H., *et al.*, Preparation of magnetic porous terpolymer and its application in cellulase immobilization. Polymer Engineering & Science, 2015. **55**(5): p. 1039-1045.

46. Zang, L., *et al.*, Preparation of magnetic chitosan nanoparticles as support for cellulase immobilization. Industrial & Engineering Chemistry Research, 2014. **53**(9): p. 3448-3454.

47. Mishra, A. and M. Sardar, Cellulase assisted synthesis of nano-silver and gold: Application as immobilization matrix for biocatalysis. International Journal of Biological Macromololecules, 2015. **77**: p. 105-113.

48. Safari Sinegani, A.A., G. Emtiazi, and H. Shariatmadari, Sorption and immobilization of cellulase on silicate clay minerals. Journal of Colloid and Interface Science, 2005. **290**(1): p. 39-44.

49. Anuradha Jabasingh, S. and C. Valli Nachiyar, Immobilization of Aspergillus nidulans SU04 cellulase on modified activated carbon. Journal of Thermal Analysis and Calorimetry, 2011. **109**(1): p. 193-202.

50. Han, K., *et al.*, Activity of glucose oxidase entrapped in mesoporous gels. Biochemical Engineering Journal, 2005. **22**(2): p. 161-166.

51. Díaz, J.F. and K.J. Balkus, Enzyme immobilization in MCM-41 molecular sieve. Journal of Molecular Catalysis B: Enzymatic, 1996. **2**(2-3): p. 115-126.

52. Yiu, H.H.P., *et al.*, Size selective protein adsorption on thiol-functionalised SBA-15 mesoporous molecular sieve. Physical Chemistry Chemical Physics, 2001. **3**(15): p. 2983-2985.

53. Yiu, H.H.P. and P.A. Wright, Enzymes supported on ordered mesoporous solids: a special case of an inorganic–organic hybrid. Journal of Materials Chemistry, 2005. **15**(35-36): p. 3690.

54. Lei, C., *et al.*, Characterization of functionalized nanoporous supports for protein confinement. Nanotechnology, 2006. **17**(22): p. 5531-5538.

55. Qiao, S.Z., *et al.*, Synthesis and bio-adsorptive properties of large-pore periodic mesoporous organosilica rods. Chemistry of Materials, 2005. **17**(24): p. 6172-6176.

56. Qiao, S.Z., *et al.*, Synthesis and lysozyme adsorption of rod-like large-pore periodic mesoporous organosilica. Progress in Solid State Chemistry, 2006. **34**(2-4): p. 249-256.

57. Budi Hartono, S., *et al.*, Improving adsorbent properties of cage-like ordered amine functionalized mesoporous silica with very large pores for bioadsorption. Langmuir, 2009. **25**(11): p. 6413-24.

58. Chibata, I., Immobilized enzymes, research and development. Kodansha scientific books. 1978: John Wiley & Sons Inc.: New York and London.

59. Cass, T. and F.S. Ligler, Immobilized biomolecules in analysis: A practical approach. Practical Approach Series, B.D. Hames, Editor. 1999, Oxford University Press: New York.

60. Takimoto, A., *et al.*, Encapsulation of cellulase with mesoporous silica (SBA-15). Microporous and Mesoporous Materials, 2008. **116**(1-3): p. 601-606.

61. Chang, R.H.-Y., J. Jang, and K.C.W. Wu, Cellulase immobilized mesoporous silica nanocatalysts for efficient cellulose-to-glucose conversion. Green Chemistry, 2011. **13**(10): p. 2844.

62. Hartono, S.B., *et al.*, Functionalized mesoporous silica with very large pores for cellulase immobilization. The Journal of Physical Chemistry C, 2010. **114**(18): p. 8353-8362.

63. Tebeka, I.R., A.G. Silva, and D.F. Petri, Hydrolytic activity of free and immobilized cellulase. Langmuir, 2009. **25**(3): p. 1582-1587.

64. Iler, R.K., Multilayers of colloidal particles. Journal of Colloid and Interface Science, 1966. **21**(6): p. 569-594.

65. Decher, G., Fuzzy nanoassemblies: Toward layered polymeric multicomposites. Science, 1997. **277**(5330): p. 1232-1237.

66. Lvov, Y., G. Decher, and H. Moehwald, Assembly, structural characterization, and thermal behavior of layer-by-layer deposited ultrathin films of poly(vinyl sulfate) and poly(allylamine). Langmuir, 1993. **9**(2): p. 481-486.

67. Onda, M., *et al.*, Molecularly flat films of linear polyions and proteins obtained by the alternate adsorption method. Japanese Journal of Applied Physics, 1997. **36**(Part 2, No. 12A): p. L1608-L1611.

68. Sano, M., Y. Lvov, and T. Kunitake, Formation of ultrathin polymer layers on solid substrates by means of polymerization-induced epitaxy and alternate adsorption. Annual Review of Materials Science, 1996. **26**(1): p. 153-187.

69. Lvov, Y., *et al.*, Successive deposition of alternate layers of polyelectrolytes and a charged virus. Langmuir, 1994. **10**(11): p. 4232-4236.

70. Kleinfeld, E.R. and G.S. Ferguson, Stepwise formation of multilayered nanostructural films from macromolecular precursors. Science, 1994. **265**(5170): p. 370-3.

71. Kotov, N.A., I. Dekany, and J.H. Fendler, Layer-by-layer self-assembly of polyelectrolyte-semiconductor nanoparticle composite films. The Journal of Physical Chemistry, 1995. **99**(35): p. 13065-13069.

72. Fendler, J.H. and F.C. Meldrum, The Colloid chemical approach to nanostructured materials. Advanced Materials, 1995. **7**(7): p. 607-632.

73. Schmitt, J., *et al.*, Metal nanoparticle/polymer superlattice films: Fabrication and control of layer structure. Advanced Materials, 1997. **9**(1): p. 61-65.

74. Bliznynuk, V.N. and V.V. Tsukruk, Composite self-assembled films from charged latex nanoparticles. Polymer Preprints Division of Polymer Chemistry of the American Chemical Society, 1997. **38**(1): p. 963-964.

75. Lvov, Y., *et al.*, Alternate assembly of ordered multilayers of SiO_2 and other nanoparticles and polyions. Langmuir, 1997. **13**(23): p. 6195-6203.

76. Lvov, Y.M., *et al.*, High-speed multilayer film assembly by alternate adsorption of silica nanoparticles and linear polycation. Chemical Communications, 1998(11): p. 1229-1230.

77. Liu, Y., A. Wang, and R.O. Claus, Layer-by-layer electrostatic self-assembly of nanoscale Fe_3O_4 particles and polyimide precursor on silicon and silica surfaces. Applied Physics Letters, 1997. **71**(16): p. 2265.

78. Ariga, K., J.P. Hill, and Q. Ji, Layer-by-layer assembly as a versatile bottom-up nanofabrication technique for exploratory research and realistic application. Physical Chemistry Chemical Physics, 2007. **9**(19): p. 2319-2340.

79. Lvov, Y. and H. Mohwald, Protein achitecture: Interfacing molecular assemblies and immobilization biotechnology (1st Edition). Lvov, Y. and H. Mohwald, Editors. 1999, CRC Press.

80. Kong, W., *et al.*, A new kind of immobilized enzyme multilayer based on cationic and anionic interaction. Macromolecular Rapid Communications, 1994. **15**(5): p. 405-409.

81. Lvov, Y., *et al.*, Assembly of multicomponent protein films by means of electrostatic layer-by-layer adsorption. Journal of the American Chemical Society, 1995. **117**(22): p. 6117-6123.

82. Kayushina, R., *et al.*, Construction and X-ray reflectivity study of self-assembled lysozyme/polyion multilayers. Thin Solid Films, 1996. **284-285**: p. 246-248.

83. Pommersheim, R., J. Schrezenmeir, and W. Vogt, Immobilization of enzymes by multilayer microcapsules. Macromolecular Chemistry and Physics, 1994. **195**(5): p. 1557-1567.

84. Burchardt, M. and G. Wittstock, Kinetic studies of glucose oxidase in polyelectrolyte multilayer films by means of scanning electrochemical microscopy (SECM). Bioelectrochemistry, 2008. **72**(1): p. 66-76.

85. Lvov, Y., K. Ariga, and T. Kunitake, Layer-by-layer assembly of alternate protein/polyion ultrathin films. Chemistry Letters, 1994. **23**(12): p. 2323-2326.

86. Hodak, J., *et al.*, Layer-by-layer self-assembly of glucose oxidase with a poly(allylamine)ferrocene redox mediator. Langmuir, 1997. **13**(10): p. 2708-2716.

87. Onda, M., *et al.*, Sequential reaction and product separation on molecular films of glucoamylase and glucose oxidase assembled on an ultrafilter. Journal of Fermentation and Bioengineering, 1996. **82**(5): p. 502-506.

88. Isgrove, F.H., *et al.*, Enzyme immobilization on nylon–optimization and the steps used to prevent enzyme leakage from the support. Enzyme and Microbial Technology, 2001. **28**(2-3): p. 225-232.

89. Bayramoglu, G., B. Kaya, and M. Yakuparica, Immobilization of lipase onto spacer-arm attached poly(GMA-HEMA-EGDMA) microspheres. Food Chemistry, 2005. **92**(2): p. 261-268.

90. Li, C., *et al.*, Characterization and immobilization of liposome-bound cellulase for hydrolysis of insoluble cellulose. Bioresource Technology, 2007. **98**(7): p. 1366-1372.

91. Wang, Y., *et al.*, Immobilization of cold-active cellulase from antarctic bacterium and its use for kelp cellulose ethanol fermentation. BioResources, 2015. **10**(1): p. 1757-1772.

92. Vansant, E.F., P. Van Der Voort, and K.C. Vrancken, Characterization and chemical modification of the silica surface. 1995, ELSEVIER: Netherlands.

93. Matos, J.R., *et al.*, Ordered mesoporous silica with large cage-like pores: structural identification and pore connectivity design by controlling the synthesis temperature and time. Journal of the American Chemical Society, 2003. **125**(3): p. 821-829.

94. Michau, M. and M. Barboiu, Self-organized proton conductive layers in hybrid proton exchange membranes, exhibiting high ionic conductivity. Journal of Materials Chemistry, 2009. **19**(34): p. 6124-6131.

95. Saini, A.K., C.M. Carlin, and H.H. Patterson, Confirmation of the presence of imine bonds in thermally cured polyimides. Journal of Polymer Science Part A: Polymer Chemistry, 1993. **31**(11): p. 2751-2758.

96. Marin, L., B. Simionescu, and M. Barboiu, Imino-chitosan biodynamers. Chemical Communications, 2012. **48**(70): p. 8778-8780.

97. Rangnekar, A., *et al.*, Retention of enzymatic activity of alpha-amylase in the reductive synthesis of gold nanoparticles. Langmuir, 2007. **23**(10): p. 5700-5706.

98. Vandenberg, E.T., *et al.*, Structure of 3-aminopropyl triethoxy silane on silicon oxide. Journal of Colloid and Interface Science, 1991. **147**(1): p. 103-118.

99. Spahn, C. and S. Minteer, Enzyme immobilization in biotechnology. Recent Patents on Engineering, 2008. **2**(3): p. 195-200.

100. Yu, Y., *et al.*, Covalent immobilization of cellulases onto a water-soluble-insoluble reversible polymer. Applied Biochemistry and Biotechnology, 2012. **166**(6): p. 1433-1441.

101. Li, Y., *et al.*, Fabrication of graphene oxide decorated with Fe_3O_4@SiO_2 for immobilization of cellulase. Journal of Nanoparticle Research, 2015. **17**(1).

102. Mao, X., *et al.*, A novel method to prepare chitosan powder and its application in cellulase immobilization. Journal of Chemical Technology & Biotechnology, 2006. **81**(2): p. 189-195.

103. Sousa Jr, R., *et al.*, Recent trends in the modeling of cellulose hydrolysis. Brazilian Journal of Chemical Engineering, 2011. **28**(4): p. 545-564.

104. Dinçer, A. and A. Telefoncu, Improving the stability of cellulase by immobilization on modified polyvinyl alcohol coated chitosan beads. Journal of Molecular Catalysis B: Enzymatic, 2007. **45**(1-2): p. 10-14.

105. Alahakoon, T., *et al.*, Immobilization of cellulases on amine and aldehyde functionalized Fe_2O_3 magnetic nanoparticles. Preparative Biochemistry Biotechnology, 2012. **42**(3): p. 234-248.

106. Wu, C., *et al.*, Active biocatalysts based on Candida rugosa lipase immobilized in vesicular silica. Process Biochemistry, 2012. **47**(6): p. 953-959.

107. Abraham, R.E., *et al.*, Suitability of magnetic nanoparticle immobilised cellulases in enhancing enzymatic saccharification of pretreated hemp biomass. Biotechnology for Biofuels, 2014. **7**: p. 90.

108. Gokhale, A.A., J. Lu, and I. Lee, Immobilization of cellulase on magnetoresponsive graphene nano-supports. Journal of Molecular Catalysis B: Enzymatic, 2013. **90**: p. 76-86.

109. Verma, M.L., *et al.*, Exploring novel ultrafine Eri silk bioscaffold for enzyme stabilisation in cellobiose hydrolysis. Bioresource Technology, 2013. **145**: p. 302-306.

110. Ungurean, M., C. Paul, and F. Peter, Cellulase immobilized by sol-gel entrapment for efficient hydrolysis of cellulose. Bioprocess and Biosystems Engineering, 2013. **36**(10): p. 1327-1338.

111. Luckarift, H.R., *et al.*, Enzyme immobilization in a biomimetic silica support. Nature Biotechnology, 2004. **22**(2): p. 211-213.